MICROFLUIDIC ASSEMBLY OF ZEIN MICROCAPSULES

BY

YIMING FENG

DISSERTATION

Submitted in partial fulfillment of the requirements
for the degree of Doctor of Philosophy in Food Science and Human Nutrition
with a concentration in Food Science
in the Graduate College of the
University of Illinois at Urbana-Champaign, 2018

Urbana, Illinois

Doctoral Committee:

Research Professor Graciela Wild Padua, Chair
Assistant Professor Youngsoo Lee, Director of Research
Professor Keith R Cadwallader
Professor Pawan Singh Takhar

ABSTRACT

Microencapsulation has been widely used for many applications to stabilize functional materials and to control the release of them. With the rapid changes in consumer needs, there are increased and diversified demands for microencapsulation technology in the food industry; for instance, flavor masking, nutrient protection, and probiotics delivery. The controlled release property of core materials from the microcapsules is one of the key factors to achieve the essential goal of incorporating microcapsules in foods. Despite the extensive research on microencapsulation in the past, it is still a challenge for the industry to customize delivery systems to meet the diverse demands, especially when the materials to be used are limited to food-grade materials. In addition, the widely used top-down processes such as high-pressure homogenization and microfluidization cannot provide sufficient control on the properties of microcapsules. Those energy-intensive processes also generate substantial shear and heat, which have negative impacts on vitamins, proteins, and bioactives in microcapsules. Hence, there is a critical need to develop a mild bottom-up process that enables accurate controls over the process and the properties of the microcapsules.

Microfluidics drew a great interest as a mean to synthesize or fabricate microcapsules. It features many advantages such as highly homogeneous and tunable product properties and non-invasive process, and makes handling of delicate materials feasible.

To date, the majority of materials used in microfluidic process are non-food grade synthetic polymers. In order to apply this technology in the food industry, it is necessary to find suitable food-grade materials. Zein is a water-insoluble protein that has shown a potential as a building block of delivery carriers for functional ingredients and is a good candidate to be used in microfluidic process. Therefore, the overall goal of this study is to develop a methodology to assemble zein microcapsules using microfluidic approach.

First, zein nanoparticles were used as building blocks to stabilize emulsions. By tuning the wettability of the zein nanoparticles with sodium caseinate, the emulsion stability was further improved. An optimal zein: caseinate ratio of 10:3 increased the interfacial coverage of oil droplets. This emulsifying ability of zein was improved by tuned wettability, which could be used as a food ingredient.

Then, shifting from the conventional process, a microfluidic process was introduced to fabricate hollow zein microcapsules with tunable permeability. The generation of zein microcapsules was driven by self-assembly of zein at the oil-water interface followed by

internal phase separation. By controlling the concentration of zein in dispersing phase and the flow rates of continuous and dispersing phases during microfluidic process, the rate of release was accurately adjusted. At the same time, the internal structure of the microcapsules was controlled from single core to multiple cores as well as the particle size of microcapsules.

Based on the established microfluidic process, the zein microcapsules were further fabricated to modify mechanical properties and degree of wrinkling. These two properties are critical engineering properties of microcapsules to function properly for many applications. The incorporation of phytic acid significantly changed the plasticity and increased the degree of wrinkling of zein microcapsules, which were confirmed by nanoindentation and image analysis.

Finally, an antimicrobial peptide nisin was encapsulated as an example to demonstrate an application of this technology. Nisin is a natural antimicrobial agent that can inhibit the growth of *Listeria monocytogenes.* However, the application of nisin has the limitation due to its instability in food matrices. Our study showed that the encapsulation of nisin in zein using a microfluidic process was able to control the release of nisin and significantly improved its antimicrobial activity against *Listeria monocytogenes* in fresh cheese. The efficacy of nisin was also extended from three days with non-encapsulated nisin to more than one week with the encapsulated nisin.

ACKNOWLEDGEMENTS

I would like to express my most sincere appreciation to my advisor, Dr. Youngsoo Lee, for his patience and motivation. Dr. Lee is someone that always being supportive and encouraging, since the day I started working in his lab as an undergraduate research assistant. I still remember every time that I propose an immature or impractical idea, he never said no but always suggest me to look more into it, which has gradually changed my scientific mindset towards a realistic and rational manner. Especially during the year of 2016 when I encountered numerous failures with the microfluidic research, Dr. Lee was always there to give me academic and moral support. Throughout my graduate research, Dr. Lee has given me a great freedom to pursue my research, and sometimes even without an objection. This thesis would not have been possible without the support and guidance from him.

Furthermore, I would like to thank my committee members, Dr. Padua, Dr. Cadwallader and Dr. Takhar. The valuable advice they have provided during committee meetings, preliminary exam, and personal conversations have helped me identify the strengths and weaknesses of my study and broadened my scientific view. It has been a pleasure to learn from their expertise and passion for research.

I am also very grateful to Dr. Soo-Yeun Lee, who has mentored me since my undergraduate study and provided me with many opportunities to collaborate with the food industry on sensory projects. She also generously spent her time to discuss about my research during lab meetings, and brought up insightful and sometimes philosophical perspectives, to help me reflect and solidify my work.

I would like to say thank you to my labmates and previous labmates in the Youngsoo Lee lab and the Soo Lee lab. I also want to express my appreciation to the FSHN staff, who are always there to do me favors.

Lastly, I would want to thank my parents, for always supporting me to pursue my dreams. The relentless love from my families and friends has sustained me through the tough days over the past years. Also, I would like to thank my girlfriend for not showing up during my Ph.D. study, so that I could completely focus on my research without being distracted.

Table of Contents

CHAPTER 1

Introduction

1.1 Significance

Microencapsulation has been widely used in many applications for the stabilization and controlled release of core such as functional materials, pharmaceuticals, nutraceuticals and cosmetics (Gouin, 2004). Conventional techniques for encapsulation in the food industry include spray drying/cooling, extrusion, fluidized bed and coacervation. In the past several years, the release fate of core from microcapsules in the gastrointestinal (GI) tract is gaining an increasing interest. The release fate of the core can be influenced by a variety of factors, such as the size and size distribution of particles, wall materials for microcapsules, formation of microstructure, as well as the space distribution of encapsulant in the microcapsules. In general, there are two types of release mechanisms associated with microcapsules: shell rupture/dissolution release and diffusion driven release through a permeable shell (Yow & Routh, 2006). Usually, a shell rupture/dissolution release usually results in a drastic release while the diffusion-driven release is considered to be slower and milder. Compared to the shell rupture/dissolution release, the diffusion-driven release provides a better control of release properties, which enables the release process to be completed in an extended timescale or under specific trigger factors.

Colloidosomes are microcapsules whose shells are consisted of colloidal particles as building blocks (Thompson, Williams, & Armes, 2014). The primary features of colloidosomes include the integrity of microcapsule during release, controllable permeability, stimulus-triggering ability and bio-compatibility. Precise control of these features would allow the design of programmable colloidosomes for specific release properties (San Miguel, Scrimgeour, Curtis, & Behrens, 2010). A variety of smart colloidosomes has been developed possessing different triggering stimuli, including pH, temperature and shear rate. To date, the majority of colloidosomes were prepared using synthetic or inorganic materials, such as polystyrene, latex and silica particles, due to their chemical stability and textural rigidity to maintain their mechanical strength at the interface. And, traditional methods for producing colloidosomes usually involve hazardous chemicals. Furthermore, utilizing of inorganic and synthetic polymer materials also limited their applications in food and pharmaceutical

industries. Thus, there is critical need to replace the building blocks using biocompatible and biodegradable materials, and to develop an alternative processing strategy without hazardous chemicals. Recently many food-grade biological materials have been successfully engineered to form solid particles, e.g., zein protein, pea protein, soy protein, whey protein and starch granules (de Folter, van Ruijven, & Velikov, 2012; Destribats, Rouvet, Gehin-Delval, Schmitt, & Binks, 2014; Feng & Lee, 2016; Song et al., 2015). Fabrication of those food-grade solid particles shed light on assembling colloidosomes using food-grade materials, with potentially greater biocompatibility for their applications in pharmaceutical, food and cosmetic industries. On the other hand, complexity in process, use of toxic chemicals and lack of control over particle uniformity are still the main challenges. So, there is a need to simplify the current technique or find an alternative structure that is analogy to colloidosomes.

Zein is a prolamine from corn that is insoluble in water but capable of self-assembly to form many types of microstructures such as films, nanoparticles, or hollow nanoparticles. Its distinct amino acid composition and rigidity in solid state make it a potential food-grade wall material for fabricating diffusion-driven controlled release systems. To date, many studies had explored the application of zein as delivery carriers, although with several limitations (Chen & Zhong, 2015; Hu, Wang, Fernandez, & Luo, 2016; Luo, Zhang, Whent, Yu, & Wang, 2011). One inherent limitation is that current zein-based delivery systems are only able to carry hydrophobic compounds, in which the encapsulation was achieved during a co-precipitation of zein and encapsulant in water. Therefore, the encapsulant has to be insoluble in water but soluble in 60%-90% ethanol. The second limitation in previous research is associated with particle size control, that only submicron (100-300nm) particles can be formed. Nevertheless, Small particles usually release encapsulated compounds rapidly due to their high surface-volume ratios and instant disintegration in the GI-tract, thus feasible for sustained release (Golomb, Fisher, & Rahamim, 1990).

To ensure a sustained release profile, the physical integrity of microcapsules during processing and release is regarded as a foremost requirement, and therefore are gaining increasing interest (Ao, Li, Zhang, & Ngai, 2011; Cayre, Noble, & Paunov, 2004; Dinsmore et al., 2002; Kaufman et al., 2015; Long, Song, York, Zhang, & Preece, 2013; Rossier-Miranda, Schroën, & Boom, 2012; Shilpi, Jain, Gupta, & Jain, 2007). In previous studies, colloidosomes were formed using silica and synthetic polymers which exhibited acceptable mechanical strength during harsh processing conditions. However, the soft nature of food proteins becomes a hurdle because the formed microcapsules could rupture during processing and release core

materials under external shearing. Thus, it is necessary to develop a methodology to characterize the mechanical properties of microcapsules first and then find a way to improve the mechanical properties. Nano-indentation is a novel technique that has been widely applied to study mechanical properties of materials in a small scale, which can be used in this study to characterize microcapsules formed by zein (Huang & Lu, 2007; Lee et al., 2012). Nevertheless, most previous studies used nano-indentation to characterize non-biological materials, and those methodologies need to be tweaked in order to fit soft matters.

Microfluidic process is a novel method to produce emulsion, and very few researches have been done in the food science discipline. Notable profound features of this method include high energy efficiency, high droplet monodispersity, potential to assemble sophisticated microstructures, and it is a continuous process (Muijlwijk, Berton-carabin, & Schroën, 2016). Currently, scaling up of microfluidic system is still the biggest hurdle that limits its applications. Recently, the strategies of scaling up microfluidic system have been extensively explored for the purposes of mass production and other applications (e.g. Scale-up and control of droplet production in coupled microfluidic flow-focusing geometries) (Maan, Nazir, Khan, Boom, & Schroën, 2015). Therefore, it is of great interest to investigate microfluidic process as a potential technique for building a delivery system.

Targetted-release is regarded as a central goal in the microencapsulation research(Abbaspourrad, Carroll, Kim, & Weitz, 2013; Li, Moosa, Croissant, & Khashab, 2015; Stephenson et al., 2014; Zhang, Zhang, Decker, & McClements, 2015). Many bioactive compounds are absorbed in the small intestine, and some even take effects in the large intestine. However, it is still a challenge to ensure the chemical stability and integrity before the compound reaches the target site. As such, triggered release becomes prominent for the purposes of achieving target release. The programmable release could be primarily formed through pH-responsive coating based on a template. Ideally, the template is able to be easily tuned to perform different release profiles, and made of bio-compatible materials. There have been very limited coating templates that were developed using food materials and the template plays a significant role as a basis for the further development of more complex delivery systems.

Many previous studies used food materials as wall material for microencapsulation, and a variety of structures were built including conventional emulsions, hydrogel particles, liposomes, solid lipid nanoparticles and double emulsions. However, they all possess strengths and drawbacks. For example, hydrogels can be used for controlled release but suffer from low

tensile strength (Hoare & Kohane, 2008), conventional emulsion is cost-effective but does not control over release rate, solid lipid nanoparticles are mechanically stable but can only be used for encapsulating lipophilic compounds.

All these limitations listed above necessitate the further development of food-grade delivery systems that feathers the similar advantages of colloidosomes. Therefore, the *rationale* of this study is to develop a controlled delivery system that is prepared 1) with biocompatible materials, 2) without using hazardous chemicals during processing, 3) with a simplified manufacturing technology, 4) for tunable permeability and mechanical properties and 5) for versatility to encapsulate various core materials.

The *significance* of this study is to utilize a cost-effective agricultural by-product, zein, as a food-grade microencapsulation wall material, to assemble bio-compatible, versatile, and programmable delivery systems, for the purposes of encapsulating and delivering bio-active compounds in food, medicine and cosmetics.

1.2 Overall goal and hypothesis

The *overall goal* of this study is to develop a food-grade microcaspule, which is capable of providing sustained release, with tunable mechanical strength, internal structure, morphogoly and release profiles. We *hypothesize* that the rate of release is a function of a series of physical and structural properties of microcapsules, and these properties can be precisely controlled in microfluidic process by flow rates formulations.

1.3 Specific objectives

The *specific objectives* of this research:

1) **Identify the effect of surface properties of zein nanoparticles on the stability of subsequent Pickering emulsions**

Hypothesis: The stability of zein Pickering emulsions is dependent upon the surface properties of zein colloidal nanoparticles. Surface modification will change the surface properties of zein colloidal nanoparticle and thus improve the stability of subsequent Pickering emulsions.

2) **Prepare hollow zein microcapsules by internal phase separation method using a microfluidic chip and analyze the release properties of the microcaptules**

Hypothesis: Zein will self-assemble at oil-water interface in microfluidic chip to form microcapsules. The release property of formed hollow zein microcapsules is a function of

microcapsule size, porosity and wall permeability, and these properties will be controlled by adjusting processing parameters and formulations.

3) **Characterize and control the nano-mechanical properties and morphology of hollow zein microcapsules**

Hypothesis: The nano-mechanical and mophological properties of hollow zein microcapsules are affected by their molecular structures, therefore disturbing the structure of zein with small molecules will change the nano-mechnical properties and morphology of the microcapsules.

4) **Evaluate the antimicrobial properties of nisin encapsulated by zein in microfluidics.**

Hypothesis: Encapsulation and controlled release of nisin will retain nisin stability therefore entend its efficacy in inhibiting microbial growth in food matrix.

1.4 References

Abbaspourrad A, Carroll NJ, Kim SH, Weitz D a. 2013. Polymer microcapsules with programmable active release. J. Am. Chem. Soc. 135:7744–7750.

Ao Z, Li Z, Zhang G, Ngai T. 2011. Colloidosomes formation by controlling the solvent extraction from particle-stabilized emulsions. Colloids Surfaces A Physicochem. Eng. Asp. [Internet] 384:592–596. Available from: http://dx.doi.org/10.1016/j.colsurfa.2011.05.011

Cayre OJ, Noble PF, Paunov VN. 2004. Fabrication of novel colloidosome microcapsules with gelled aqueous cores. J. Mater. Chem. 14:3351.

Chen H, Zhong Q. 2015. A novel method of preparing stable zein nanoparticle dispersions for encapsulation of peppermint oil. Food Hydrocoll. [Internet] 43:593–602. Available from: http://linkinghub.elsevier.com/retrieve/pii/S0268005X14002616

Destribats M, Rouvet M, Gehin-Delval C, Schmitt C, Binks BP. 2014. Emulsions stabilised by whey protein microgel particles: towards food-grade Pickering emulsions. Soft Matter [Internet] 10:6941–54. Available from: http://www.ncbi.nlm.nih.gov/pubmed/24675994

Dinsmore a D, Hsu MF, Nikolaides MG, Marquez M, Bausch a R, Weitz D a. 2002. Colloidosomes: Selectively Permeable Capsules Composed of Colloidal Particles. Science (80-.). [Internet] 298:1006–1009. Available from: http://www.sciencemag.org/cgi/doi/10.1126/science.1074868

Feng Y, Lee Y. 2016. Surface modification of zein colloidal particles with sodium caseinate to stabilize oil-in-water pickering emulsion. Food Hydrocoll. [Internet] 56:292–302. Available from: http://linkinghub.elsevier.com/retrieve/pii/S0268005X15301971

de Folter JWJ, van Ruijven MWM, Velikov KP. 2012. Oil-in-water Pickering emulsions stabilized by colloidal particles from the water-insoluble protein zein. Soft Matter [Internet] 8:6807. Available from: http://xlink.rsc.org/?DOI=c2sm07417f

Golomb G, Fisher P, Rahamim E. 1990. The relationship between drug release rate, particle size and swelling of silicone matrices. J. Control. Release [Internet] 12:121–132. Available from: http://linkinghub.elsevier.com/retrieve/pii/016836599090088B

Gouin S. 2004. Microencapsulation: Industrial appraisal of existing technologies and trends. Trends Food Sci. Technol. 15:330–347.

Hoare TR, Kohane DS. 2008. Hydrogels in drug delivery: Progress and challenges. Polymer (Guildf). [Internet] 49:1993–2007. Available from: http://dx.doi.org/10.1016/j.polymer.2008.01.027

Hu S, Wang T, Fernandez ML, Luo Y. 2016. Development of tannic acid cross-linked hollow zein nanoparticles as potential oral delivery vehicles for curcumin. Food Hydrocoll. [Internet] 61:821–831. Available from: http://linkinghub.elsevier.com/retrieve/pii/S0268005X16302946

Huang G, Lu H. 2007. Measurements of two independent viscoelastic functions by nanoindentation. Exp. Mech. 47:87–98.

Kaufman G, Nejati S, Sarfati R, Boltyanskiy R, Loewenberg M, Dufresne ER, and others. 2015. Soft microcapsules with highly plastic shells formed by interfacial polyelectrolyte–nanoparticle complexation. Soft Matter [Internet] 11:7478–7482. Available from: http://xlink.rsc.org/?DOI=C5SM00973A

Lee J, Zhang M, Bhattacharyya D, Yuan YC, Jayaraman K, Mai YW. 2012. Micromechanical behavior of self-healing epoxy and hardener-loaded microcapsules by nanoindentation. Mater. Lett. [Internet] 76:62–65. Available from: http://dx.doi.org/10.1016/j.matlet.2012.02.052

Li S, Moosa B a., Croissant JG, Khashab NM. 2015. Electrostatic Assembly/Disassembly of Nanoscaled Colloidosomes for Light-Triggered Cargo Release. Angew. Chemie Int. Ed. [Internet] 54:6804–6808. Available from: http://doi.wiley.com/10.1002/anie.201501615

Long Y, Song K, York D, Zhang Z, Preece JA. 2013. Engineering the mechanical and physical properties of organic-inorganic composite microcapsules. Colloids Surfaces A Physicochem. Eng. Asp. [Internet] 433:30–36. Available from: http://dx.doi.org/10.1016/j.colsurfa.2013.04.055

Luo Y, Zhang B, Whent M, Yu LL, Wang Q. 2011. Preparation and characterization of zein/chitosan complex for encapsulation of α-tocopherol, and its in vitro controlled release study. Colloids Surfaces B Biointerfaces [Internet] 85:145–152. Available from: http://www.ncbi.nlm.nih.gov/pubmed/21440424

Maan AA, Nazir A, Khan MKI, Boom R, Schroën K. 2015. Microfluidic emulsification in food processing. J. Food Eng. [Internet] 147:1–7. Available from:

http://linkinghub.elsevier.com/retrieve/pii/S0260877414003896

Muijlwijk K, Berton-carabin C, Schroën K. 2016. Cross-flow microfluidic emulsification from a food perspective. Trend food Sci. Technol. 49:51–63.

Rossier-Miranda FJ, Schroën K, Boom R. 2012. Microcapsule production by an hybrid colloidosome-layer-by-layer technique. Food Hydrocoll. [Internet] 27:119–125. Available from: http://dx.doi.org/10.1016/j.foodhyd.2011.08.007

San Miguel A, Scrimgeour J, Curtis JE, Behrens SH. 2010. Smart colloidosomes with a dissolution trigger. Soft Matter 6:3163.

Shilpi S, Jain A, Gupta Y, Jain SK. 2007. Colloidosomes: an emerging vesicular system in drug delivery. Crit. Rev. Ther. Drug Carrier Syst. 24:361–391.

Song X, Pei Y, Qiao M, Ma F, Ren H, Zhao Q. 2015. Preparation and characterizations of Pickering emulsions stabilized by hydrophobic starch particles. Food Hydrocoll. [Internet] 45:256–263. Available from: http://linkinghub.elsevier.com/retrieve/pii/S0268005X14004445

Stephenson G, Parker RM, Lan Y, Yu Z, Scherman O a, Abell C. 2014. Supramolecular colloidosomes: fabrication, characterisation and triggered release of cargo. Chem. Commun. [Internet] 50:7048. Available from: http://www.ncbi.nlm.nih.gov/pubmed/24848874

Thompson KL, Williams M, Armes SP. 2014. Colloidosomes: Synthesis, properties and applications. J. Colloid Interface Sci. [Internet] 447:217–228. Available from: http://linkinghub.elsevier.com/retrieve/pii/S0021979714009187

Yow HN, Routh AF. 2006. Formation of liquid core-polymer shell microcapsules. Soft Matter 2:940.

Zhang Z, Zhang R, Decker EA, McClements DJ. 2015. Development of food-grade filled hydrogels for oral delivery of lipophilic active ingredients: pH-triggered release. Food Hydrocoll. [Internet] 44:345–352. Available from: http://dx.doi.org/10.1016/j.foodhyd.2014.10.002

CHAPTER 2

Literature review

2.1 Introduction

2.1.1 Controlled delivery in foods: Significance and hurdles

The fabrication of microcapsules as a carrier for delivering and stabilizing bioactive compounds have been extensively studied and widely applied in biomedical, food and cosmetic industries (Gouin 2004; Kaufman and others 2015). Recently, numerous efforts have been made towards sophisticated design of delivery systems, for the purposes of improving bioavailability of core materials and achieving their bioactivity in human bodies (Hejazi and Amiji 2003; Oh and others 2008; Marsanasco and others 2011; Chen and others 2014; Morais and Burgess 2014; Ozturk and others 2014; K. Pan, Luo, and others 2014; Ruiz-Rodriguez and others 2014; Koga and others 2015; Yang and others 2015; Zou and others 2015; Katouzian and Jafari 2016; J. Li and others 2016; Liu and Tang 2016; Zhang and others 2016). For instance, the utilization of solid lipid nanoparticle goes through three primary stages)of micellization, adsorption and metabolism, to become biologically available (Yao and others 2014). Hence, it is of great interest to customize delivery systems meeting various criteria and achieve different functionalities such as release of core materials at appropriate site within the human digestive system (McClements 2010). In addition to bioactive compounds, sustained release of functional ingredients in food matrices also play a vital role in improving food quality. For example, controlled release of tocopherol and quercetin in oil-rich foods were reported to inhibit lipid oxidation (Chen and others 2012; Lee and Yam 2013). Also slow release of antimicrobial agents have been deployed to prevent the contamination by pathogen in foods during processing and storage (Bhaskara Rao and others 2014; Vonasek and others 2014; Kashiri and others 2016).

2.1.2 Overview of microfluidics and the growing interest in food related applications

Microfluidics is a terminology to refer the way of manipulating fluids in channels with dimensions of tens of micrometers (Whitesides 2006). In the past decade, the application of microfluidics has been rapidly extended to biomedical imaging, drug discovery, biomolecule synthesis and diagnostics (Teh and others 2008), due to its superior ability to precisely control

small volume of liquid segments and act as reaction confinements (Mark and others 2010). Recently, utilization of microfluidic devices in food applications has gained increasing interest, primarily as a rapid detection tool to resolve food safety issues (Ma and others 2018), a platform to study basic emulsion physics (Muijlwijk and others 2017) and to quantify active and hazardous compounds (Amine and others 2017; Al Haddabi and others 2017; Oscar and others 2017). Beyond the conventional analytical roles of microfluidics, there is a growing interest to use microfluidics as a micro-reactor to assemble sophisticated structures with distinctive features (Yow and Routh 2006; Fang and Cathala 2011; Abbaspourrad and others 2013; Yuan and Williams 2014; Maan and others 2015; Khalid and others 2016; M. Li and others 2016; Schloss and others 2016; Akbari and others 2017; Liu and others 2018). Compare to conventional processing techniques, microfluidic process features many unique advantages. As an emulsification tool, microfluidic process does not require additional energy input unlike high-shear or high-pressure homogenization (Othman and others 2015). The mild process therefore would not develop temperature fluctuations during the process. When it functions as a micro-reactor or micro-factory, the efficacy of reaction could be drastically accelerated due to its better mass and heat transfer rate (Tian and others 2016). Moreover, as a continuous process, the properties of products can be accurately controlled by adjusting flow rates. Benefit from all these advantages, microfluidic process is recognized as an emerging technique in many fields. Figure 2.1 displays the growing interest on microfluidic studies, based on the number of publications counted by ISI Web of Science database. Compare to the entire field, the application of microfluidics in food-related research is still at early stage but it is growing rapidly.

2.1.3 Principles of microfluidic devices

Understanding the fluid dynamics behind microfluidic devices is one of the prerequisites to develop a microfluidic-based system. In a microfluidic device, mixing of fluids from different channels is the one of the most common scenarios, which was applied for biomedical diagnosis, drug delivery and droplet formations (Calado and others 2016; Feng and Lee 2017). In general, the mixing of fluids in microfluidic devices could be classified into two types: miscible mixing and immiscible droplet generation.

The mixing of miscible fluids in a microfluidic device usually enables the occurrence of chemical reactions. Optimization of the mixing efficacy, therefore, becomes essential to enhance the performance of microfluidic device as a micro-reactor (Soleymani and others

2007). Experimental and simulation studies found that the design patterns of vortices, mixing angles, precise control of flow rates and pressure drop are also indispensable factors that could have impact on mixing efficacy (Soleymani and others 2007; Calado and others 2016). A mathematical model has also been proposed to describe the extent of mixing using a parameter αmix (eq. 1) (Hoffmann and others 2006; Calado and others 2016).

$$\alpha_{mix} = 1 - \sqrt{I_S} = 1 - \frac{\sigma}{\sigma_{max}} \quad (1)$$

Where σ and σmax are the standard deviation and the maximum standard deviation of the concentration field, while IS represents the local fluid concentration.

Another type of mixing regime involves two immiscible fluids, followed by the formation of droplets. This method has been widely used to produce monodispersed emulsions. The monodispersed emulsions could be generated in two manners, shear induced emulsification and spontaneous emulsification (Maan and others 2011). A shear induced emulsification refers to a further size reduction of pre-mixed emulsions, when passing through a constriction (Nazir and others 2010; Maan and others 2011). The formation of spherical droplets in the spontaneous emulsification process, on the other hand, is due to Laplace pressure differences in the dispersed phase on the terrace and in the channel (Sugiura and others 2001). The figure 2.2 shows a diagram that compares spontaneous emulsification and shear-induced emulsification (Van Der Graaf and others 2006; Nazir and others 2010).

2.1.4 Microfluidic control and chip gemometries

The control over a microfluidic device is mainly achieved through the adjustment of flow rates. Precise control of flow rates during microfluidic processes is the key to control the properties of final products in both droplet generation of two immiscible fluids and mixing of two miscible fluids. Depending on the flow rate, the droplets can be generated by three mechanisms in a focused flow microfluidic device, namely, dripping regime, narrow jetting regime and wide jetting regime (Figure 2.3) (Utada and others 2007). Regulated by the dynamic equilibrium between surface tension and viscous dragging force (shown in the equation 2), different droplet generation regimes could be achieved by adjusting the flow rates of continues phase and dispersing phase. When the flow rates of both phases are low, a dripping regime is preferred; while increasing the flow rate of continuous phase would lead to a narrow jetting regime, and the further increase in the flow rate of disperse phase could switch the droplet generation mechanism to a wide jetting regime (Utada and others 2007).

$$\eta_{out}\mu_{out}d_{drop} \sim \gamma d_{tip} \quad (2)$$

Where μout is the mean velocity of the continuous phase, ηout is the viscosity of the continuous phase, ddrop is the diameter of droplets, γ is the surface tension, and dtip is diameter of the tip.

Conventional microfluidic devices were controlled primarily by adjusting flow rates, while recently developed programmable microfluidic platforms provide more state of the art possibilities such as hydrodynamic trapping, droplet generation on demand, sequential loading and merging of droplets, and storage (Tsui and others 2013; Jin and others 2015). These cutting edge technologies granted the capability of utilizing microfluidic devices to produce extremely sophisticated structures, such as synthetic cells (Weiss and others 2017).

The terrace geometry of microfluidic devices is another vital factor. According to the literature, the droplet size of emulsion formed at the terrace is proportional to the reversed shear rate, which can be expressed mathematically using the equation (3) (Thorsen and others 2001).

$$r \sim \frac{\sigma}{\eta\dot{\varepsilon}} \quad (3)$$

Where r is the droplet radius, σ is the interfacial tension between the dispersing phase and continuous phase, η is the viscosity of the continuous phase, and $\dot{\varepsilon}$ is the shear rate. T-junction has been reported to generate the most extensive shear rate compared to flow-focusing and Y-junction, which favors the formation of emulsion droplets with highly monodispersed particle size (Steegmans and others 2009). In regards to the droplet size control, the droplet size in Y-junction is only a function of the flow rate and viscosity of continuous phase, while having no correlation to the properties of disperse phase (Steegmans and others 2009). However, in the cases of flow-focusing and T-junction, droplet size depends on the viscosity and flow rate of both phases (Carrier and others 2014; Park and others 2016). Therefore, when Y-junction is considered a more feasible approaching to building a scale-up microfluidic device, for its simplicity in controlling droplet size (Steegmans and others 2009). The terrace angle is also a critical parameter that affects the mixing efficacy. Figure 2.4 shows the effect of mixing angle on the mixing efficacy, where the blue and red color represent two streams that are engaged at the joint of two microchannels (Soleymani and others 2007).

2.1.5 Dilivery systems assembled using microfluidics

Higher shear or pressure induced homogenization are conventionally used in many encapsulation applications, which are top-down processes and are feasible for mass production

(Mijatovic and others 2005). However, top-down processes are associated with extensive mechanical attritions and considerable energy cost, and usually result in heterogeneous product attributes, including particle sizes, shape, and surface and mechanical properties (Hu and others 2008; Ali and others 2009). In many cases, controlled release of orally administrated bioactive compounds is necessary to ensure their functionalities, because most of these compounds are absorbed in small intestine by epithelium cells (Rossier-Miranda and others 2009; Tippetts and others 2012; Huq and others 2013). Therefore, it is of great interest to employ a bottom-up process to accurately control the engineering properties microcapsules. Some pioneering studies have already utilized microfluidic droplet system as a bottom-up approach to synthesize homogeneous microcapsules (Subramaniam and others 2005; Amici and others 2008). In encapsulation applications, many strategies using microfluidic chips have been developed to precisely control size and other properties of the particles (Headen and others 2014; Kim and others 2015; Olenskyj and others 2017). A number of microfluidic chip designs also emerged to produce sophisticated capsule structures (Zhang and others 2007; Workman and others 2008; Shum and others 2010; Zhao and Middelberg 2013). Benefited from mild processing conditions, microfluidic devices are suitable for manipulating delicate core materials, especially when live microorganisms such as prebiotics and yeasts are the targets(Gach and others 2016). However, there is still very few works done with food-related applications.

2.2 The structures assembled by microfluidic process

2.2.1 Emulsion

Emulsion is the most common structure that can be formed in a droplet-based microfluidic device. Different from conventional energy-dense emulsification processes, which break up the disperse phase through shear-induced collision (K. Pan, Chen, and others 2014), pressurization(TAN and NAKAJIMA 2005), or ultrasound-induced cavitation (van Zwieten and others 2017), the emulsion droplets form with a bottom-up manner in a microfluidic junction (Mijatovic and others 2005). This approach is ideal to produce monodisperse emulsion droplets with complications. In addition to the commonly used O/W and W/O single emulsions, double, quadruple and quintuple emulsions could be produced by shear-driven microfluidic systems (Abate and Weitz 2009). In the past, high-order emulsions were produced by a two-step top-down emulsification with two levels of energy input intensity (Li and others 2012). However, this approach lacks control of particle size and structure

because the higher energy process could partially break up the coarse emulsions formed in the prior step, and lead to heterogeneous droplet morphology.

Several chip configurations are widely used for the microfluidic emulsification process, namely T-junction, co-flow, focus-flow and microchannel plates (Fu and others 2012; Carrier and others 2014; Nabavi and others 2015; Khalid and others 2016). The figure 2.5 shows a schematic diagram of each droplet microfluidic configurations. In addition to those classical chip designs, many chips were customized with different junction angles (Marquis and others 2012). Selection of microfluidic configuration is based upon the needs of application, and typically, T-junction microfluidics provides the most extensive shear at the terrace, while membrane microfluidics features higher yield production.

Recently, microfluidic production of Janus particles have been gaining increasing attention, for their applications as bacteria detection agents, robust emulsifiers and other important structuralbuilding blocks (Teh and others 2008; Vladisavljević 2015; Nisisako 2016; Q. Zhang and others 2017). Janus particles are typically consisted of two distinct segments, that are chemically and physically amphiphilic or bipolar (Marquis and others 2012). Traditional routes to prepare Janus particles were based upon asymmetrical chemical modification on the unprotected side of substrates, such as sputtering, stamp coating and Langmuir desorption (J. Zhang and others 2017). Those approaches involve multiple steps and are lack of precise control. Microfluidics provide a more facile and precise control to prepare Janus particles, simply through the merging two channels containing different polymers at the junction (Nie and others 2006; Nisisako and others 2006). A schematic diagram in the figure 2.6 shows an example of such a practice (Marquis and others 2012).

2.2.2 Polymer nanoparticles

Many successes were also achieved to produce nanoparticles with microfluidic devices. The generation of nanoparticles in microfluidic chips were usually triggered by nanoprecipitation effects, through anti-solvation process. Briefly, a flow of polymeric solution is merged with a flow of anti-solvent solution at the junction of two microchannels, while the diffusion occurs and the concentration of solvent and anti-solvent gradually changes until an equilibrium is reached to precipitate the polymer nanoparticles. Compared to conventional methods, microfluidic production of particles are featured by its accurate control over nanoparticle properties and homogeneity. During the formation the nanoparticles, many factors, in particular fluid dynamics are crucial that could impact the properties of nanoparticles. For

instance, a turbulent flow could result in heterogeneous nanoparticles, due to its chaotic condition and spatially varied shear rate distribution.Shearing speed has a great impact on the particle size distribution of formed nanoparticles (Zhong and Jin 2009). Therefore, producing nanoparticles in a laminar flow could result in a more predictable and homogeneous particle sizes. A schematic diagram of microfluidic nanoprecipitation is shown in the figure 2.7.

Several materials have demonstrated acceptable feasibility to form nanoparticles in a microfluidic device, such as PLGA-PEG nanoparticles (Karnik and others 2008), PLA nanoparticles (Othman and others 2015), chitosan-ATP nanoparticles (Pessoa and others 2017), and zein nanoparticles (Olenskyj and others 2017). Further mathematical simulation suggests that the size of the nanoparticle is highly associated with the mixing ratio between polymeric solution and anti-solvent, hydraulic pressure upon mixing, flow velocity, and shear stress (Olenskyj and others 2017). Our previous work also found that the PDI (polydispersity index) of the nanoparticle could be reduced to less than 0.1, compared to the conventional value around 0.15~0.2 (A. Patel and others 2010; Y. Pan and others 2014). In addition to the flow parameters and fluid dynamics, the geometry of microfluidic devices also play important roles. D-bends and D-barriers were reported to give rise to chaotic mixing conditions and disturb the formation of nanoparticle structures (Pessoa and others 2017). Other factors, such as viscosity of fluids and hydrophobicity of microfluidic channels also need to be carefully considered. In order to take all of these factors into account, a computational fluid dynamics (CFD) simulation will be helpful to predict the final properties of the particles (Marra and others 2017; Olenskyj and others 2017).

2.2.3 Complexes

The formation of nano-scale or micro-scale complexes are usually driven by electrostatic coacervation processes (De Kruif and others 2004). Polyelectrolytes, such as gelatin, pectin, sodium alginate, gum arabic and globular proteins, can react with oppositely charged polyelectrolytes to form coacervated complexes (BURGESS and SINGH 1993; Luo and others 2011; Luo and Wang 2014; Luo and others 2015). Clogging is a critical issue when performing coacervation process on a microfluidic platform, where the process needs to be precisely regulated to avoid possible generation of large particles. In a recent study, β-lactoglubulin/Gum Arabic complex was formed in a microfluidic device, and the thermodynamic facts were elucidated (Amine and others 2017). In addition to those conventionally used polyelectrolytes, complexation could also be formed between DNA and polymers, for the purposes of delivering DNA into cells as a nano-medicine (Ho and others

2011). Many other food materials possess the potential to form complexes, which could be explored more in the future. Examples include complexing proteins and polysaccharides (Chen and others 2016), proteins and proteins (A.R. Patel and others 2010; Feng and Lee 2016), as well as dextrin and lipophilic vitamins (Vilanova and Solans 2015; Saldanha do Carmo and others 2017). Attributed to the potentially greater homogeneity and stability, complexes formed in microfluidic process could feature predictable and reliable bioavailability in the gastrointestinal tract.

2.2.4 Hydrogels

Hydrogels have already been widely applied in clinical and food practices, as oral administration delivery carrier (Zhang and others 2015), transdermal drug delivery (Costa and others 2017), enzyme immobilization (Kim and others 2009; Qian and others 2014), and release media for antimicrobials (Veiga and Schneider 2013). Most hydrogels networks are formed through chemical or physical cross-linking, that could be triggered by metal ions, pH and temperature (Hoare and Kohane 2008). In microfluidic devices, temperature fluctuation could result in fluid expansion and irreversible microchannel deformation, therefore it is not considered feasible to use temperature as a trigger. Instead, ion-induced gelation has been commonly employed to form hydrogels in microfluidic devices (Amici and others 2008; Ogończyk and others 2011; Marquis and others 2012; Akay and others 2017). Calcium and magnesium ions were usually used as gelling agents.

Throughout the hydrogel formation process, gelation is a second step following the W/O droplet generation. The gelling agent, usually calcium ions, could be introduced in three manners, by a third channel (Fang and Cathala 2011), chemical reactions between acids and calcium carbonate, or sequential exposure (Amici and others 2008; Kim and others 2017). The figure 2.8 shows a schematic example of introducing calcium ions in microfluidic channels by sequential exposure of pectin droplets in oil and calcium chloride, respectively (Kim and others 2017).

2.2.5 Solid lipid nanoparticles

Solid lipid nanoparticle is another important type of delivery matrix, usually formed by a lipid with high melting point and a surfactant (Schwarz and others 1994; Naseri and others 2015). Solid lipids nanoparticles can be degraded rapidly in the gastric-intestinal phase with almost no toxic effects, therefore they are regarded as an ideal delivery tool (Schwarz and others 1994). Conventional approaches to produce solid lipid nanoparticles involve high

pressure homogenization or microfluidization, in order to form a O/W nanoemulsion (Hentschel and others 2008; K. Pan and others 2013; Mcclements 2015; Naseri and others 2015; Yi and others 2016; Ravanfar and others 2018). An immediate cooling process should be performed to solidify the nanoemulsion before the droplets start coalescence. Unlike the conventional methods, the solid lipid nanoparticles are formed by solvent diffusion-induced supersaturation in microfluidic chips whereno extensive energy input is required (Yun and others 2009; Belliveau and others 2012). It is desirable to encapsulate delicate materials such as DNAs due to its mild processing environment.

2.2.6 Other structures

Attributed to its precise control capability, microfluidic devices can be used to form a series of unique structures that require rigorous conditions. Microfluidic platform has been reported as a single-step process for fabricating many sophisticated supramolecular microcapsules, for example, non-spherical particles(Shum and others 2010), porous microcapsules(Zhang and others 2012), dendritic microcapsules (Zheng and others 2014), cross-linked protein capsules(Zhou and others 2014), and protein crystals (Hansen and others 2002; Li and Ismagilov 2010; Maeki and others 2014; Zhu and others 2014; Abdallah and others 2016; Maeki, Yamazaki, and others 2016; Maeki, Yamaguchi, and others 2016). Those special structural designs significantly expanded the controlled-release capability, and enables microfluidic devices to be used to meet the demands for various application.

The formation of other structures that require accurate reacting ratios, or need to follow a procedure that contains a number of sequential steps, could also be performed on microfluidic platforms. For instance, layer-by-layer coating is a useful technique to modify surface properties and has been used for microencapsulation applications (Mak and others 2008; Kozlovskaya and others 2010; Rossier-Miranda and others 2012; Shchepelina and others 2012; Liu and others 2014). Limitations of conventional layer-by-layer approaches is related to process complexity, where residue washing and mixing ratios are very critical to control the quality of layers (Liu and others 2014). These issues could be potentially resolved using microfluidic devices.

2.3 Food-grade materials: Current achievements and prospectives

2.3.1 Synthetic polymers

Compare to biologically derived materials, it is more cost-effective to use edible synthetic polymers for food-related applications due to their process simplicity, abundancy and high purity (Shit and Shah 2014). Those food-grade polymers, such as polymethyl methacrylate (PMMA), polyethylene glycol (PEG), polyethyleneimine (PEI) and poly-lactic-co-glycolic acid (PLGA), have demonstrated excellent chemical resistance and biocompatibility (Lawton 2004; X. Pan and others 2013), and been widely applied as encapsulation wall materials, packing materials and edible films (Klose and others 2006; X. Pan and others 2013; Liu and others 2014; Rajan and others 2014).

Synthetic polymers, attributed to their well identified chemical and physical properties, are ideal options to be processed in microfluidics as building blocks. A classical method is to polymerize monomers at the interface after the formation of O/W or W/O droplets, by means of UV light, heat, initiator, or cross-linking agents (Shum and others 2010; Abbaspourrad and others 2013; Headen and others 2014; Wang and others 2014; Kim and others 2015; Liu and others 2018). The barrier or shell structure that formed at the interface further leads to a phase separation and formation of microcapsules. To date, a series of stimuli-triggered release systems have been reported using this approach, such as pH responsive microcapsules (Abbaspourrad and others 2013), thermal responsive microcapsules (Kim and others 2007) and microcapsules with tunable permeability (Rossier-Miranda and others 2009; Wang and others 2014; Kim and others 2015).

2.3.2 Proteins

Food protein-based materials are widely used for encapsulation and delivery of bioactive compounds in food matrices, featured for their high nutritional value and sustainability, and also they are Generally Recognized as Safe (GRAS) (Tavares and others 2014; Coltelli and others 2015). However, limited successes have been achieved with protein in microfluidic processes, due to their complicated folding and unfolding patterns (Greenfield 2006), and highly dependable interfacial adsorption behaviors (Tcholakova and others 2003). To date, zein, a corn protein that is capable of self-assembly (Wang and Padua 2010; Wang and Padua 2012), has been used in microfluidic devices to successfully encapsulate core materials with controllable release properties (Feng and Lee 2017). Gelatin, which is a protein from animal source, could form microbeads in microfluidic channels by means of in-situ gelation (Wassén and others 2012; Park and others 2016). Other proteins like casein, which is also amphiphilic and able to self-assembly (K. Pan, Luo, and others 2014; Turovsky and others 2015), may also be a feasible material for microfluidics.

2.3.3 Carbohydrates

The most common food-grade materials explored for microfluidic processes are carbohydrate-based biopolymers. For example, hydrogels or microbeads can be formed by ion induced gelling of pectin (Fang and Cathala 2011; Ogończyk and others 2011; Kim and others 2017) and alginate (Amici and others 2008; Akay and others 2017). However, only water-soluble compounds are suitable to be encapsulated with the gelation method, because they need to be solubilized along with pectin or alginate. This issue could be possibly resolved by a two-step microencapsulation, such as using a nanoparticle to entrap lipophilic compound first, followed by encapsulation of nanoparticles through in-situ gelation (Ogończyk and others 2011). The microfluidic devices could hence be designed with two functional segments, one to create nanoparticles (Olenskyj and others 2017) and the other one to form hydrogel, so that the encapsulation of lipophilic compound could be accomplished in a continuous process. It is also noteworthy that potato starch, which is capable of gelation due to its high amylose content, can also be used to produce microcapsules when coupled with saponin, a surfactant (Skurtys and Aguilera 2009). This study implied that other starches, which possess high amylose content, might also be candidates to be used in the microfluidic systems.

2.3.4 Lipids

Many solid lipid nanoparticles or nanostructured lipid carriers have been developed with food-grade lipids (Hentschel and others 2008; Gonnet and others 2010; McClements 2010; McClements 2012; Modi and Anderson 2013; Dan 2016), however, to the authors' best knowledge, similar work has not been done on microfluidic chips. Featured by the design versatility and control accuracy of microfluidic devices, it would be possible to produce sophisticated lipid nanoparticles with designated nanosturcutres to achieve various functionalities. Food lipids, such as anhydrous milk fat (Tm, melting temperature, around 37°C), coconut oil (Tm around 25°C) and palm oil (Tm around 35°C) could be good options. In some cases, necessary chemical modification such as cationization (Belliveau and others 2012) may be needed to adjust the polarity of lipids. A recent study reported promising features of lipid-based lyotropic liquid crystals as oral and transdermal delivery carrier (Rajabalaya and others 2017), and such fat crystal may be generated in microfluidics through thermal quenching approach using food-grade lipids (Kim and Vanapalli 2013).

2.4 Challenges and future interests

In spite of many advantages benefited from microfluidic processes, scalability is still the biggest challenge for their production-oriented applications. In the past decade, a considerable effort has been made to increase the yield of microfluidic production. To summarize, there are several classical strategies. One strategy is integration of independent microchannel units, as shown in the figure 2.9 (Han and others 2017). There are three levels of integration, which are from channel to 2-D array, 2-D array to 3-D module, and 3-D module to systems, respectively. As such, a high flow rate combinations (20 ml/min for the dispersed phase, and 80 ml/min for the continuous phase) could be achieved as a result of 80 integrated droplet microfluidic units.

In addition to simple integration of microchannel units, another approach focuses on increasing the number of microchannels on a single chip. A high-density microfluidic chip with thousands of microchannels has been developed (Thorsen and others 2002).

Another challenge could be related to the inhomogeneity of food materials. In conventional top-down processes, the existence of impurity may be a significant issue. However, the inhomogeneity of food materials could be detrimental in microfluidic processes, especially when the raw material is being handled at a very small scale. For instance, a high local concentration of impurities could result in clogging in the microfluidic channels. Furthermore, the impurities could accumulate at microchannels, which alters flow parameters and hydraulic pressure. Those issues may be resolved by a periodical auto-cleaning system, but it will increase the cost in the meantime. Future work is still needed to increase the yield of microfluidic production and avoid clogging during process with a cost-effective approach.

2.5 Conclusions

Assembling food-grade delivery systems in microfluidic platforms is gaining more and more interest. In this review, we discussed the basic principles of microfluidic systems, and categorized five common delivery matrices that have been reported, with food-grade or nonfood-grade materials. Recently, several types of food-grade materials have been successfully applied in microfluidic process, and most of them are carbohydrate-based polyelectrolytes and synthetic polymers. Nevertheless, very few work has been reported using proteins and lipids as building blocks of the structure, which could be a promising future direction. Scalability and reliability have always been issues for the mass production using microfluidics, and future studies could focus more on prevention of clogging during production, especially the when biomaterials are used.

2.6 Tables and figures

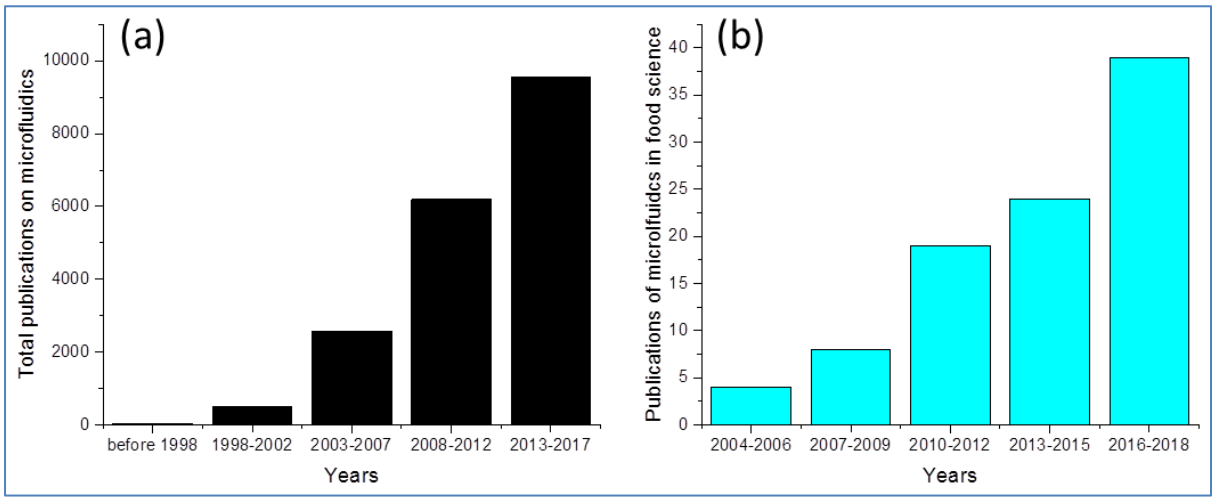

Figure 2.1. Publications per year found in Sci-finder using search terms “microfluidics”. (a) shows the number of publications in all disciplines, and (b) shows the number of publications in food science and technology.

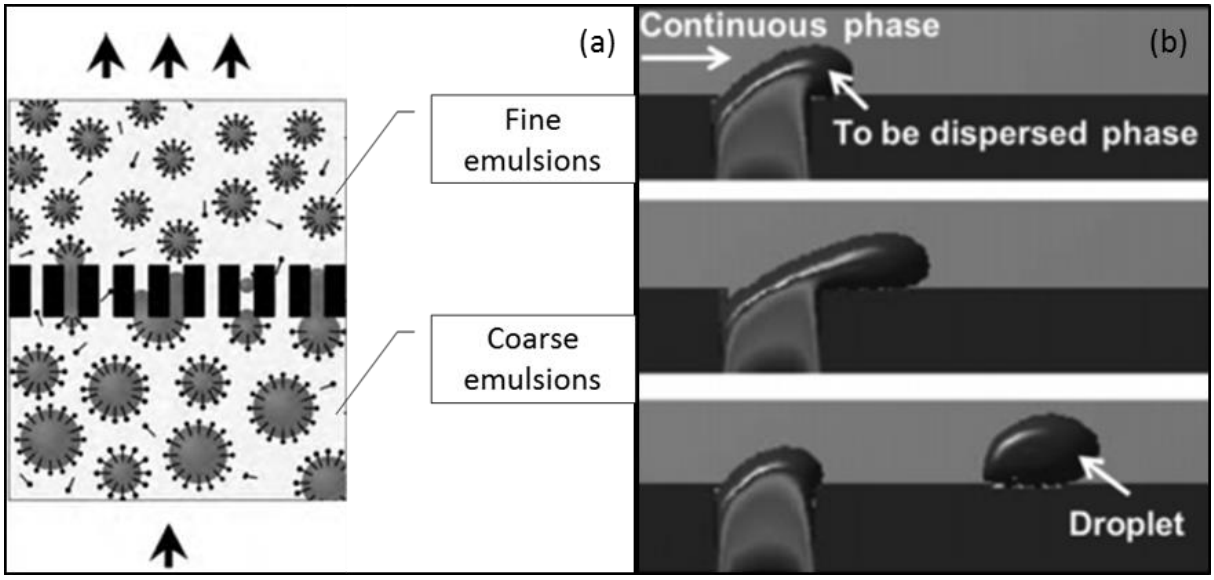

Figure 2.2. Two methods for the droplet formation using microfluidic chips: (a) shear-induced microfluidic emulsification. Reprinted from Journal of Membrane Science, Vol 362, Akmal Nazir,Karin and Schroën,Remko Boom, Premix emulsification: A review, Pages 1-11, Copyright (2010), with permission from Elsevier; (b) Spontaneous microfluidic emulsification. Reprinted with permission from Van der Graaf, S., Nisisako, T., Schroen, C. G. P. H., Van Der Sman, R. G. M., & Boom, R. M. (2006). Lattice Boltzmann simulations of droplet formation in a T-shaped microchannel. Langmuir, 22(9), 4144-4152. Copyright (2006) American Chemical Society.

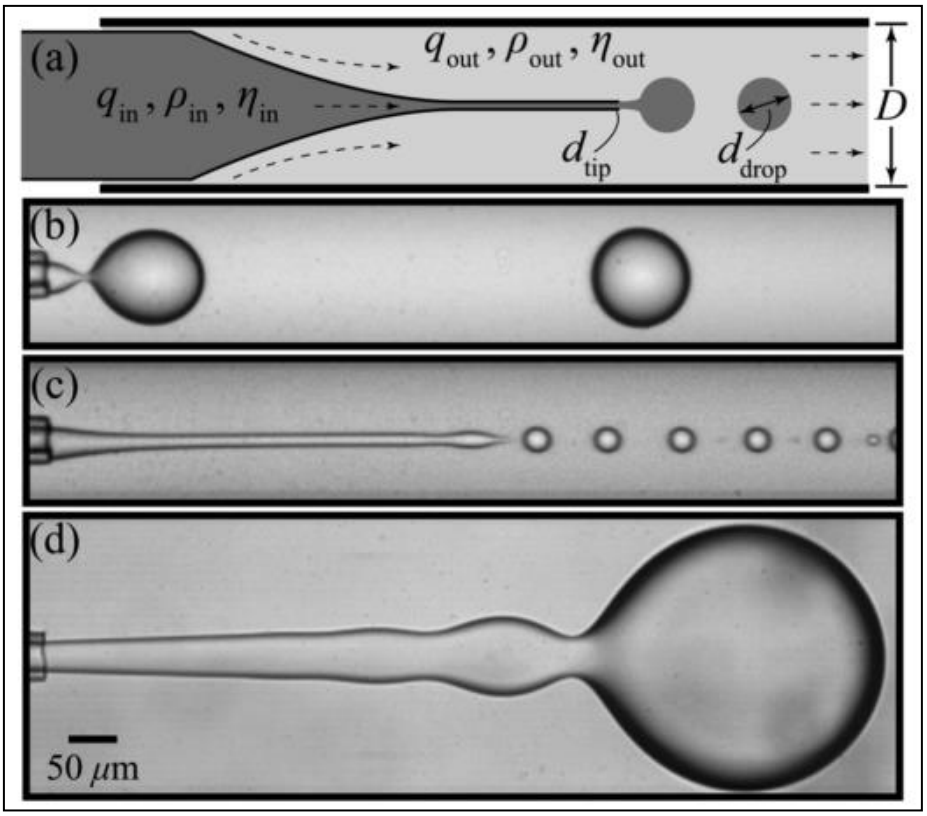

Figure 2.3. Three regimes of droplet formation. Reprinted from Physical Review Letters, Vol 99, Andrew S. Utada et al., Dripping to Jetting Transitions in Coflowing Liquid Streams, Pages 094502, Copyright (2007), with permission from American Physical Society.

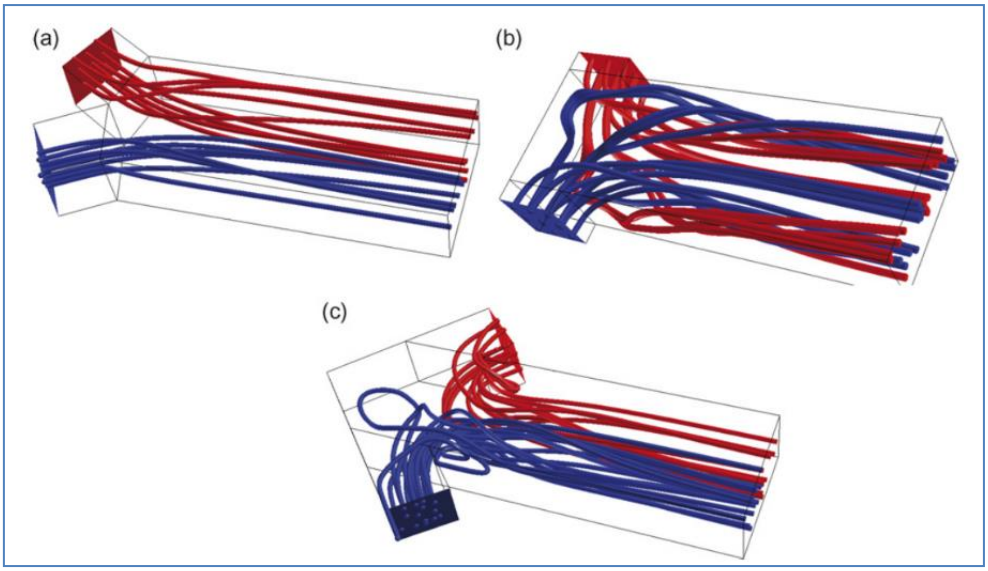

Figure 2.4. The streamline patterns inside of the mixing channel for mixing angles (a) θ =30◦; (b) θ =90◦; and (c) θ =135◦. Colour is used to distinguish between the streams entering the mixing channel from each inlet channel. Reprinted from Chemical Engineering Journal, Vol 135, A. Soleymani, E. Kolehmainen and I. Turunen, Numerical and experimental investigations of liquid mixing in T-type, Pages s219-s228, Copyright (2008), with permission from Elsevier.

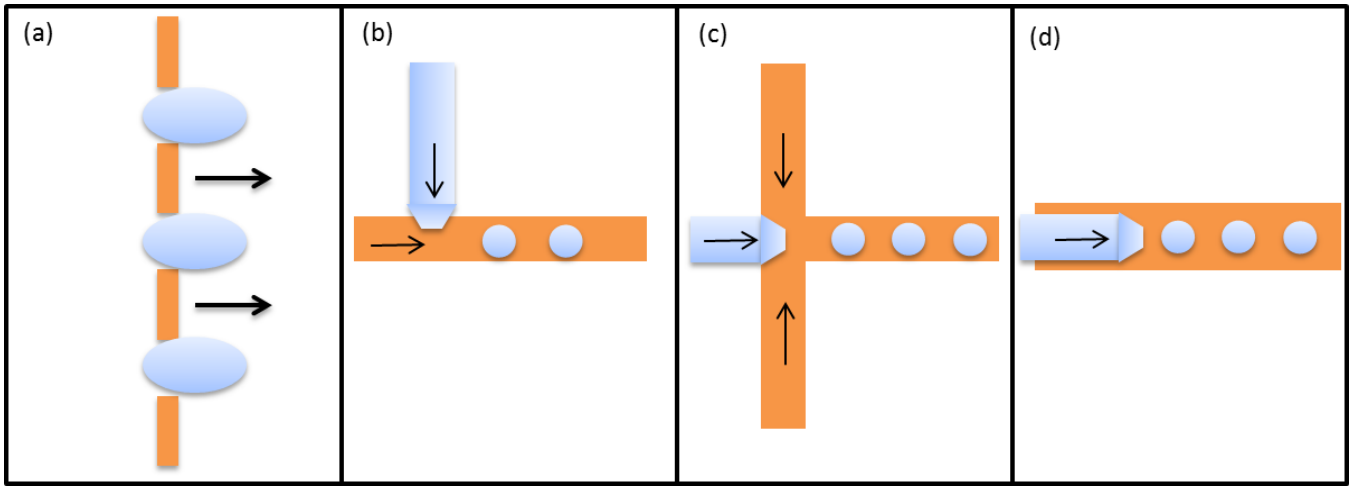

Figure 2.5. Schematic diagram of droplet microfluidic configurations, (a) membrane droplet microfluidics, (b) T-junction droplet microfluidics, (c) flow-focusing droplet microfluidics, and (d) co-flow droplet microfluidics.

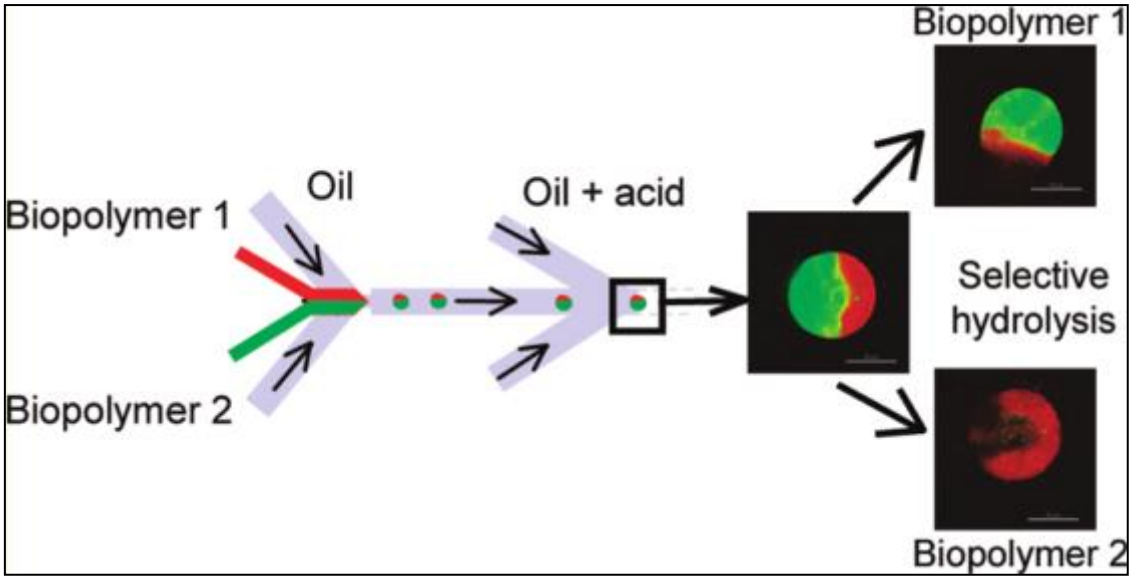

Figure 2.6. An example of fabricating Janus particles in microfluidics. Reprinted with permission from Marquis, M., Renard, D., & Cathala, B. (2012). Microfluidic generation and selective degradation of biopolymer-based Janus microbeads. Biomacromolecules, 13(4), 1197-1203. Copyright (2012) American Chemical Society.

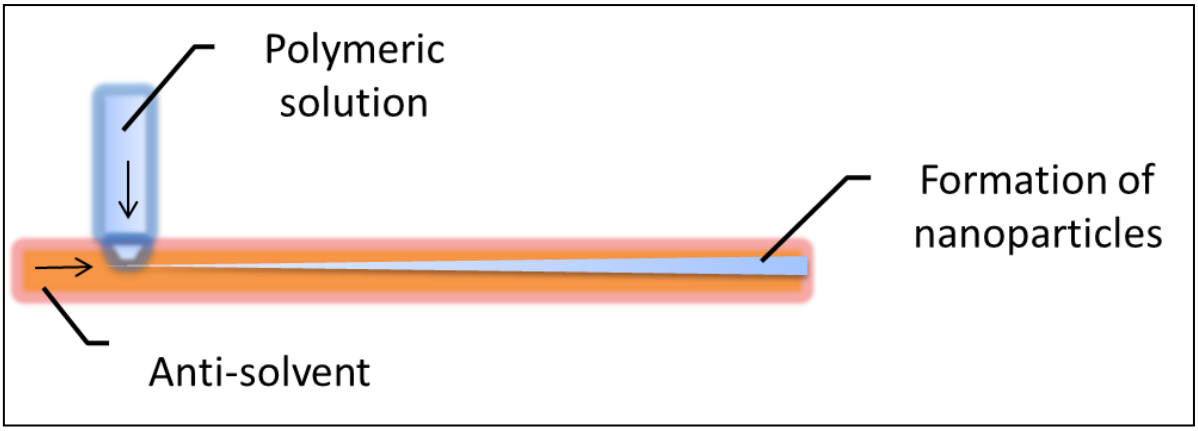

Figure 2.7. A schematic diagram illustrating the generation of polymeric nanoparticles in microfluidics by anti-solvent nanoprecipitation method.

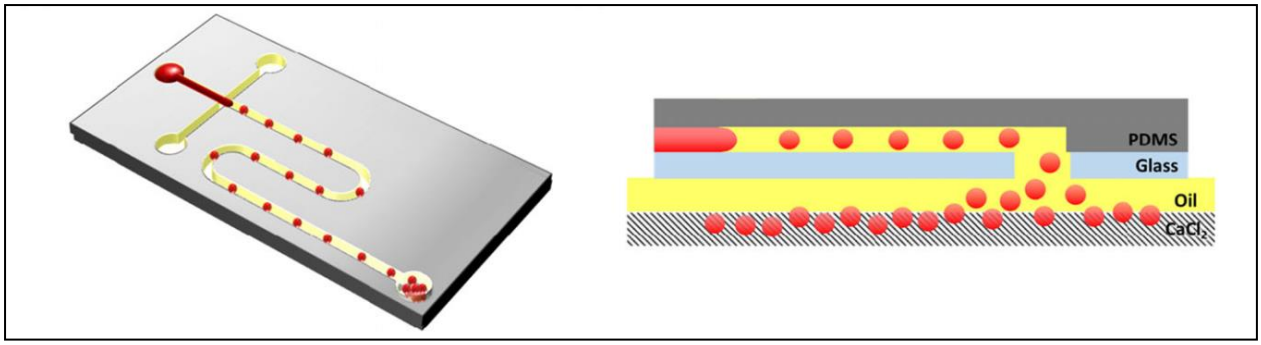

Figure 2.8. Sequential exposure of pectin hydrogel in oil and calcium chloride. Reprinted with permission from Kim, C., Park, K. S., Kim, J., Jeong, S. G., & Lee, C. S. (2017). Microfluidic synthesis of monodisperse pectin hydrogel microspheres based on in situ gelation and settling collection. Journal of Chemical Technology and Biotechnology, 92(1), 201-209. Copyright (2017) John Wiley and Sons.

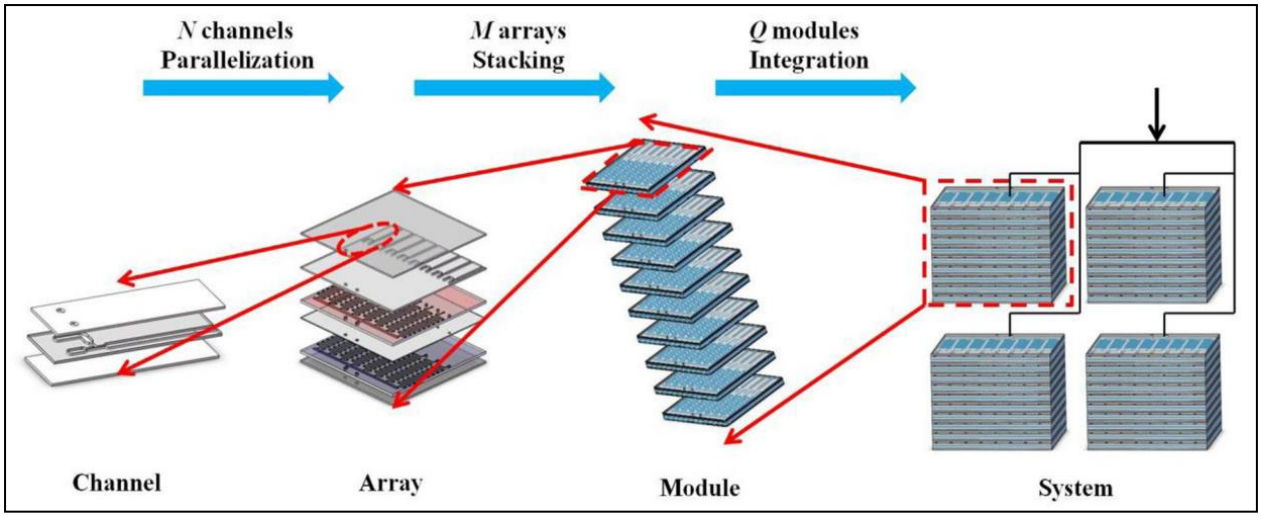

Figure 2.9. Three-dimensional scale up of microfluidic channels. Reprinted from Chemical Engineering Journal, Vol 326, Tengteng Han,Li Zhang,Hong Xu,Jin Xuan, Factory-on-chip: Modularised microfluidic reactors for continuous mass production of functional materials, Pages 765-773, Copyright (2017), with permission from Elsevier.

2.7 References

Abate AR, Weitz DA. 2009. High-order multiple emulsions formed in poly(dimethylsiloxane) microfluidics. Small 5:2030–2032.

Abbaspourrad A, Datta SS, Weitz D a. 2013. Controlling release from pH-responsive microcapsules. Langmuir 29:12697–12702.

Abdallah BG, Roy-Chowdhury S, Fromme R, Fromme P, Ros A. 2016. Protein Crystallization in an Actuated Microfluidic Nanowell Device. Cryst. Growth Des. [Internet] 16:2074–2082. Available from: http://pubs.acs.org/doi/10.1021/acs.cgd.5b01748

Akay S, Heils R, Trieu HK, Smirnova I, Yesil-Celiktas O. 2017. An injectable alginate-based hydrogel for microfluidic applications. Carbohydr. Polym. [Internet] 161:228–234. Available from: http://dx.doi.org/10.1016/j.carbpol.2017.01.004

Akbari S, Pirbodaghi T, Kamm RD, Hammond PT. 2017. A versatile microfluidic device for high throughput production of microparticles and cell microencapsulation. Lab Chip [Internet] 17:2067–2075. Available from: http://xlink.rsc.org/?DOI=C6LC01568A

Alargova RG, Paunov VN, Velev OD. 2006. Formation of polymer microrods in shear flow by emulsification - Solvent attrition mechanism. Langmuir 22:765–774.

Ali HSM, York P, Blagden N. 2009. Preparation of hydrocortisone nanosuspension through a bottom-up nanoprecipitation technique using microfluidic reactors. Int. J. Pharm. [Internet] 375:107–113. Available from: http://linkinghub.elsevier.com/retrieve/pii/S0378517309001732

Amici E, Tetradis-Meris G, de Torres CP, Jousse F. 2008. Alginate gelation in microfluidic channels. Food Hydrocoll. 22:97–104.

Amine C, Boire A, Davy J, Marquis M, Renard D. 2017. Droplets-based millifluidic for the rapid determination of biopolymers phase diagrams. Food Hydrocoll. [Internet] 70:134–142. Available from: http://linkinghub.elsevier.com/retrieve/pii/S0268005X17302023

Belliveau NM, Huft J, Lin PJ, Chen S, Leung AK, Leaver TJ, and others. 2012. Microfluidic synthesis of highly potent limit-size lipid nanoparticles for in vivo delivery of siRNA. Mol. Ther. - Nucleic Acids 1:1–9.

Bhaskara Rao B V., Mukherji R, Shitre G, Alam F, Prabhune AA, Kale SN. 2014. Controlled release of antimicrobial Cephalexin drug from silica microparticles. Mater. Sci. Eng. C

[Internet] 34:9–14. Available from: http://dx.doi.org/10.1016/j.msec.2013.10.002

Binks BP, Rodrigues JA, Frith WJ. 2007. Synergistic interaction in emulsions stabilized by a mixture of silica nanoparticles and cationic surfactant. Langmuir [Internet] 23:3626–36. Available from: http://pubs.acs.org/doi/abs/10.1021/la0634600

BURGESS DJ, SINGH ON. 1993. Spontaneous Formation of Small Sized Albumin/acacia Coacervate Particles. J. Pharm. Pharmacol. 45:586–591.

Calado B, dos Santos A, Semiao V. 2016. Characterization of the mixing regimes of Newtonian fluid flows in asymmetrical T-shaped micromixers. Exp. Therm. Fluid Sci. [Internet] 72:218–227. Available from: http://www.sciencedirect.com/science/article/pii/S0894177715003337

Carrier O, Funfschilling D, Li HZ. 2014. Effect of the fluid injection configuration on droplet size in a microfluidic T junction. Phys. Rev. E - Stat. Nonlinear, Soft Matter Phys. 89:1–6.

Chen FP, Ou S, Tang CH. 2016. Core-shell Soy Protein-Soy Polysaccharide Complex (Nano)particles as Carriers for Improved Stability and Sustained-Release of Curcumin. J Agric Food Chem [Internet]. Available from: http://www.ncbi.nlm.nih.gov/pubmed/27243766

Chen H, Zhang Y, Zhong Q. 2015. Physical and antimicrobial properties of spray-dried zein–casein nanocapsules with co-encapsulated eugenol and thymol. J. Food Eng. [Internet] 144:93–102. Available from: http://linkinghub.elsevier.com/retrieve/pii/S026087741400329X

Chen H, Zhong Q. 2014. Processes improving the dispersibility of spray-dried zein nanoparticles using sodium caseinate. Food Hydrocoll. [Internet] 35:358–366. Available from: http://dx.doi.org/10.1016/j.foodhyd.2013.06.012

Chen J, Zheng J, McClements DJ, Xiao H. 2014. Tangeretin-loaded protein nanoparticles fabricated from zein/β-lactoglobulin: preparation, characterization, and functional performance. Food Chem. [Internet] 158:466–72. Available from: http://www.ncbi.nlm.nih.gov/pubmed/24731371

Chen X, Lee DS, Zhu X, Yam KL. 2012. Release kinetics of tocopherol and quercetin from binary antioxidant controlled-release packaging films. J. Agric. Food Chem. 60:3492–3497.

Coltelli M-B, Wild F, Bugnicourt E, Cinelli P, Lindner M, Schmid M, and others. 2015. State of the Art in the Development and Properties of Protein-Based Films and Coatings and Their Applicability to Cellulose Based Products: An Extensive Review. Coatings [Internet] 6:1. Available from: http://www.mdpi.com/2079-6412/6/1/1/htm

Costa ALR, Gomes A, Ushikubo FY, Cunha RL. 2017. Gellan microgels produced in planar microfluidic devices. J. Food Eng. [Internet] 209:18–25. Available from: http://dx.doi.org/10.1016/j.jfoodeng.2017.04.007

Dan N. 2016. Transport and release in nano-carriers for food applications. J. Food Eng. [Internet] 175:136–144. Available from: http://www.sciencedirect.com/science/article/pii/S026087741530087X

Destribats M, Rouvet M, Gehin-Delval C, Schmitt C, Binks BP. 2014. Emulsions stabilised by whey protein microgel particles: towards food-grade Pickering emulsions. Soft Matter [Internet] 10:6941–54. Available from: http://www.ncbi.nlm.nih.gov/pubmed/24675994

Dickinson E. 2010. Food emulsions and foams: Stabilization by particles. Curr. Opin. Colloid Interface Sci. [Internet] 15:40–49. Available from: http://linkinghub.elsevier.com/retrieve/pii/S1359029409001010

Dickinson E. 2011. Mixed biopolymers at interfaces: Competitive adsorption and multilayer structures. Food Hydrocoll. [Internet] 25:1966–1983. Available from: http://dx.doi.org/10.1016/j.foodhyd.2010.12.001

Dickinson E. 2012. Use of nanoparticles and microparticles in the formation and stabilization of food emulsions. Trends Food Sci. Technol. [Internet] 24:4–12. Available from: http://linkinghub.elsevier.com/retrieve/pii/S0924224411001981

Dickinson E. 2015. Structuring of colloidal particles at interfaces and the relationship to food emulsion and foam stability. J. Colloid Interface Sci. [Internet] 449:38–45. Available from: http://linkinghub.elsevier.com/retrieve/pii/S0021979714007292

Dickinson E, Golding M. 1997. Depletion flocculation of emulsions containing unadsorbed sodium caseinate. Food Hydrocoll. [Internet] 11:13–18. Available from: http://dx.doi.org/10.1016/S0268-005X(97)80005-7

Evers CHJ, Andersson T, Lund M, Skepö M. 2012. Adsorption of unstructured protein β-casein to hydrophobic and charged surfaces. Langmuir 28:11843–11849.

Fang A, Cathala B. 2011. Smart swelling biopolymer microparticles by a microfluidic

approach: Synthesis, in situ encapsulation and controlled release. Colloids Surfaces B Biointerfaces [Internet] 82:81–86. Available from: http://dx.doi.org/10.1016/j.colsurfb.2010.08.020

Feng Y, Lee Y. 2016. Surface modification of zein colloidal particles with sodium caseinate to stabilize oil-in-water pickering emulsion. Food Hydrocoll. [Internet] 56:292–302. Available from: http://linkinghub.elsevier.com/retrieve/pii/S0268005X15301971

Feng Y, Lee Y. 2017. Microfluidic fabrication of hollow protein microcapsules for rate-controlled release. RSC Adv. [Internet] 7:49455–49462. Available from: http://xlink.rsc.org/?DOI=C7RA08645H

de Folter JWJ, van Ruijven MWM, Velikov KP. 2012. Oil-in-water Pickering emulsions stabilized by colloidal particles from the water-insoluble protein zein. Soft Matter [Internet] 8:6807. Available from: http://xlink.rsc.org/?DOI=c2sm07417f

Fu T, Wu Y, Ma Y, Li HZ. 2012. Droplet formation and breakup dynamics in microfluidic flow-focusing devices: From dripping to jetting. Chem. Eng. Sci. [Internet] 84:207–217. Available from: http://dx.doi.org/10.1016/j.ces.2012.08.039

Gach PC, Shih SCC, Sustarich J, Keasling JD, Hillson NJ, Adams PD, and others. 2016. A Droplet Microfluidic Platform for Automating Genetic Engineering. ACS Synth. Biol. 5:426–433.

Gao Z-M, Yang X-Q, Wu N-N, Wang L-J, Wang J-M, Guo J, and others. 2014. Protein-based pickering emulsion and oil gel prepared by complexes of zein colloidal particles and stearate. J. Agric. Food Chem. [Internet] 62:2672–8. Available from: http://www.ncbi.nlm.nih.gov/pubmed/24621373

Ghouchi Eskandar N, Simovic S, Prestidge CA. 2007. Synergistic effect of silica nanoparticles and charged surfactants in the formation and stability of submicron oil-in-water emulsions. Phys. Chem. Chem. Phys. [Internet] 9:6426. Available from: http://www.ncbi.nlm.nih.gov/pubmed/18060160

Golemanov K, Tcholakova S, Kralchevsky P a., Ananthapadmanabhan KP, Lips a. 2006. Latex-particle-stabilized emulsions of anti-bancroft type. Langmuir 22:4968–4977.

Gonnet M, Lethuaut L, Boury F. 2010. New trends in encapsulation of liposoluble vitamins. J. Control. Release [Internet] 146:276–290. Available from: http://dx.doi.org/10.1016/j.jconrel.2010.01.037

Gouin S. 2004. Microencapsulation: Industrial appraisal of existing technologies and trends. Trends Food Sci. Technol. 15:330–347.

Van Der Graaf S, Nisisako T, Schroën CGPH, Van Der Sman RGM, Boom RM. 2006. Lattice Boltzmann simulations of droplet formation in a T-shaped microchannel. Langmuir 22:4144–4152.

Greenfield NJ. 2006. Using circular dichroism spectra to estimate protein secondary structure. Nat. Protoc. [Internet] 1:2876–2890. Available from: http://www.nature.com/nprot/journal/v1/n6/abs/nprot.2006.202.html

Al Haddabi B, Al Lawati HAJ, Suliman FEO. 2017. A comprehensive evaluation of three microfluidic chemiluminescence methods for the determination of the total phenolic contents in fruit juices. Food Chem. [Internet] 214:670–677. Available from: http://dx.doi.org/10.1016/j.foodchem.2016.07.119

Han T, Zhang L, Xu H, Xuan J. 2017. Factory-on-chip: Modularised microfluidic reactors for continuous mass production of functional materials. Chem. Eng. J. [Internet] 326:765–773. Available from: http://dx.doi.org/10.1016/j.cej.2017.06.028

Hansen CL, Skordalakes E, Berger JM, Quake SR. 2002. A robust and scalable microfluidic metering method that allows protein crystal growth by free interface diffusion. Proc. Natl. Acad. Sci. [Internet] 99:16531–16536. Available from: http://www.pnas.org/cgi/doi/10.1073/pnas.262485199

Headen DM, Aubry G, Lu H, García AJ. 2014. Microfluidic-Based Generation of Size-Controlled, Biofunctionalized Synthetic Polymer Microgels for Cell Encapsulation. Adv. Mater. [Internet] 26:3003–3008. Available from: http://doi.wiley.com/10.1002/adma.201304880

Hejazi R, Amiji M. 2003. Chitosan-based gastrointestinal delivery systems. J. Control. Release 89:151–165.

Hentschel A, Gramdorf S, Müller RH, Kurz T. 2008. β-Carotene-Loaded Nanostructured Lipid Carriers. J. Food Sci. [Internet] 73:N1–N6. Available from: http://doi.wiley.com/10.1111/j.1750-3841.2007.00641.x

Ho YP, Grigsby CL, Zhao F, Leong KW. 2011. Tuning physical properties of nanocomplexes through microfluidics-assisted confinement. Nano Lett. 11:2178–2182.

Hoare TR, Kohane DS. 2008. Hydrogels in drug delivery: Progress and challenges. Polymer

(Guildf). [Internet] 49:1993–2007. Available from: http://dx.doi.org/10.1016/j.polymer.2008.01.027

Hoffmann M, Schlüter M, Räbiger N. 2006. Experimental investigation of liquid-liquid mixing in T-shaped micro-mixers using μ-LIF and μ-PIV. Chem. Eng. Sci. 61:2968–2976.

Hu TT, Wang JX, Shen ZG, Chen JF. 2008. Engineering of drug nanoparticles by HGCP for pharmaceutical applications. Particuology 6:239–251.

Huq T, Khan A, Khan R a, Riedl B, Lacroix M. 2013. Encapsulation of probiotic bacteria in biopolymeric system. Crit. Rev. Food Sci. Nutr. [Internet] 53:909–16. Available from: http://www.ncbi.nlm.nih.gov/pubmed/23768183

Jin SH, Jeong H-H, Lee B, Lee SS, Lee C-S. 2015. A programmable microfluidic static droplet array for droplet generation, transportation, fusion, storage, and retrieval. Lab Chip [Internet] 15:3677–3686. Available from: http://xlink.rsc.org/?DOI=C5LC00651A

Karnik R, Gu F, Basto P, Cannizzaro C, Dean L, Kyei-Manu W, and others. 2008. Microfluidic platform for controlled synthesis of polymeric nanoparticles. Nano Lett. [Internet] 8:2906–2912. Available from: http://pubs.acs.org/doi/abs/10.1021/nl801736q

Kashiri M, Cerisuelo JP, Domínguez I, López-Carballo G, Hernández-Muñoz P, Gavara R. 2016. Novel antimicrobial zein film for controlled release of lauroyl arginate (LAE). Food Hydrocoll. 61:547–554.

Katouzian I, Jafari SM. 2016. Nano-encapsulation as a promising approach for targeted delivery and controlled release of vitamins. Trends Food Sci. Technol. [Internet] 53:34–48. Available from: http://dx.doi.org/10.1016/j.tifs.2016.05.002

Kaufman G, Nejati S, Sarfati R, Boltyanskiy R, Loewenberg M, Dufresne ER, and others. 2015. Soft microcapsules with highly plastic shells formed by interfacial polyelectrolyte–nanoparticle complexation. Soft Matter [Internet] 11:7478–7482. Available from: http://xlink.rsc.org/?DOI=C5SM00973A

Khalid N, Kobayashi I, Neves MA, Uemura K, Nakajima M, Nabetani H. 2016. Microchannel emulsification study on formulation and stability characterization of monodisperse oil-in-water emulsions encapsulating quercetin. Food Chem. [Internet] 212:27–34. Available from: http://dx.doi.org/10.1016/j.foodchem.2016.05.154

Kim B, Jeon TY, Oh Y-K, Kim S-H. 2015. Microfluidic Production of Semipermeable Microcapsules by Polymerization-Induced Phase Separation. Langmuir [Internet]

31:6027–6034. Available from: http://pubs.acs.org/doi/abs/10.1021/acs.langmuir.5b01129

Kim B, Lee Y, Lee K, Koh WG. 2009. Immobilization of enzymes within hydrogel microparticles to create optical biosensors for the detection of organophosphorus compounds. Curr. Appl. Phys. [Internet] 9:e225–e228. Available from: http://dx.doi.org/10.1016/j.cap.2009.06.043

Kim C, Park KS, Kim J, Jeong SG, Lee CS. 2017. Microfluidic synthesis of monodisperse pectin hydrogel microspheres based on in situ gelation and settling collection. J. Chem. Technol. Biotechnol. 92:201–209.

Kim J, Vanapalli SA. 2013. Microfluidic production of spherical and nonspherical fat particles by thermal quenching of crystallizable oils. Langmuir 29:12307–12316.

Kim JW, Fernández-Nieves A, Dan N, Utada AS, Marquez M, Weitz D a. 2007. Colloidal assembly route for responsive colloidosomes with tunable permeability. Nano Lett. 7:2876–2880.

Klose D, Siepmann F, Elkharraz K, Krenzlin S, Siepmann J. 2006. How porosity and size affect the drug release mechanisms from PLGA-based microparticles. Int. J. Pharm. 314:198–206.

Koga CC, Andrade JE, Ferruzzi MG, Lee Y. 2015. Stability of Trans-Resveratrol Encapsulated in a Protein Matrix Produced Using Spray Drying to UV Light Stress and Simulated Gastro-Intestinal Digestion. J. Food Sci. [Internet] 81. Available from: http://www.ncbi.nlm.nih.gov/pubmed/26677808

Kozlovskaya V, Kharlampieva E, Drachuk I, Cheng D, Tsukruk V V. 2010. Responsive microcapsule reactors based on hydrogen-bonded tannic acid layer-by-layer assemblies. Soft Matter 6:3596.

De Kruif CG, Weinbreck F, De Vries R. 2004. Complex coacervation of proteins and anionic polysaccharides. Curr. Opin. Colloid Interface Sci. 9:340–349.

Lawton JW. 2004. Plasticizers for Zein: Their Effect on Tensile Properties and Water Absorption of Zein Films. Cereal Chem. 81:1–5.

Lee DS, Yam KL. 2013. Effect of tocopherol loading and diffusivity on effectiveness of antioxidant packaging. CyTA - J. Food [Internet] 11:89–93. Available from: http://www.tandfonline.com/doi/abs/10.1080/19476337.2012.696281

Li B, Jiang Y, Liu F, Chai Z, Li Y, Li Y, and others. 2012. Synergistic effects of whey protein-polysaccharide complexes on the controlled release of lipid-soluble and water-soluble vitamins in W1/O/W2 double emulsion systems. Int. J. Food Sci. Technol. [Internet] 47:248–254. Available from: http://doi.wiley.com/10.1111/j.1365-2621.2011.02832.x

Li J, Hwang I-C, Chen X, Park HJ. 2016. Effects of chitosan coating on curcumin loaded nano-emulsion: study on stability and in vitro digestibility. Food Hydrocoll. [Internet] 60:138–147. Available from: http://www.sciencedirect.com/science/article/pii/S0268005X16300972

Li KK, Zhang X, Huang Q, Yin SW, Yang XQ, Wen QB, and others. 2014. Continuous preparation of zein colloidal particles by Flash NanoPrecipitation (FNP). J. Food Eng. [Internet] 127:103–110. Available from: http://dx.doi.org/10.1016/j.jfoodeng.2013.12.001

Li L, Ismagilov RF. 2010. Protein Crystallization Using Microfluidic Technologies Based on Valves, Droplets, and SlipChip. Annu. Rev. Biophys. [Internet] 39:139–158. Available from: http://www.annualreviews.org/doi/10.1146/annurev.biophys.050708.133630

Li M, Joung D, Hughes B, Waldman SD, Kozinski JA, Hwang DK. 2016. Wrinkling Non-Spherical Particles and Its Application in Cell Attachment Promotion. Sci. Rep. [Internet] 6:30463. Available from: http://www.nature.com/articles/srep30463

Liang H-N, Tang C. 2014. Pea protein exhibits a novel Pickering stabilization for oil-in-water emulsions at pH 3.0. LWT - Food Sci. Technol. [Internet] 58:463–469. Available from: http://linkinghub.elsevier.com/retrieve/pii/S002364381400173X

Liu EY, Jung S, Weitz DA, Yi H, Choi C-H. 2018. High-throughput double emulsion-based microfluidic production of hydrogel microspheres with tunable chemical functionalities toward biomolecular conjugation. Lab Chip [Internet] 18:323–334. Available from: http://xlink.rsc.org/?DOI=C7LC01088E

Liu F, Tang C-H. 2013. Soy protein nanoparticle aggregates as pickering stabilizers for oil-in-water emulsions. J. Agric. Food Chem. [Internet] 61:8888–98. Available from: http://www.ncbi.nlm.nih.gov/pubmed/23977961

Liu F, Tang C-H. 2015. Soy glycinin as food-grade Pickering stabilizers: Part. I. Structural characteristics, emulsifying properties and adsorption/arrangement at interface. Food Hydrocoll. [Internet]:1–14. Available from:

http://linkinghub.elsevier.com/retrieve/pii/S0268005X15001897

Liu F, Tang C-H. 2016. Soy glycinin as food-grade Pickering stabilizers: Part. III. Fabrication of gel-like emulsions and their potential as sustained-release delivery systems for β-carotene. Food Hydrocoll. [Internet] 56:434–444. Available from: http://linkinghub.elsevier.com/retrieve/pii/S0268005X16300029

Liu F, Tang CH. 2014. Emulsifying properties of soy protein nanoparticles: Influence of the protein concentration and/or emulsification process. J. Agric. Food Chem. [Internet] 62:2644–2654. Available from: http://pubs.acs.org/doi/abs/10.1021/jf405348k

Liu H, Gu X, Hu M, Hu Y, Wang C. 2014. Facile fabrication of nanocomposite microcapsules by combining layer-by-layer self-assembly and Pickering emulsion templating. RSC Adv. [Internet] 4:16751. Available from: http://xlink.rsc.org/?DOI=c4ra00089g

Luo Y, Pan K, Zhong Q. 2015. Casein/pectin nanocomplexes as potential oral delivery vehicles. Int. J. Pharm. [Internet] 486:59–68. Available from: http://dx.doi.org/10.1016/j.ijpharm.2015.03.043

Luo Y, Wang Q. 2014. Recent development of chitosan-based polyelectrolyte complexes with natural polysaccharides for drug delivery. Int. J. Biol. Macromol. [Internet] 64:353–367. Available from: http://linkinghub.elsevier.com/retrieve/pii/S0141813013006673

Luo Y, Zhang B, Whent M, Yu LL, Wang Q. 2011. Preparation and characterization of zein/chitosan complex for encapsulation of α-tocopherol, and its in vitro controlled release study. Colloids Surfaces B Biointerfaces [Internet] 85:145–152. Available from: http://www.ncbi.nlm.nih.gov/pubmed/21440424

Ma L, Nilghaz A, Choi JR, Liu X, Lu X. 2018. Rapid detection of clenbuterol in milk using microfluidic paper-based ELISA. Food Chem. [Internet] 246:437–441. Available from: https://doi.org/10.1016/j.foodchem.2017.12.022

Maan AA, Nazir A, Khan MKI, Boom R, Schroën K. 2015. Microfluidic emulsification in food processing. J. Food Eng. [Internet] 147:1–7. Available from: http://linkinghub.elsevier.com/retrieve/pii/S0260877414003896

Maan AA, Schroën K, Boom R. 2011. Spontaneous droplet formation techniques for monodisperse emulsions preparation - Perspectives for food applications. J. Food Eng. [Internet] 107:334–346. Available from: http://dx.doi.org/10.1016/j.jfoodeng.2011.07.008

Maeki M, Teshima Y, Yoshizuka S, Yamaguchi H, Yamashita K, Miyazaki M. 2014. Controlling protein crystal nucleation by droplet-based microfluidics. Chem. - A Eur. J. 20:1049–1056.

Maeki M, Yamaguchi H, Tokeshi M, Miyazaki M. 2016. Microfluidic Approaches for Protein Crystal Structure Analysis. Anal. Sci. 32:3–9.

Maeki M, Yamazaki S, Pawate AS, Ishida A, Tani H, Yamashita K, and others. 2016. A microfluidic-based protein crystallization method in 10 micrometer-sized crystallization space. CrystEngComm [Internet] 18:7722–7727. Available from: http://xlink.rsc.org/?DOI=C6CE01671E

Mak WC, Cheung KY, Trau D. 2008. Influence of different polyelectrolytes on layer-by-layer microcapsule properties: Encapsulation efficiency and colloidal and temperature stability. Chem. Mater. 20:5475–5484.

Mark D, Haeberle S, Roth G, von Stetten F, Zengerle R. 2010. Microfluidic lab-on-a-chip platforms: requirements, characteristics and applications. Chem. Soc. Rev. [Internet] 39:1153. Available from: http://xlink.rsc.org/?DOI=b820557b

Marquis M, Renard D, Cathala B. 2012. Microfluidic generation and selective degradation of biopolymer-based Janus microbeads. Biomacromolecules 13:1197–1203.

Marra F, De Vivo A, Sarghini F. 2017. Virtualization of fluid-dynamics in micro-air assisted extruders for food microfluidic based encapsulation. J. Food Eng. 213:89–98.

Marsanasco M, Márquez AL, Wagner JR, del V. Alonso S, Chiaramoni NS. 2011. Liposomes as vehicles for vitamins E and C: An alternative to fortify orange juice and offer vitamin C protection after heat treatment. Food Res. Int. [Internet] 44:3039–3046. Available from: http://dx.doi.org/10.1016/j.foodres.2011.07.025

Mcclements DJ. 2015. Nanoscale Nutrient Delivery Systems for Food Applications: Improving Bioactive Dispersibility, Stability, and Bioavailability. J. Food Sci. 80:N1602–N1611.

McClements DJ. 2010. Emulsion Design to Improve the Delivery of Functional Lipophilic Components. Annu. Rev. Food Sci. Technol. 1:241–269.

McClements DJ. 2012. Advances in fabrication of emulsions with enhanced functionality using structural design principles. Curr. Opin. Colloid Interface Sci. [Internet] 17:235–245. Available from: http://linkinghub.elsevier.com/retrieve/pii/S1359029412000702

Mijatovic D, Eijkel JCT, van den Berg a. 2005. Technologies for nanofluidic systems: top-down vs. bottom-up--a review. Lab Chip [Internet] 5:492–500. Available from: http://www.ncbi.nlm.nih.gov/pubmed/15856084

Modi S, Anderson BD. 2013. Determination of drug release kinetics from nanoparticles: Overcoming pitfalls of the dynamic dialysis method. Mol. Pharm. 10:3076–3089.

Morais JM, Burgess DJ. 2014. In vitro release testing methods for vitamin E nanoemulsions. Int. J. Pharm. [Internet] 475:393–400. Available from: http://dx.doi.org/10.1016/j.ijpharm.2014.08.063

Muijlwijk K, Colijn I, Harsono H, Krebs T, Berton-Carabin C, Schroën K. 2017. Coalescence of protein-stabilised emulsions studied with microfluidics. Food Hydrocoll. 70:96–104.

Nabavi SA, Vladisavljević GT, Gu S, Ekanem EE. 2015. Double emulsion production in glass capillary microfluidic device: Parametric investigation of droplet generation behaviour. Chem. Eng. Sci. [Internet] 130:183–196. Available from: http://linkinghub.elsevier.com/retrieve/pii/S0009250915001736

Naseri N, Valizadeh H, Zakeri-Milani P. 2015. Solid lipid nanoparticles and nanostructured lipid carriers: Structure preparation and application. Adv. Pharm. Bull. [Internet] 5:305–313. Available from: http://dx.doi.org/10.15171/apb.2015.043

Nazir A, Schroën K, Boom R. 2010. Premix emulsification: A review. J. Memb. Sci. [Internet] 362:1–11. Available from: http://dx.doi.org/10.1016/j.memsci.2010.06.044

Nel AE, Mädler L, Velegol D, Xia T, Hoek EM V, Somasundaran P, and others. 2009. Understanding biophysicochemical interactions at the nano-bio interface. Nat. Mater. [Internet] 8:543–557. Available from: http://dx.doi.org/10.1038/nmat2442

Nesterenko A, Drelich A, Lu H, Clausse D, Pezron I. 2014. Influence of a mixed particle/surfactant emulsifier system on water-in-oil emulsion stability. Colloids Surfaces A Physicochem. Eng. Asp. [Internet] 457:49–57. Available from: http://linkinghub.elsevier.com/retrieve/pii/S0927775714004944

Nie Z, Li W, Seo M, Xu S, Kumacheva E. 2006. Janus and ternary particles generated by microfluidic synthesis: Design, synthesis, and self-assembly. J. Am. Chem. Soc. 128:9408–9412.

Nisisako T. 2016. Recent advances in microfluidic production of Janus droplets and particles. Curr. Opin. Colloid Interface Sci. [Internet] 25:1–12. Available from:

http://dx.doi.org/10.1016/j.cocis.2016.05.003

Nisisako T, Torii T, Takahashi T, Takizawa Y. 2006. Synthesis of monodisperse bicolored janus particles with electrical anisotropy using a microfluidic co-flow system. Adv. Mater. 18:1152–1156.

Niu F, Zhou J, Niu D, Wang C, Liu Y, Su Y, and others. 2015. Food Hydrocolloids Synergistic effects of ovalbumin / gum arabic complexes on the stability of emulsions exposed to environmental stress. Food Hydrocoll. [Internet] 47:14–20. Available from: http://dx.doi.org/10.1016/j.foodhyd.2015.01.002

Ogończyk D, Siek M, Garstecki P. 2011. Microfluidic formulation of pectin microbeads for encapsulation and controlled release of nanoparticles. Biomicrofluidics 5:1–12.

Oh JK, Drumright R, Siegwart DJ, Matyjaszewski K. 2008. The development of microgels/nanogels for drug delivery applications. Prog. Polym. Sci. 33:448–477.

Olenskyj AG, Feng Y, Lee Y. 2017. Continuous microfluidic production of zein nanoparticles and correlation of particle size with physical parameters determined using CFD simulation. J. Food Eng. [Internet] 211:50–59. Available from: http://linkinghub.elsevier.com/retrieve/pii/S0260877417301668

Oscar SV, Fernando OCL, del Pilar CMM. 2017. Total polyphenols content in white wines on a microfluidic flow injection analyzer with embedded optical fibers. Food Chem. [Internet] 221:1062–1068. Available from: http://dx.doi.org/10.1016/j.foodchem.2016.11.055

Othman R, Vladisavljević GT, Hemaka Bandulasena HC, Nagy ZK. 2015. Production of polymeric nanoparticles by micromixing in a co-flow microfluidic glass capillary device. Chem. Eng. J. [Internet] 280:316–329. Available from: http://linkinghub.elsevier.com/retrieve/pii/S1385894715007718

Ozturk B, Argin S, Ozilgen M, McClements DJ. 2014. Formation and stabilization of nanoemulsion-based vitamin E delivery systems using natural surfactants: Quillaja saponin and lecithin. J. Food Eng. [Internet] 142:57–63. Available from: http://dx.doi.org/10.1016/j.jfoodeng.2014.06.015

Pan K, Chen H, Davidson PM, Zhong Q. 2014. Thymol nanoencapsulated by sodium caseinate: Physical and antilisterial properties. J. Agric. Food Chem. 62:1649–1657.

Pan K, Luo Y, Gan Y, Baek SJ, Zhong Q. 2014. pH-driven encapsulation of curcumin in self-

assembled casein nanoparticles for enhanced dispersibility and bioactivity. Soft Matter [Internet] 10:6820. Available from: http://dx.doi.org/10.1039/C4SM00239C

Pan K, Zhong Q, Baek SJ. 2013. Enhanced dispersibility and bioactivity of curcumin by encapsulation in casein nanocapsules. J. Agric. Food Chem. 61:6036–6043.

Pan X, Mercadé-Prieto R, York D, Preece J a, Zhang Z. 2013. Structure and Mechanical Properties of Consumer-Friendly PMMA Microcapsules. Ind. Eng. Chem. Res. [Internet] 52:11253–11265. Available from: http://pubs.acs.org/doi/abs/10.1021/ie303451s%5Cnhttp://pubs.acs.org/doi/pdf/10.1021/ie303451s%5Cnhttp://dx.doi.org/10.1021/ie303451s

Pan Y, Tikekar R V., Wang MS, Avena-Bustillos RJ, Nitin N. 2014. Effect of barrier properties of zein colloidal particles and oil-in-water emulsions on oxidative stability of encapsulated bioactive compounds. Food Hydrocoll. [Internet] 43:82–90. Available from: http://dx.doi.org/10.1016/j.foodhyd.2014.05.002

Park KS, Kim C, Nam JO, Kang SM, Lee CS. 2016. Synthesis and characterization of thermosensitive gelatin hydrogel microspheres in a microfluidic system. Macromol. Res. 24:529–536.

Patel A, Hu Y, Tiwari JK, Velikov KP. 2010. Synthesis and characterisation of zein–curcumin colloidal particles. Soft Matter [Internet] 6:6192. Available from: http://xlink.rsc.org/?DOI=c0sm00800a

Patel AR, Bouwens ECM, Velikov KP. 2010. Sodium caseinate stabilized zein colloidal particles. J. Agric. Food Chem. [Internet] 58:12497–503. Available from: http://www.ncbi.nlm.nih.gov/pubmed/21077613

Pessoa ACSN, Sipoli CC, de la Torre LG. 2017. Effects of diffusion and mixing pattern on microfluidic-assisted synthesis of chitosan/ATP nanoparticles. Lab Chip [Internet] 17:2281–2293. Available from: http://xlink.rsc.org/?DOI=C7LC00291B

Qi F, Wu J, Sun G, Nan F, Ngai T, Ma G. 2014. Systematic studies of Pickering emulsions stabilized by uniform-sized PLGA particles: preparation and stabilization mechanism. J. Mater. Chem. B [Internet] 2:7605–7611. Available from: http://dx.doi.org/10.1039/C4TB01165A

Qian YC, Chen PC, He GJ, Huang XJ, Xu ZK. 2014. Preparation of polyphosphazene hydrogels for enzyme immobilization. Molecules 19:9850–9863.

Rajabalaya R, Musa MN, Kifli N, David SR. 2017. Oral and transdermal drug delivery systems: Role of lipid-based lyotropic liquid crystals. Drug Des. Devel. Ther. 11:393–406.

Rajan SS, Cavera VL, Zhang X, Singh Y, Chikindas ML, Sinko PJ. 2014. Polyethylene glycol-based hydrogels for controlled release of the antimicrobial subtilosin for prophylaxis of bacterial vaginosis. Antimicrob. Agents Chemother. 58:2747–2753.

Ravanfar R, Comunian TA, Dando R, Abbaspourrad A. 2018. Optimization of microcapsules shell structure to preserve labile compounds: A comparison between microfluidics and conventional homogenization method. Food Chem. [Internet] 241:460–467. Available from: http://dx.doi.org/10.1016/j.foodchem.2017.09.023

Rossier-Miranda FJ, Schroën CGPH, Boom RM. 2009. Colloidosomes: Versatile microcapsules in perspective. Colloids Surfaces A Physicochem. Eng. Asp. 343:43–49.

Rossier-Miranda FJ, Schroën K, Boom R. 2012. Microcapsule production by an hybrid colloidosome-layer-by-layer technique. Food Hydrocoll. [Internet] 27:119–125. Available from: http://dx.doi.org/10.1016/j.foodhyd.2011.08.007

Ruiz-Rodriguez PE, Meshulam D, Lesmes U. 2014. Characterization of Pickering O/W Emulsions Stabilized by Silica Nanoparticles and Their Responsiveness to In vitro Digestion Conditions. Food Biophys.:406–415.

Saldanha do Carmo C, Maia C, Poejo J, Lychko I, Gamito P, Nogueira I, and others. 2017. Microencapsulation of α-tocopherol with zein and β-cyclodextrin using spray drying for colour stability and shelf-life improvement of fruit beverages. RSC Adv. [Internet] 7:32065–32075. Available from: http://xlink.rsc.org/?DOI=C6RA25946D

San-Miguel A, Behrens SH. 2012. Influence of nanoscale particle roughness on the stability of pickering emulsions. Langmuir 28:12038–12043.

Schloss AC, Liu W, Williams DM, Kaufman G, Hendrickson HP, Rudshteyn B, and others. 2016. Fabrication of Modularly Functionalizable Microcapsules Using Protein-Based Technologies. ACS Biomater. Sci. Eng. 2:1856–1861.

Schwarz C, Mehnert W, Lucks JS, Müller RH. 1994. Solid lipid nanoparticles (SLN) for controlled drug delivery. I. Production, characterization and sterilization. J. Control. Release [Internet] 30:83–96. Available from: http://www.sciencedirect.com/science/article/pii/0168365994900477

Shchepelina O, Lisunova MO, Drachuk I, Tsukruk V V. 2012. Morphology and properties of

microcapsules with different core releases. Chem. Mater. 24:1245–1254.

Shit SC, Shah PM. 2014. Edible Polymers: Challenges and Opportunities. J. Polym. [Internet] 2014:1–13. Available from: http://www.hindawi.com/journals/jpol/2014/427259/

Shum HC, Abate AR, Lee D, Studart AR, Wang B, Chen CH, and others. 2010. Droplet microfluidics for fabrication of non-spherical particles. Macromol. Rapid Commun. 31:108–118.

Skurtys O, Aguilera JM. 2009. Formation of O/W macroemulsions with a circular microfluidic device using saponin and potato starch. Food Hydrocoll. [Internet] 23:1810–1817. Available from: http://dx.doi.org/10.1016/j.foodhyd.2009.01.014

Soleymani A, Kolehmainen E, Turunen I. 2007. Numerical and experimental investigations of liquid mixing in T-type micromixers. Chem. Eng. J. 135.

Steegmans MLJ, Schroën KGPH, Boom RM. 2009. Characterization of emulsification at flat microchannel y junctions. Langmuir 25:3396–3401.

Subramaniam AB, Abkarian M, Stone H a. 2005. Controlled assembly of jammed colloidal shells on fluid droplets. Nat. Mater. 4:553–556.

Sugiura S, Nakajima M, Iwamoto S, Seki M. 2001. Interfacial tension driven monodispersed droplet formation from microfabricated channel array. Langmuir 17:5562–5566.

Svensson O, Kurut A, Skepö M. 2014. Adsorption of β-casein to hydrophilic silica surfaces. Effect of pH and electrolyte. Food Hydrocoll. 36:332–338.

Tan C, Nakajima M. 2005. β-Carotene nanodispersions: preparation, characterization and stability evaluation. Food Chem. [Internet] 92:661–671. Available from: http://linkinghub.elsevier.com/retrieve/pii/S0308814604006727

Tavares GM, Croguennec T, Carvalho AF, Bouhallab S. 2014. Milk proteins as encapsulation devices and delivery vehicles: Applications and trends. Trends Food Sci. Technol. [Internet] 37:5–20. Available from: http://linkinghub.elsevier.com/retrieve/pii/S0924224414000454

Tcholakova S, Denkov ND, Banner T. 2004. Role of surfactant type and concentration for the mean drop size during emulsification in turbulent flow. Langmuir 20:7444–7458.

Tcholakova S, Denkov ND, Ivanov IB, Campbell B. 2002. Coalescence in beta-Lactoglobulin-Stabilized Emulsions : Effects of Protein Adsorption and Drop Size. Langmuir 18:8960–

8971.

Tcholakova S, Denkov ND, Ivanov IB, Campbell B. 2006. Coalescence stability of emulsions containing globular milk proteins. Adv. Colloid Interface Sci. 123–126:259–293.

Tcholakova S, Denkov ND, Lips A. 2008. Comparison of solid particles, globular proteins and surfactants as emulsifiers. Phys. Chem. Chem. Phys. [Internet] 10:1608–27. Available from: http://www.ncbi.nlm.nih.gov/pubmed/18060160

Tcholakova S, Denkov ND, Sidzhakova D, Ivanov IB, Campbell B. 2003. Interrelation between drop size and protein adsorption at various emulsification conditions. Langmuir 19:5640–5649.

Teh S-Y, Lin R, Hung L-H, Lee AP. 2008. Droplet microfluidics. Lab Chip [Internet] 8:198. Available from: http://xlink.rsc.org/?DOI=b715524g

Thomar P, Nicolai T. 2015. Dissociation of native casein micelles induced by sodium caseinate. Food Hydrocoll. [Internet]. Available from: http://dx.doi.org/10.1016/j.foodhyd.2015.03.016

Thorsen T, Maerkl SJ, Quake SR. 2002. Microfluidic Large-Scale Integration. Science (80-.). 298:5593.

Thorsen T, Roberts RW, Arnold FH, Quake SR. 2001. Dynamic pattern formation in a vesicle-generating microfluidic device. Phys. Rev. Lett. 86:4163–4166.

Tian ZH, Xu JH, Wang YJ, Luo GS. 2016. Microfluidic synthesis of monodispersed CdSe quantum dots nanocrystals by using mixed fatty amines as ligands. Chem. Eng. J. [Internet] 285:20–26. Available from: http://dx.doi.org/10.1016/j.cej.2015.09.104

Tikekar R V., Pan Y, Nitin N. 2013. Fate of curcumin encapsulated in silica nanoparticle stabilized Pickering emulsion during storage and simulated digestion. Food Res. Int. [Internet] 51:370–377. Available from: http://dx.doi.org/10.1016/j.foodres.2012.12.027

Tippetts M, Martini S, Brothersen C, McMahon DJ. 2012. Fortification of cheese with vitamin D3 using dairy protein emulsions as delivery systems. J. Dairy Sci. [Internet] 95:4768–74. Available from: http://www.sciencedirect.com/science/article/pii/S0022030212004900%5Cnhttp://www.ncbi.nlm.nih.gov/pubmed/22916880

Tsui JH, Lee W, Pun SH, Kim J, Kim DH. 2013. Microfluidics-assisted in vitro drug screening

and carrier production. Adv. Drug Deliv. Rev. 65:1575–1588.

Turovsky T, Khalfin R, Kababya S, Schmidt A, Barenholz Y, Danino D. 2015. Celecoxib Encapsulation in ??-Casein Micelles: Structure, Interactions, and Conformation. Langmuir 31:7183–7192.

Utada AS, Fernandez-Nieves A, Stone HA, Weitz DA. 2007. Dripping to Jetting Transitions in Coflowing Liquid Streams. Phys. Rev. Lett. [Internet] 99:94502. Available from: http://link.aps.org/doi/10.1103/PhysRevLett.99.094502

Veiga AS, Schneider JP. 2013. Antimicrobial hydrogels for the treatment of infection. Biopolymers 100:637–644.

Vilanova N, Solans C. 2015. Vitamin A Palmitate–β-cyclodextrin inclusion complexes: Characterization, protection and emulsification properties. Food Chem. [Internet] 175:529–535. Available from: http://dx.doi.org/10.1016/j.foodchem.2014.12.015

Vladisavljević GT. 2015. Structured microparticles with tailored properties produced by membrane emulsification. Adv. Colloid Interface Sci. [Internet] 225:53–87. Available from: http://linkinghub.elsevier.com/retrieve/pii/S000186861500144X

Vonasek E, Le P, Nitin N. 2014. Encapsulation of bacteriophages in whey protein films for extended storage and release. Food Hydrocoll. [Internet] 37:7–13. Available from: http://dx.doi.org/10.1016/j.foodhyd.2013.09.017

Wang L-J, Hu Y-Q, Yin S-W, Yang X-Q, Lai F-R, Wang S-Q. 2015. Fabrication and Characterization of Antioxidant Pickering Emulsions Stabilized by Zein/Chitosan Complex Particles (ZCPs). J. Agric. Food Chem. [Internet] 63:2514–2524. Available from: http://pubs.acs.org/doi/abs/10.1021/jf505227a

Wang LJ, Yin YC, Yin SW, Yang XQ, Shi WJ, Tang CH, and others. 2013. Development of novel zein-sodium caseinate nanoparticle (ZP)-stabilized emulsion films for improved water barrier properties via emulsion/solvent evaporation. J. Agric. Food Chem. [Internet] 61:11089–11097. Available from: http://pubs.acs.org/doi/full/10.1021/jf4029943

Wang W, Zhang MJ, Chu LY. 2014. Functional polymeric microparticles engineered from controllable microfluidic emulsions. Acc. Chem. Res. 47:373–384.

Wang Y, Padua GW. 2010. Formation of zein microphases in ethanol-water. Langmuir 26:12897–12901.

Wang Y, Padua GW. 2012. Nanoscale characterization of zein self-assembly. Langmuir 28:2429–2435.

Wassén S, Rondeau E, Sott K, Lorén N, Fischer P, Hermansson AM. 2012. Microfluidic production of monodisperse biopolymer particles with reproducible morphology by kinetic control. Food Hydrocoll. [Internet] 28:20–27. Available from: http://dx.doi.org/10.1016/j.foodhyd.2011.11.004

Weiss M, Frohnmayer JP, Benk LT, Haller B, Heitkamp T, Börsch M, and others. 2017. Sequential Bottom-up Assembly of Synthetic Cells. Nat. Mater.

Whitesides GM. 2006. The origins and the future of microfluidics. Nature [Internet] 442:368–73. Available from: http://www.ncbi.nlm.nih.gov/pubmed/16871203

Workman VL, Dunnett SB, Kille P, Palmer DD. 2008. On-chip alginate microencapsulation of functional cells. Macromol. Rapid Commun. 29:165–170.

Wu J, Shi M, Li W, Zhao L, Wang Z, Yan X, and others. 2015. Pickering emulsions stabilized by whey protein nanoparticles prepared by thermal cross-linking. Colloids Surfaces B Biointerfaces [Internet] 127:96–104. Available from: http://linkinghub.elsevier.com/retrieve/pii/S0927776515000363

Yang Y, Decker EA, Xiao H, McClements DJ. 2015. Enhancing vitamin E bioaccessibility: factors impacting solubilization and hydrolysis of α-tocopherol acetate encapsulated in emulsion-based delivery systems. Food Funct. [Internet] 6:83–96. Available from: http://pubs.rsc.org/en/content/articlehtml/2015/fo/c4fo00725e

Yao M, Xiao H, McClements DJ. 2014. Delivery of Lipophilic Bioactives: Assembly, Disassembly, and Reassembly of Lipid Nanoparticles. Annu. Rev. Food Sci. Technol. Vol 5 5:53–81.

Ye A. 2008. Interfacial composition and stability of emulsions made with mixtures of commercial sodium caseinate and whey protein concentrate. Food Chem. 110:946–952.

Yi J, Fan Y, Zhang Y, Zhao L. 2016. Characterization of catechin-α-lactalbumin conjugates and the improvement in β-carotene retention in an oil-in-water nanoemulsion. Food Chem. [Internet] 205:73–80. Available from: http://dx.doi.org/10.1016/j.foodchem.2016.03.005

Yow HN, Routh AF. 2006. Formation of liquid core-polymer shell microcapsules. Soft Matter 2:940.

Yuan Q, Williams R a. 2014. Precision emulsification for droplet and capsule production. Adv. Powder Technol. [Internet] 25:122–135. Available from: http://dx.doi.org/10.1016/j.apt.2013.10.006

Yun J, Zhang S, Shen S, Chen Z, Yao K, Chen J. 2009. Continuous production of solid lipid nanoparticles by liquid flow-focusing and gas displacing method in microchannels. Chem. Eng. Sci. [Internet] 64:4115–4122. Available from: http://dx.doi.org/10.1016/j.ces.2009.06.047

Zhang H, Tumarkin E, Sullan RMA, Walker GC, Kumacheva E. 2007. Exploring microfluidic routes to microgels of biological polymers. Macromol. Rapid Commun. 28:527–538.

Zhang J, Coulston RJ, Jones ST, Geng J, Scherman O a, Abell C. 2012. One-Step Fabrication of Supramolecular Microcapsules from Microfluidic Droplets. Science (80-.). [Internet] 335:690–694. Available from: http://www.ncbi.nlm.nih.gov/pubmed/22323815

Zhang J, Grzybowski BA, Granick S. 2017. Janus Particle Synthesis, Assembly, and Application. Langmuir 33:6964–6977.

Zhang Q, Savagatrup S, Kaplonek P, Seeberger PH, Swager TM. 2017. Janus Emulsions for the Detection of Bacteria. ACS Cent. Sci. 3:309–313.

Zhang Y, Niu Y, Luo Y, Ge M, Yang T, Yu L, and others. 2014. Fabrication, characterization and antimicrobial activities of thymolloaded zein nanoparticles stabilized by sodium caseinate-chitosan hydrochloride double layers. Food Chem. [Internet] 142:269–275. Available from: http://dx.doi.org/10.1016/j.foodchem.2013.07.058

Zhang Z, Zhang R, Decker EA, McClements DJ. 2015. Development of food-grade filled hydrogels for oral delivery of lipophilic active ingredients: pH-triggered release. Food Hydrocoll. [Internet] 44:345–352. Available from: http://dx.doi.org/10.1016/j.foodhyd.2014.10.002

Zhang Z, Zhang R, McClements DJ. 2016. Encapsulation of β-carotene in alginate-based hydrogel beads: Impact on physicochemical stability and bioaccessibility. Food Hydrocoll. [Internet] 61:1–10. Available from: http://dx.doi.org/10.1016/j.foodhyd.2016.04.036

Zhao CX, Middelberg APJ. 2013. One-step fabrication of titania hollow spheres by controlled interfacial reaction in a droplet-based microfluidic system. Microfluid. Nanofluidics 14:703–709.

Zheng Y, Yu Z, Parker RM, Wu Y, Abell C, Scherman O a. 2014. Interfacial assembly of dendritic microcapsules with host–guest chemistry. Nat. Commun. [Internet] 5:5772. Available from: http://www.nature.com/doifinder/10.1038/ncomms6772

Zhong Q, Jin M. 2009. Zein nanoparticles produced by liquid–liquid dispersion. Food Hydrocoll. [Internet] 23:2380–2387. Available from: http://linkinghub.elsevier.com/retrieve/pii/S0268005X09001374

Zhou J, Hyun DC, Liu H, Wu H, Xia Y. 2014. Protein capsules with cross-linked, semipermeable, and enzyme-degradable surface barriers for controlled release. Macromol. Rapid Commun. 35:1436–1442.

Zhu Y, Zhu LN, Guo R, Cui HJ, Ye S, Fang Q. 2014. Nanoliter-scale protein crystallization and screening with a microfluidic droplet robot. Sci. Rep. 4:1–9.

Zou L, Liu W, Liu C, Xiao H, McClements DJ. 2015. Designing excipient emulsions to increase nutraceutical bioavailability: emulsifier type influences curcumin stability and bioaccessibility by altering gastrointestinal fate. Food Funct. [Internet] 6:2475–2486. Available from: http://xlink.rsc.org/?DOI=C5FO00606F

van Zwieten R, Verhaagen B, Schroën K, Fernández Rivas D. 2017. Emulsification in novel ultrasonic cavitation intensifying bag reactors. Ultrason. Sonochem. [Internet] 36:446–453. Available from: http://dx.doi.org/10.1016/j.ultsonch.2016.12.004

CHAPTER 3

Surface modification of zein colloidal particles with sodium caseinate to stabilize oil-in-water Pickering emulsion[1]

3.1 Abstract

Zein colloidal nanoparticles can adsorb at the oil-water interface to form Pickering emulsion. However, zein Pickering emulsion is usually not stable due to the poor wettability of zein colloidal nanoparticles. The objective of this study was to modify the surface of zein nanoparticles using sodium caseinate (NaCas) and assess the properties of zein/NaCas nanocomplexes and the resultant oil-in-water Pickering emulsions. One percent (w/w) of zein/NaCas colloidal nanocomplexes were formed, with the zein:NaCas ratios (w/w) ranging from 10:1 to 10:4 at pH=3 by an ultrasound treatment. The zeta-potential of the zein/NaCas nanocomplexes showed altered surface charges, indicating that NaCas adsorbed on the surface of the zein colloidal nanoparticles. Three-phase contact angle measurements suggested that the original zein colloidal nanoparticles were preferentially wetted in water. The incorporation of 0.1%-0.2% (w/w) NaCas significantly enhanced its wettability in the oil, and intermediate wettability was achieved at a zein:NaCas ratio of 10:3. Confocal laser scanning microscopy (CLSM) showed that the incorporation of NaCas improved the interfacial coverage of the Pickering emulsions. When the zein:NaCas ratio ranged from 10:1 to 10:3, the interface was composed of zein/NaCas nanocomplexes. At a zein:NaCas ratio of 10:4, NaCas can competitively adsorbed to the interface and formed a hybrid interfacial structure. The Zein/NaCas nanocomplexes stabilized the Pickering emulsions and exhibited greater centrifugal stability than plain zein emulsions at most pHs and ionic strengths. The underlying mechanisms of the improved emulsion stability are discussed in this paper. This study explored a novel approach to stabilizing Pickering emulsions via the surface modification method using a food-grade protein.

Keywords

Pickering emulsion, zein, sodium caseinate, surface modification , wettability, synergistic effects, limited coalescence

[1] ***The contents of this section have been published in: Feng, Y., & Lee, Y. (2016). Surface modification of zein colloidal particles with sodium caseinate to stabilize oil-in-water pickering emulsion. Food Hydrocolloids, 56, 292-302. With the reprint permission from the publisher.***

3.2 Introduction

Emulsions are commonly used in food and pharmaceutical industries for encapsulation and delivery of bioactive compounds (McClements 2012). Conventional emulsions are stabilized by biopolymers and low-molecular-mass (LMM) surfactants, which have been extensively studied in the past few decades (Tikekar and others 2013). Alternatively, colloidal particles stabilized Pickering emulsions have attracted considerable interest in recent years, due to their superior stability against coalescence and irreversible adsorption to the oil-water interface. The resulting capsules are called colloidosomes (Dickinson 2010).

Unlike biopolymers and LMM surfactants, colloidal particles can adsorb at interface to form a rigid shell, that is potentially thicker layer resulting in reduced mobility, which may offer enhanced stability to encapsulants (Tikekar and others 2013). In order to improve the compatibility of Pickering emulsifiers in pharmaceutical and food formulations, many pioneering studies derivied Pickering emulsifiers from biological origin, e.g., pea protein (Liang and Tang 2014), soy protein aggregates (Liu and Tang 2013; Liu and Tang 2014), whey protein microgel particles (Destribats and others 2014) and zein protein nanoparticles (de Folter and others 2012; Gao and others 2014).

It is widely recognized that the wettability of colloidal nanoparticles in the oil-water interface can substantially affect the emulsion stability, and the wettability is usually expressed using oil-water three phase contact angle, θ. An appropriate θ angle is a hinge that ensures the types of emulsion (O/W or W/O) and irreversible adsorption. Generally, the θ angle to achieve irreversible adsorption is neither too close to 0o nor 180o (Dickinson, 2012). However, most of the known inorganic and biological colloidal particles have been found to be too hydrophilic, thus results in slow diffusion and low interfacial coverage during emulsification (Gao and others 2014; Qi and others 2014). Several approaches have been explored to improve the surface properties of both inorganic and biological materials, including utilizing small molecular surfactants, lecithin and hydrophobin to synergistically stabilize Pickering emulsions (Binks and others 2007; Ghouchi Eskandar and others 2007; Gao and others 2014; Nesterenko and others 2014). To be compatible with the food and pharmaceutical industry, there is a need to avoid the usage of surfactants due to their toxicity. Alternatively, recent studies applied processing techniques such as heating and sonication to generate colloidal particles without using surfactants (Destribats and others 2014; Liu and Tang 2015).

Zein colloidal nanoparticles have been found as a potential effective Pickering stabilizer (de Folter and others 2012; Gao and others 2014), and the intermediate oil-water wettability of

zein films were reported at various pH and ionic strength (de Folter and others 2012). It is noteworthy that the wettability of zein has been reported differently in the past. Typically zein films are prepared following the "evaporation induced self-assembly" (EISA) process, which is considered as a slow process and involves complicated configurational alterations. Therefore, many structural rearrangements are allowed to occur, such as the transformation from α-helix into β-sheet, dense packing, molecular alignment, sphere growing, and eventually forms a highly-organized structure (Wang & Padua, 2012). However, zein colloidal particles that used for stabilizing emulsions were formed by the liquid-liquid dispersion, which is commonly recognized as a physical process consisting of the breakup of the droplets, solvent attrition and solidification (Alargova and others 2006; Zhong and Jin 2009). In order to represent the more realistic environment that the zein colloidal particles experience, a study measured the three-phase contact angle of zein colloidal particles and indicated their poor wettability in aqueous phase (Gao and others 2014). To improve the feasibility of zein as Pickering emulsifier, surface modification with sodium stearate has been proposed (Gao and others 2014). However, the incorporation of surfactant also induced toxicity.

Sodium caseinate (NaCas) was utilized to improve the stability and dispersibility of zein colloidal particles in the aqueous phase through surface adsorption, and this technique has also been vast applied for encapsulation purposes (Ye 2008; A.R. Patel and others 2010; Chen and Zhong 2014; Li and others 2014). Two mechanisms (electrostatic coacervation and direct molecular interactions) were proposed to interpret the process (A.R. Patel and others 2010), but there remains a lack of mechanistic information. A recent study suggested that β-casein can act as a molecular chameleon and adsorb to a variety of surfaces by changing its own molecular arrangement according to pH, ionic strength and the specific surface types (Evers and others 2012; Svensson and others 2014). It is still unknown whether NaCas behaves like β-casein when it interacts with zein colloidal surface, but the adsorption implies the possible occurrence of surface modification, both chemically and physically. This surface modification could also tailor the surface roughness, which was proved to substantially alter a particle's wettability (San-Miguel and Behrens 2012). To date, there is no systematic study that investigates the adsorption of NaCas on zein colloidal particles, in addition to the concomitantly formed zein/NaCas nanocomplexes.

Food-grade Pickering emulsions have recently been a subject of renewed interest, but there are still many challenges towards their applications. The main problem associated with biological Pickering emulsifiers is that they are inherently hydrophilic resulting in insufficient droplet coverage, and require surfactants as synergistic stabilizers (Gao and others 2014).

Herein, we present novel research on the surface properties of zein/NaCas colloidal nanocomplexes. The objective of this study is to investigate a potential approach to tweaking the surface properties using an amphiphilic protein, sodium caseinate (NaCas). Furthermore, we studied the surface properties of zein/NaCas colloidal nanocomplexes, including the wettability and surface charge, as a function of pH and the zein/NaCas ratios. The zein/NaCas nanocomplexes were used to prepare oil-in-water Pickering emulsions, and the macroscopic stability of the Pickering emulsions against environmental stresses as well as the interfacial properties of the Pickering emulsions were characterized and discussed.

3.3 Materials and methods

3.3.1 Materials

Zein (Z3625), sodium caseinate (C8654), protein assay kits including Biuret reagent (B3934) and Folin and Ciocalteu's phenol reagent (F6678), and sodium azide (S2002) were obtained from Sigma Aldrich Inc. (St. Louis, MO, USA). Sodium chloride (S271-3) was purchased from Fisher Scientific (Pittsburgh, PA, USA). Canola oil (Crisco Inc., Orrville, OH, USA) was purchased from a local store. Ethanol (anhydrous denatured 200 proof) was obtained from Cole-Parmer Inc. (Vernon Hills, IL, USA). The other chemicals reagents used were all of analytical grade.

3.3.2 Preparation and characterization of zein/NaCas nanocomplexes

Particle size

For the dynamic light scattering (DLS) measurement, the freshly prepared emulsion after vacuum treatment was examined at 25°C by ZetaPALS zeta potential analyzer (Brookhaven Instruments Co., Holtsville, NY). Intensity-weighted particle size distribution was collected from the average of three readings, and the D_{90} values were obtained for each distribution of particle sizes in the intensity profiles. Three to five measurements on the DLS were completed for each sample.

Preparation of zein colloidal nanoparticles.

Zein colloidal nanoparticles were prepared following the liquid-liquid dispersion method. Six gram of zein was dissolved into 100ml 70% ethanol solution to form a stock solution. The stock solution was then dispersed to 150ml DI water under a high speed (12,000 rpm) homogenization (IKA-ULTRA-TURRAX® T25 basic, IKA® Works, Inc., Wilmington,

NC, USA), to form zein colloidal nanoparticles dispersion. In order to remove large zein aggregates, the dispersion was subjected to centrifugation (model IEC CENTRA CL2, Thermo Scientific Inc., Waltham, MA, USA) at 100 g for 10 min. Excessive ethanol and water were evaporated by rotary evaporator (HaakeBuchler Instruments Inc., Saddle Brook, NJ, USA) at 65oC, and the sample was centrifuged at 100 g for 10 min again (model IEC CENTRA CL2, Thermo Scientific Inc., Waltham, MA, USA) to ensure the removal of large particles formed during heat treatment. The final concentration of zein colloidal nanoparticles dispersion is 1% (w/w).

Formation of zein/NaCas nanocomplexes.

To avoid aggregation, the pH of zein colloidal dispersions was adjusted to be around 2.8 using HCl. The zein/NaCas nanocomplexes were prepared at pH=3 by adding various amounts of NaCas into zein colloidal nanoparticles dispersions, under constant magnetic stirring at 500 rpm for 10min (IKA RO10, Works, Inc., Wilmington, NC, USA). In total, zein/NaCas nanocomplexes with four different weight ratios were prepared, 10:1, 10:2, 10:3 and 10:4 (zein: NaCas, w/w). The samples (40 ml) were then treated with a sonicator equipped a standard 1/8'' diameter probe (Ultrasonic processor Q55, Qsonica, Newtown, CT, USA) at 50 % power for 30 seconds to facilitate the NaCas adsorption. The final pH of zein/NaCas nanocomplexes dispersions were adjusted to 3.0. Sodium azide (0.01%, w/w) was added as preservative.

Zeta-potential measurements.

The zeta-potential measurements were conducted using a zeta potential analyzer (model ZetaPALS, Brookhaven Instruments Corporation, Brookhaven, NY, USA) at various pHs ranging from 3.0 to 9.0. All samples were diluted by 100 times with DI water, and the pH was adjusted using HCl or NaOH solution. An average value of three measurements was reported for each sample.

Contact angle measurements.

Three-phase contact angle (θ) was measured using VCA Optima system (AST Products Inc., Billerica, MA, USA). Samples were prepared into films by oven-drying (Gallenkamp, Weiss, UK) at 70oC overnight. The protein film was then immersed in canola oil, and a droplet of DI water (2μL) was placed on the substrate. After the equilibrium was reached, the contact angle was determined using the instrumental software. All measurements were replicated for at least three times.

Scanning Electron Microscope (SEM).

Morphological structure of zein colloidal nanoparticles, zein/NaCas nanocomplexes and NaCas were obtained using a scanning electron microscope equipped with a field emission electron gun (model Philips XL30 ESEM-FEG, FEI Company, Hillsboro, OR, USA). Samples were subjected to freeze-drying (Labconco Freezone 6, Labconco Corp., Kansas city, MO, USA) for 48 hours followed by adhering to a conductive carbon tape and sputter coating (model Dest-1 TSC, Denton Vacuum LLC., Moorestown, NJ, USA) with a gold layer before imaging.

3.3.3 Preparation and characterization of emulsions

Preparation of emulsions.

All emulsions were prepared using the same emulsifier concentration (1%, w/v), oil fraction (Φ=0.5, v/v) at same pH (pH=3.0). Specifically, canola oil was added slowly into the aqueous phase, while mixing with a high-speed homogenizer at 12,000 rpm (IKA-ULTRA-TURRAX® T25 basic, IKA® Works, Inc., Wilmington, NC, USA). Samples were homogenized for another 2min after all the oil was added. pH and ionic strength of the obtained emulsions were adjusted using HCl, NaOH and NaCl solutions. The emulsion type was determined quantitatively by a drop test. Briefly, a drop of each emulsion sample was added into pure canola oil or pure water. If the emulsion droplet remains intact in the oil phase, it indicates an oil-in-water emulsion. Vice versa, it will be a water-in-oil emulsion.

Centrifugal Stability.

An accelerated stability test was conducted to check the stability of emulsions. In general, 1ml of freshly prepared emulsions with different levels of pH (3.0, 5.0, 7.0 and 9.0) and salt (NaCl) concentration (0M, 0.006M, 0.06M, and 0.6M) were vortexed and placed into micro-centrifuge tubes. Samples were then subjected to centrifugation at 9400g for 10min (model MiniSpin® plus, Eppendorf, Westbury, NY, USA). The amount of released oil was quantified by weighing, and the weight was further converted to volume in accordance with its density. The percentage of the released oil during centrifugation over the total amount of oil was reported. All measurements were conducted in triplicate.

Emulsion morphology and droplet size.

The morphology and droplet size were characterized using an optical microscopy equipped with a camera (Axio Imager A1, Zeiss, Germany). The digital images were taken at 20X magnifications and analyzed in pixels using ImageJ software (1.48v, National Institute of

Health, Bethesda, MD, USA). The size distributions were collected with at least 40 droplets from each sample. The surface average diameter (d3,2) was calculated by the following equation:

$$D_{3,2} = \frac{\sum n_i d_i^3}{\sum n_i d_i^2} \quad (1)$$

Where n_i is the total number of droplets with diameter d_i.

Confocal Laser Scanning Microscope (CLSM).

Emulsion samples (1ml) were stained with the mixture (40μL) of Nile blue (0.1%) and Nile red (0.1%) for 2 hours. A Zeiss LSM 700 confocal microscope (Zeiss, Germany) was operated using two excitation lines (488nm for the Nile blue dye and 634nm for the Nile red dye) to visualize the emulsions. Images were taken at a magnification of 20x, and further processed using the instrumental software.

Surface protein loading (τ).

The surface protein loading (τ) was quantified using a modified procedure that was described in a previous study (Liang and Tang 2014). The freshly prepared emulsions were centrifuged at 1000g (model IEC CENTRA CL2, Thermo Scientific Inc., Waltham, MA, USA) for 20min, to allow the complete separation of creaming phase (top) and the serum phase (bottom.) The protein concentration in the serum phase was determined using the Lowry method, The surface protein loading τ (mg/m2) can be calculated by the following equation:

$$\tau(mg/m^2) = (C_0 - C_f) * d_{3,2}/6\emptyset \quad (2)$$

Where C0 is the initial protein concentration in the aqueous phase, Cf is the final concentration of protein in the serum fraction determined by Lowry method, d3,2 is the surface average diameter of emulsion droplets, and Φ is the volume fraction of oil.

3.3.4 Statistical analysis.

All the measurements were conducted at least in triplicate. Data were analyzed using OriginPro 2015 software (OriginLab Corp., Northampton, MA) and Microsoft Excel 2010 (Microsoft Corp., Seattle, WA). Analysis of variance (ANOVA) and least significant difference (LSD) were used to compare the means. The significance level was set at 0.05.

3.4 Results and discussion

3.4.1 Mechanisms of the zein/NaCas interactions.

Morphology of zein/NaCas nanocomplexes

The SEM pictures shown in Figure. 3.1 provide the visualization of zein/NaCas nanocomplexes, zein colloidal nanoparticles and NaCas at pH 3.0. The surface of the plain zein particles was smooth while the addition of various amounts of NaCas was able to change the surface roughness indicating the surface adsorption. At the zein:NaCas ratio of 10:4, there was no smooth zein surface existing in Fig 2E, which indicates the complete surface coverage by NaCas. Figure 3.2 shows the effect of pH 3 and 5 on the NaCas adsorption. At the same zein:NaCas ratio (10:3), the adsorption of NaCas is observed at pH 3.0 (indicated by the arrow), but not at pH = 5.0. Thus, the adsorption of NaCas on the zein colloidal particles is a pH-dependent process and did not occur at pH 5.0, which may be due to the isoelectric coagulation of NaCas. The driving force of this type of adsorption was discussed to be either direct electrostatic interaction or molecular interaction (A.R. Patel and others 2010). The results from this experiment suggest the direct molecular interaction as the driving force. At pH 3.0, both zein and NaCas are positively charged, while the adsorption occurred regardless of their repulsive electrostatic forces. The specific molecular rearrangement of NaCas involved during this process is not discussed in this paper, as it is beyond the scope of the current study. To the authors' knowledge, this is the first time visualizing zein/NaCas nanocomplexes with SEM.

Zeta-potential.

Figure 3.3 shows the zeta-potential (mV) as a function of pH for zein/NaCas nanocomplexes with different zein:NaCas ratios. A rapid shift of the isoelectric point was observed from the plain zein (around 6.5) to the zein:NaCas ratio 10:1 nanocomplexes (around 5.6), indicating that NaCas of this amount was able to cover a considerable portion of the zein surface. However, even at the zein:NaCas ratio of 10:4 where complete surface coverage was observed from the Fig 1, the isoelectric point of the zein/NaCas nanocomplexes was 5.3, and did not coincide with the isoelectric point of NaCas at 5.0. This disparity is probably ascribed to the molecular rearrangement of NaCas at the zein colloidal surface, and result in an uneven surface charge distribution of NaCas between the exposed and adsorbed side.

Wettability

The wettability of the plain zein was studied in previous studies with disparate results reported, including intermediately wetted (de Folter and others 2012), predominately wetted in aqueous phase (Gao and others 2014), and mainly wetted in the oil phase (Wang et al., 2015). The differences in the findings could be attributed to the various preparation methodologies

and the resulting microstructures. Samples derived through the evaporation induced self-assembly (EISA) process exhibited intermediate wettability, due to the formation of a self-assembled and orderly arrayed laminar structure (Wang & Padua, 2012). Since Pickering emulsions are stabilized by the intact zein colloidal particles instead of laminar zein molecules, it would be more reasonable to report the wettability of zein particles in this study. Even so, contradictory wettability results were found when measuring the zein colloidal particles, (Gao et al., 2014; Wang et al., 2015), according to different sample preparation techniques (oven drying and freezing drying) applied. Here, we selected the oven-drying method since it produced the three-phase contact angle (θ) less than 90º, because it is in agreement with the previous drop test, which confirmed the formation of oil-in-water (O/W) emulsion (de Folter and others 2012). In this study, we measured the wettability of plain zein colloidal particles, zein/NaCas nanocomplexes with different zein:NaCas ratios, and the plain NaCas following the methodology described in a previous study (Qi and others 2014). Figure 3.4 illustrates the change of oil-water three phase contact angle as a function of zein:NaCas ratio. Our results also confirmed that plain zein colloidal particles are preferentially wetted by the aqueous phase, while the incorporation of NaCas significantly enhanced their wettability in the oil phase. At the zein:NaCas ratios of 10:2 and 10:3, the intermediate wettability (θ~90°) was achieved. There was no significant difference of the contact angle between zein/NaCas nanocomplexes with the zein:NaCas ratio of 10:4 and the plain NaCas, indicating the complete surface coverage of NaCas. The increase in wettability upon NaCas adsorption is mainly caused by the change of surface composition. On the other hand, the enhancement of surface roughness could also contribute to the alteration of wettability (San-Miguel and Behrens 2012).

It is worth addressing that the three-phase contact angle exceeded 90º at the zein:NaCas ratio of 10:4, but its stabilized emulsion did not invert to a W/O emulsion. This could be attributed to contact angle hysteresis, which is a ramification of many factors such as surface roughness, adsorption of solution impurities and rearrangement of surface by the solvent (Ghouchi Eskandar and others 2007). In this experiment, the adsorption of fatty acid chains on the protein films could have further increase the surface hydrophobicity.

Zein/NaCas ratio

The adsorption of NaCas on zein colloidal particles has been recently studied for the purposes of improving the colloidal stability, protein digestibility and spray-drying redispersibility, and the produced zein/NaCas nanocomplexes were mainly applied as wall materials for encapsulation (A.R. Patel and others 2010; Wang and others 2013; Chen and

Zhong 2014; Li and others 2014). In previous studies, zein/NaCas nanocomplexes were formed through dispersing zein ethanol/water binary solution into deionized water containing NaCas under high-speed shearing (A.R. Patel and others 2010; Zhang and others 2014; Chen and others 2015). The essential zein:NaCas ratio was estimated at 1:0.29 (w/w) to achieve monolayer coverage (A.R. Patel and others 2010). However, another study observed the precipitation of zein/NaCas nanocomplexes when the zein:NaCas ratio reached 1:0.35-1:0.5, and the reason was concluded as unsaturated surface coverage (Zhang and others 2014). Therefore, in order to investigate the actual zein:NaCas ratio that forms monolayer coverage, and to ensure that the precipitation of zein/NaCas nanocomplexes were not induced by the isoelectric coagulation of NaCas, our experiment strictly controlled the pH below the isoelectric point of NaCas (pI = 5.0 was obtained from our experiment) throughout the adsorption process. The formation of zein/NaCas nanocomplexes was facilitated using an ultrasound treatment (Gao and others 2014). At pH = 3.0, all the samples with different zein: NaCas ratios from 10:0 to 10:4 were macroscopically stable, indicating that the precipitation of zein/NaCas nanocomplexes observed in previous studies could be induced by the isoelectric aggregation of NaCas. No visible plain zein colloidal surface (flat) was found at the zein:NaCas ratio of 10:4, indicating the saturated surface coverage. Results from our experiment suggest the complete surface coverage is reached at the zein:NaCas ratio between 10:3 to 10:4.

3.4.2 Characterization of Pickering emulsions

Centrifugal stability

The emulsion stability was evaluated via centrifugal method, by virtue of many advantages such as improved reproducibility and accuracy (Qi and others 2014). Moreover, the centrifugal stability is a characteristic of the emulsion itself (Tcholakova, Denkov, & Lips, 2008). Typically, Pickering emulsions exhibit poor centrifugal stability when comparing to the conventional emulsions stabilized by proteins and small molecular surfactants, primarily due to the differences in the emulsion droplet sizes and the destabilization mechanisms (Tcholakova et al., 2008; Tcholakova, Denkov, Ivanov, & Campbell, 2002, 2006). To ensure the reliability of using the centrifugal method, two emulsions systems being compared have to possess the similar droplet size. Generally, larger droplets are more susceptible to the coalescence and many previous studies reported the linear correlation between the critical osmotic pressure and drop radius (Tcholakova et al., 2002, 2006). Therefore, we will not discuss the centrifugal stability of emulsions stabilized by the plain NaCas due to the significant size difference while the data is still presented here for the validation purposes. Table 3.1

demonstrates the percentage of oil that released after high-speed centrifugation (9400g) for 10 min at different pH and ionic strengths. Different superscript letters indicate the significant difference within the same column ($P<0.05$).

The effect of pH of ionic strength

Four levels of pH (3.0, 5.0, 7.0 and 9.0) and four levels of ionic strengths (0M, 0.006M, 0.06M, and 0.6M) were selected to study the emulsion stability, which was aiming to mimic the majority of the circumstances in food systems. Overall, emulsions at pH 3.0 and pH 9.0 showed better stability than those at pH 5.0 and pH 7.0, for the reason of the isoelectric coagulation of zein and NaCas at pH 5.0 to 7.0. It has been noted that samples with the zein:NaCas ratios of 10:0, 10:1 and 10:2 were not stable at pH 7.0, probably due to the isoelectric coagulation of zein particles. However, the zein:NaCas ratio of 10:3 and 10:4 provided superb stability at pH 7.0, suggesting the isoelectric aggregation was suppressed, probably due to the greater extent of surface coverage by NaCas. Change of pH and ionic strength affects the emulsion stability in two ways. First, the electrostatic repulsion between emulsion droplets are highly depend on the pH and ionic strength. At the pH close to pI or high ionic strength, emulsions become less stable because the coalescence is hindered solely by the steric barrier of Pickering emulsifiers, whereas the electronic repulsion diminishes. Second, the wettability of Pickering emulsifiers can also be affected by pH and ionic strength. In general, a pH close to pI or high ionic strength result in increased wettability angle of particles at the oil-water interface, hence, either promote or depress the emulsion stability (Wu and others 2015). In this experiment, there is no clear trend of emulsion stability subjected to the adjustment of pH and ionic strength, because of the potential counteraction or synergism of two mechanisms, in accordance with different combination of pH and ionic strength.

Although it is not the focus of this study, we interestingly found that the 0:10 samples exhibited superior stability at all the pHs and ionic strengths tested including pH 5.0, the isoelectric point of NaCas. It could be a consequence of the NaCas coagulation at pH 5.0 and high ionic strength. The extensive coagulation occurred within or between the adsorbed and non-adsorbed NaCas forms a dense 2-D network, and thus provided the extra stability against the centrifugal pressure (Destribats and others 2014). In addition, the increase of viscosity could also contribute to the improved stability.

Effect of NaCas on the synergistic stabilization

The synergistic effect of NaCas in stabilizing Pickering emulsions can be concluded as three mechanisms. Firstly, the NaCas improves interfacial properties by facilitating the interfacial adsorption. Figure 3.8 shows that the surface coverage was enhanced while adjust the zein:NaCas ratio from 10:0 to 10:3. Second, if the amount of NaCas reaches a critical ratio, the excessive NaCas can competitively adsorb to the interface and minimize of interstitial distance. According to the previous study, the critical osmotic pressure decreases substantially with an increase of the interparticle distance (Tcholakova et al., 2008). The evidence and underlying mechanisms of enhanced interfacial adsorption and competitive adsorption will be discussed further in this paper. Third, the excessive NaCas that is not adsorbed gives rise to the depletion flocculation and bridging to provide the extra physical stability. In general, the presence of non-adsorbed NaCas in the gap between emulsion droplets is able to create an attractive force (depletion force), which helps to stabilize the emulsion (Dickinson 2015). It was reported that the magnitude of depletion force is proportional to the number density of NaCas sub-micelles (Dickinson and Golding 1997). In our case, they would specifically be referred as the amount of free NaCas sub-micelles after depositing to zein particle surface.

Droplet size and morphology.

Figure 3.6 illustrates the optical microscopy pictures of the emulsion samples. ImageJ was utilized to analyze the images and calculate the area average droplet size ($d_{3,2}$), and the results are shown in the Table 2. The droplet size initially increased with increasing NaCas fraction until reaching the maximum at the zein:NaCas ratio of 10:3, followed by dropping down at the zein:NaCas ratio of 10:4. When an emulsion system encompasses two or more different types of emulsifiers, the behavior of each component during the emulsification process is complicated. In this study, Pickering emulsions were prepared using zein colloidal particles and zein/NaCas nanocomplexes. There could be two possible behaviors of NaCas during the emulsification process, 1) remain on the surface of zein colloidal particles or 2) migrate to the oil-water interface to stabilize the oil droplets. When there were more than one emulsifiers or surface active compounds, the competitive adsorption between two emulsifiers was widely recognized (Ghouchi Eskandar and others 2007; Dickinson 2011; Niu and others 2015). On the other hand, the interactions between different components should also be considered. Surfactant was found to anchor on a colloidal particle surface to form a agglomeration, and followed by the adsorption of such agglomerated particles at oil-water interface (Nesterenko and others 2014).

In order to understand the behavior of NaCas, it is important to learn about the forces that can take effect on it during emulsification. Unlike conventional emulsions where it is the diffusion that drives emulsifiers onto the interface, hydrodynamic forces are recognized as the driving force for the Pickering emulsions (Destribats et al., 2014; Tcholakova et al., 2008). Hydrodynamic interactions were reported to have influences on the substances with the size ranging from 10^2 to 10^6 nm (Nel and others 2009). According to the literature, the radius of NaCas upon removal of colloidal calcium phosphate (CCP) is about 10nm (Thomar and Nicolai 2015), which is similar to the thickness of NaCas layer that adsorbed on zein particle surface, observed from our SEM images (Figure 3.8). Therefore, NaCas is unlikely to be sheared off under high speed homogenization environment. In order to confirm the statement, we hypothesize that zein/NaCas nanocomplexes act as intact emulsifier units during emulsification, and use the so-called "limited coalescence" or "partial coalescence" model to verify it. The limited coalescence model infers that dispersing droplets are experiencing coalescence upon the formation until its surface reaches a threshold emulsifier adsorption, τ^* (Tcholakova et al., 2008). Generally, the limited coalescence theory is only suitable in the emulsifier-poor regime, where it is emulsifier concentration that predominately influences the droplet size, other than the power density during energy dissipation. Moreover, a recent study reported the limited coalescence phenomenon for emulsions containing excessive emulsifiers (Destribats and others 2014). Thus, it becomes unnecessary in this experiment to identify whether or not the emulsions are in the emulsifier-poor regime.

A mathematical model was built to study the limited coalescence quantitatively. (Tcholakova, Denkov, Sidzhakova, Ivanov, & Campbell, 2003):

$$d_{3,2} \approx \frac{6\phi}{(1-\phi)} \frac{\tau^*}{C_{INI}} \quad (3)$$

Here C_{INI} is the initial emulsifier concentration (wt%), τ^* is the threshold surface adsorption or coverage to hamper droplets from coalescence, and φ is the volume fraction of the dispersed phase. In many studies, the proportional correlation between $d_{3,2}$ and $1/C_{INI}$ was found in the emulsifier-poor regime, and recently in the emulsifier-rich regime (Destribats et al., 2014; Golemanov, Tcholakova, Kralchevsky, Ananthapadmanabhan, & Lips, 2006; Tcholakova, Denkov, & Banner, 2004; Tcholakova et al., 2003). In this experiment, we were able to identify a linear region where the zein:NaCas ratio is between 10:0 and 10:3, $d_{3,2}$ was found to be proportional ($R^2 = 0.95$) to the $1/C_{zein\ ini}$ (the initial concentration of zein, wt%), despite the fact that overall emulsifier concentration was remaining at 1% (wt%)(Figure 3.7).

However, the emulsion sample with the zein:NaCas ratio of 10:4 significantly deviated from the linear fitting. The plot indicates that NaCas did not participate in the interfacial adsorption until the zein:NaCas ratio reached 10:4, at which ratio we consider it entails excessive NaCas, originally existing as multilayer deposition on zein surface. During the emulsification, those multilayer NaCas acted as free emulsifier units, which was able to diffuse and competitively adsorb to the oil-water interface, and resulted in the formation of smaller droplet size with a multi-components interface that consists of both zein/NaCas nanocomplexes and NaCas sub-micelles (Figure 3.8). To further confirm the hypothesis, we have also studied the correlation between droplet size and emulsifier concentration using plain zein colloidal partilces (data is shown in the supplemental material). The linear region observed with zein/NaCas nanocomplexes perfectly overlaps with the linear fitting with plain zein.

Interfacial properties

The interfacial properties were characterized quantitatively by the surface protein loading and visually using the confocal laser scanning microscope (CLSM). A distinct feature of Pickering emulsions is the formation of a densely packed layer at the oil-water interface, which provides the steric barrier to hinder droplet coalescence (Ghouchi Eskandar and others 2007). The surface protein loading data is shown in Table 2. The obtained results strongly suggest that zein/NaCas nanocomplexes stabilized emulsions are Pickering emulsions, according to their significantly higher protein density at the interface compared to the conventional emulsion, which is, the NaCas emulsion in this study. However, the incorporation of NaCas from zein:NaCas ratio 10:0-10:2 significantly increased the surface protein concentration, yet the further addition of NaCas caused the surface protein to decrease ($p<0.05$).

In a previous study that prepared Pickering emulsions using zein/sodium stearate complexes, the enhancement of interfacial adsorption or accumulation was concluded as a result of the alteration of wettability (Gao and others 2014). Nevertheless, in this study, the surface loading significantly dropped down when the zein:NaCas ratio further increases to 10:4, and this is in a contrary trend with the observed wettability. This may indicate that the adsorption of NaCas occupied the interface thus hindered the further adsorption of zein/NaCas nanocomplexes.

Figure 3.7 presents the visualization of droplet interface characterized with CLSM. Figure 3.7A shows an emulsion droplet stabilized by the plain zein colloidal nanoparticles,

where large aggregates of zein colloidal particles can be seen at the oil-water interface, and the droplet surface is sparsely covered by the emulsifiers. Our supplemental material indicates that zein colloidal particles have the tendency to agglomerate reversibly in the aqueous phase. The agglomeration substantially reduced the efficacy of zein colloidal particles as Pickering emulsifiers. According to the Figure 3.7B, C, D and E, the incorporation of NaCas gradually changes the interfacial structure to be smooth and homogeneous, potentially attributed to the following three reasons: 1) zein agglomeration was inhibited by the presence of NaCas (shown in the supplemental information); 2) surface modification of zein colloidal particles with altered wettability improved the interfacial adsorption; 3) the excessive NaCas is able to cover the interstitial space between particles. Figure 3.8 illustrates three types of interfacial structures, which varies in accordance with the zein:NaCas ratios.

3.5 Conclusions

Adsorption of NaCas onto zein colloidal nanoparticles is able to modify the surface the zein particles and form zein/NaCas nanocomplexes. The wettability and surface charge of the nanocomplexes are tunable through adjusting the zein:NaCas ratio. Zein colloidal particles are inherently hydrophilic while the incorporation of different amount of NaCas can significantly tweak the three phase contact angle. The monolayer surface adsorption of NaCas and intermediate wettability are both found to be close to 10:3. The obtained zein/NaCas nanocomplexes were then used to prepare Pickering emulsions and the emulsions using nanocomplexes with the zein:NaCas ratios of 10:3 and 10:4 exhibits enhanced surface coverage and centrifugal stability. Limited coalescence theory shows that the nanocomplexes stabilize oil droplets as intact particles when the zein:NaCas ratio is between 10:1 and 10:3. However, after the monolayer adsorption is achieved, the excessive NaCas will competitively adsorb to the interface to form a particle-polymer hybrid interfacial structure. The non-adsorbed NaCas can trigger flocculation at high ionic strength or pH close to the isoelectric point of NaCas. In this study, the emulsification was conducted using a top-down approach, where the high shear emulsification was used to break down the oil phase. As an alternative, a bottom-up approach was also made to generate Pickering emulsions in microfluidic channels, however, the fresh formed droplets are highly susceptible to coalescence and followed by phase separation. The limited mobility of colloidal particles at low shear rate lead to insufficient interfacial coverage at the oil-water interface and unstable emulsion system. As such, it is not practical to used colloidal particles as building blocks in bottom-up processes.

3.6 Tables and figures

Table 3.1. Volume percentage of released oil (%) after high-speed centrifugation at 9400g for 10min. Emulsions were prepared using emulsifiers with different zein:NaCas ratios, followed by the adjustment of the pH and ionic strengths. Different superscript letters indicate the significant difference within the same column (P<0.05).

pH 3.0					pH 5.0				
Z/N ratios	Ionic strengths [NaCl]				Z/N ratios	Ionic strengths [NaCl]			
	0M	0.006M	0.06M	0.6M		0M	0.006M	0.06M	0.6M
10:0	25.71^{ab}	65.79^{b}	83.05^{b}	75.43^{ab}	10:0	81.75^{a}	80.69^{a}	86.42^{a}	89.62^{a}
10:1	28.44^{a}	63.46^{b}	65.64^{c}	64.42^{bc}	10:1	67.90^{b}	66.86^{b}	67.93^{b}	60.90^{b}
10:2	19.05^{abc}	79.47^{a}	92.00^{a}	80.22^{ab}	10:2	62.87^{bc}	78.45^{a}	81.50^{a}	88.42^{a}
10:3	2.57^{c}	3.79^{c}	32.46^{d}	58.51^{c}	10:3	61.09^{c}	66.77^{b}	52.14^{c}	3.03^{d}
10:4	5.10^{bc}	7.07^{c}	68.42^{c}	77.59^{ab}	10:4	84.49^{a}	80.99^{a}	79.03^{a}	78.34^{c}
0:10	0.15^{c}	0.38^{c}	0.00^{e}	1.13^{d}	0:10	0.00^{d}	0.00^{c}	0.00^{d}	0.00^{d}

pH 7.0					pH 9.0				
Z/N ratios	Ionic strengths [NaCl]				Z/N ratios	Ionic strengths [NaCl]			
	0M	0.006M	0.06M	0.6M		0M	0.006M	0.06M	0.6M
10:0	82.12^{a}	74.73^{b}	79.83^{a}	77.78^{a}	10:0	7.76^{a}	17.07^{a}	78.74^{a}	87.93^{a}
10:1	94.47^{a}	99.53^{a}	94.50^{a}	87.46^{a}	10:1	4.52^{b}	7.00^{b}	34.84^{b}	76.21^{b}
10:2	85.09^{a}	45.87^{c}	36.66^{b}	24.91^{b}	10:2	4.77^{b}	6.59^{b}	6.84^{c}	15.88^{c}
10:3	1.59^{b}	1.87^{d}	3.33^{c}	2.37^{c}	10:3	1.46^{c}	1.27^{b}	1.11^{c}	1.74^{d}
10:4	5.65^{b}	6.67^{d}	5.41^{c}	8.17^{c}	10:4	3.76^{bc}	4.30^{b}	4.53^{c}	6.42^{d}
0:10	3.01^{b}	3.62^{d}	4.05^{c}	3.27^{c}	0:10	1.44^{c}	1.59^{b}	1.94^{c}	2.92^{d}

Means within the columns followed by the same letters are not significantly different ($P <$ 0.05).

Table 3.2. Effect of the zein:NaCas ratios on the emulsion droplet size (d3,2) and the surface protein concentration τ (mg/m2). Different superscript letters indicate the significant difference within the same column (P<0.05).

Zein:NaCas ratios (w/w)	$D_{3,2}$ (μm)	Surface protein concentration τ (mg/m^2)
10:0	52.12	123.62 ± 3.34^{b}
10:1	58.09	114.39 ± 3.33^{b}
10:2	64.87	133.84 ± 2.76^{a}
10:3	66.31	115.23 ± 11.81^{b}
10:4	61.33	100.42 ± 4.50^{c}
0:10	26.29	3.70 ± 1.16^{d}

Means within the columns followed by the same letters are not significantly different ($P < 0.05$).

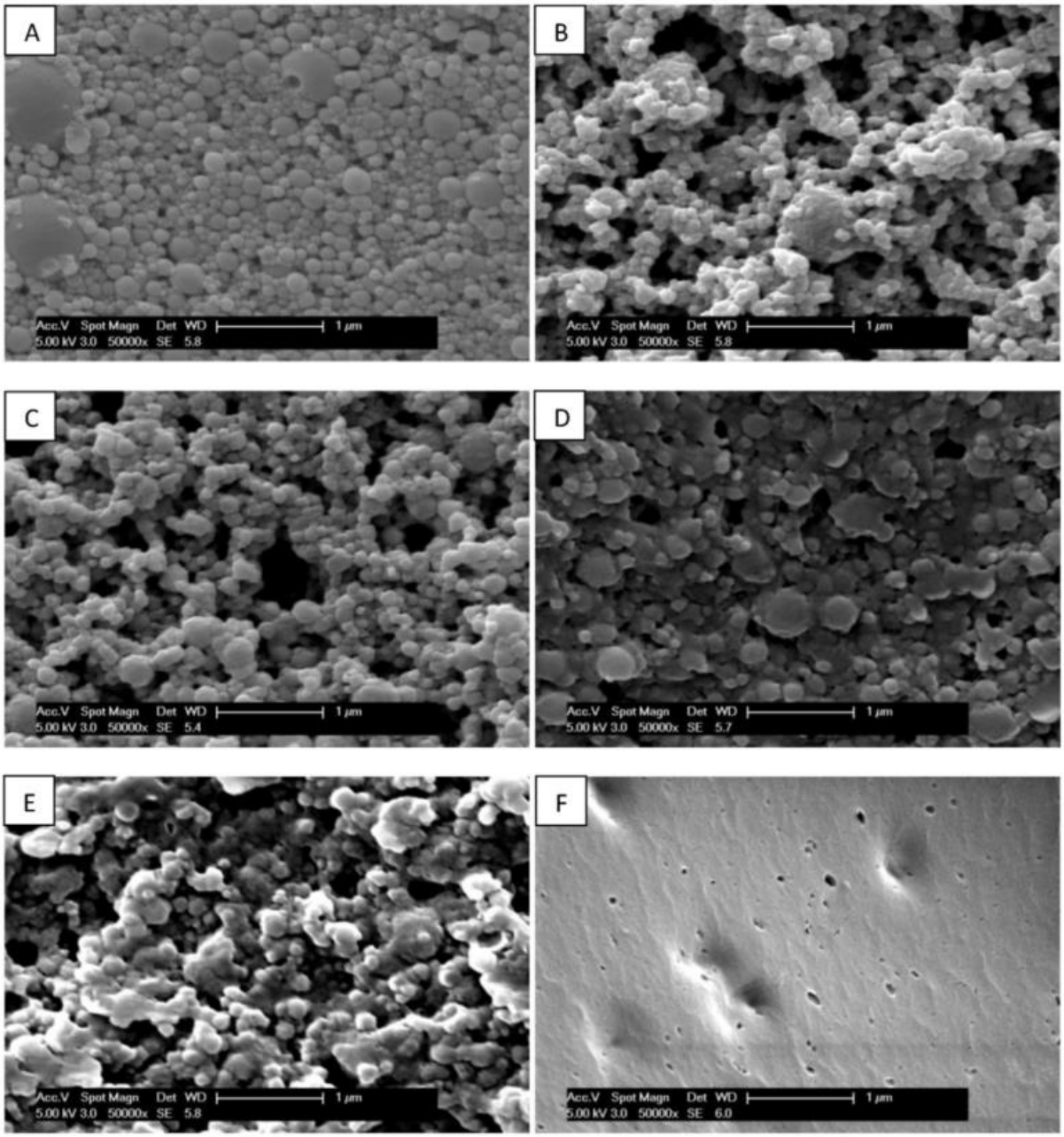

Figure 3.1. Scanning electron microscope (SEM) pictures of the plain zein colloidal particles (A), the zein/NaCas nanocomplexes with the zein:NaCas ratio of 10:1 (B), 10:2 (C), 10:3 (D), 10:4 (E), and the plain NaCas (F) prepared at pH 3.0.

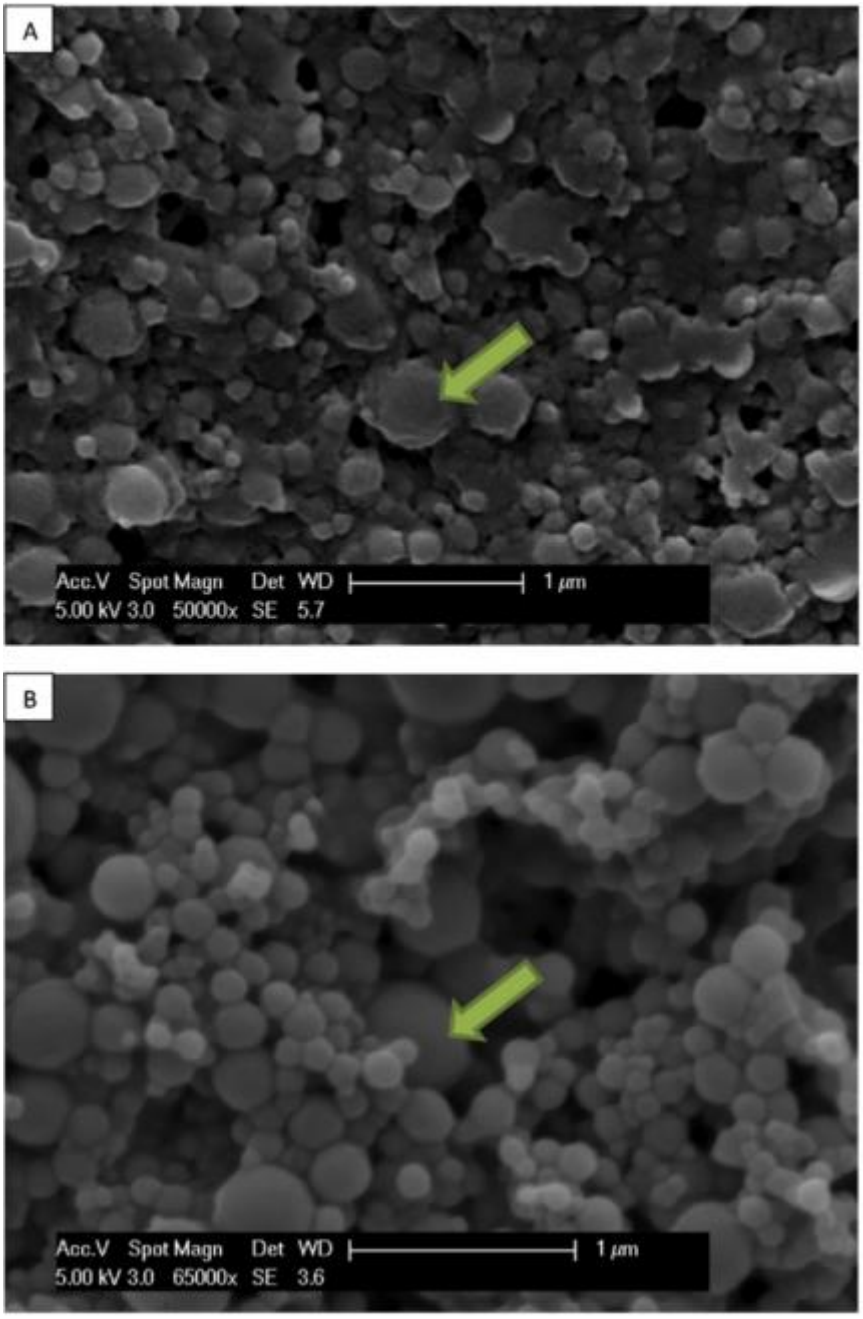

Figure 3.2. Scanning electron microscope (SEM) pictures of the zein/NaCas nanocomplexes with the zein:NaCas ratio of 10:3 at pH 3.0 (A), and 5.0 (B).

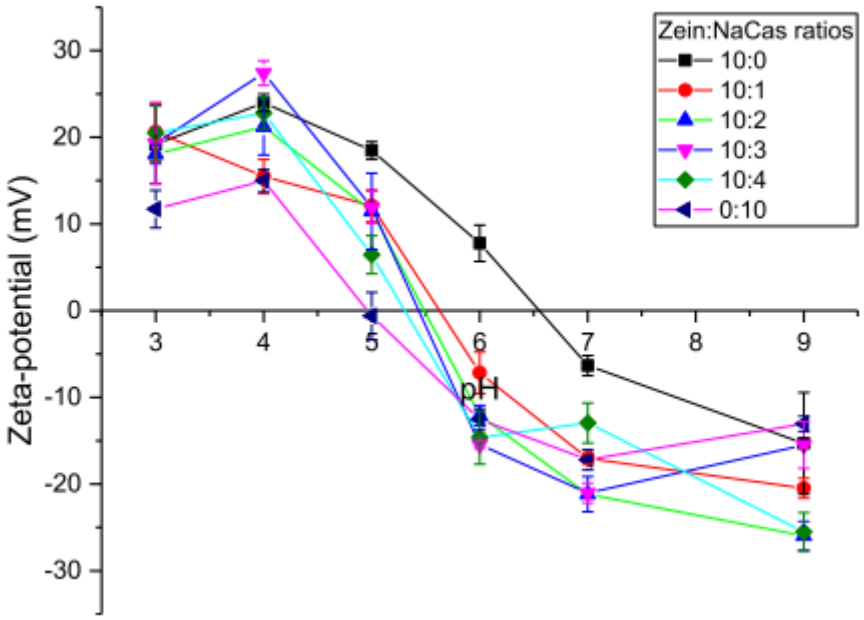

Figure 3.3. Zeta-potential versus pH curves at different zein:NaCas ratios.

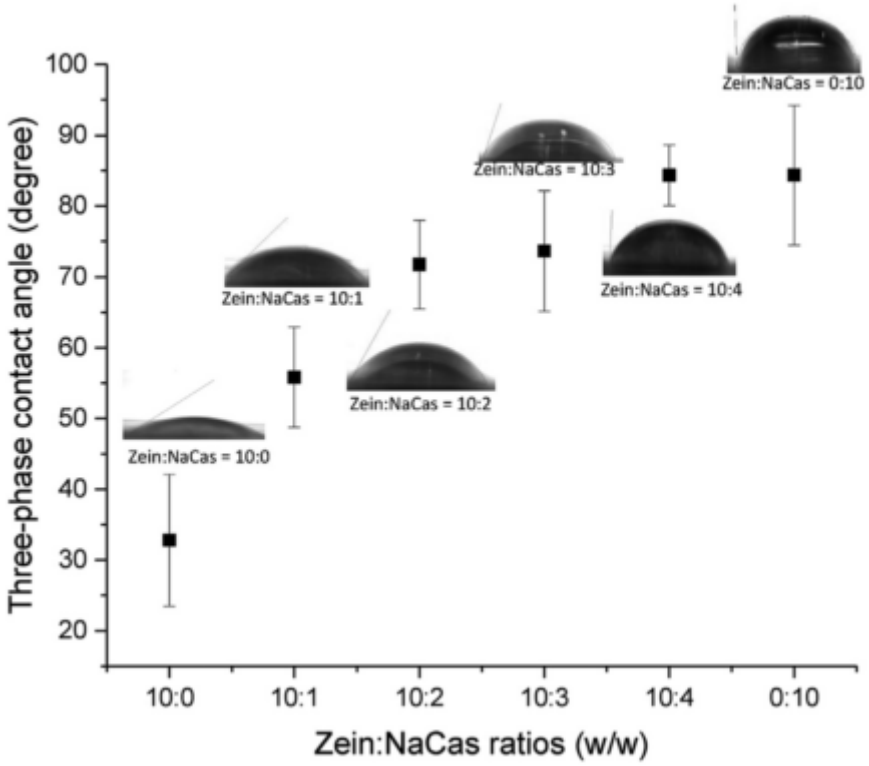

Figure 3.4. Three-phase contact angle (q) of protein films with different zein:NaCas ratios.

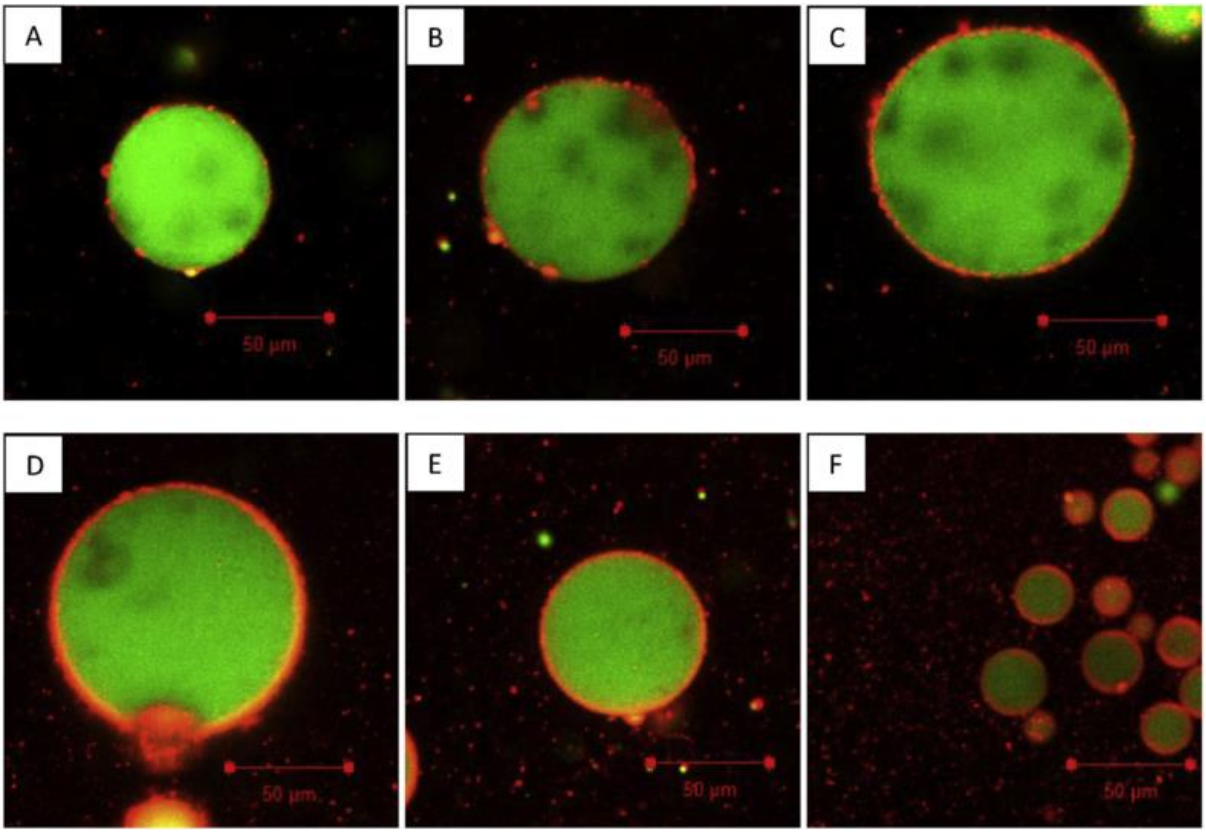

Figure 3.5. Confocal laser scanning microscope (CLSM) pictures of emulsion droplet prepared with the plain zein colloidal particles (A), the zein/NaCas nanocomplexes with the zein:NaCas ratio of 10:1 (B), 10:2 (C), 10:3 (D), 10:4 (E), and the plain NaCas (F) at pH 3.0.

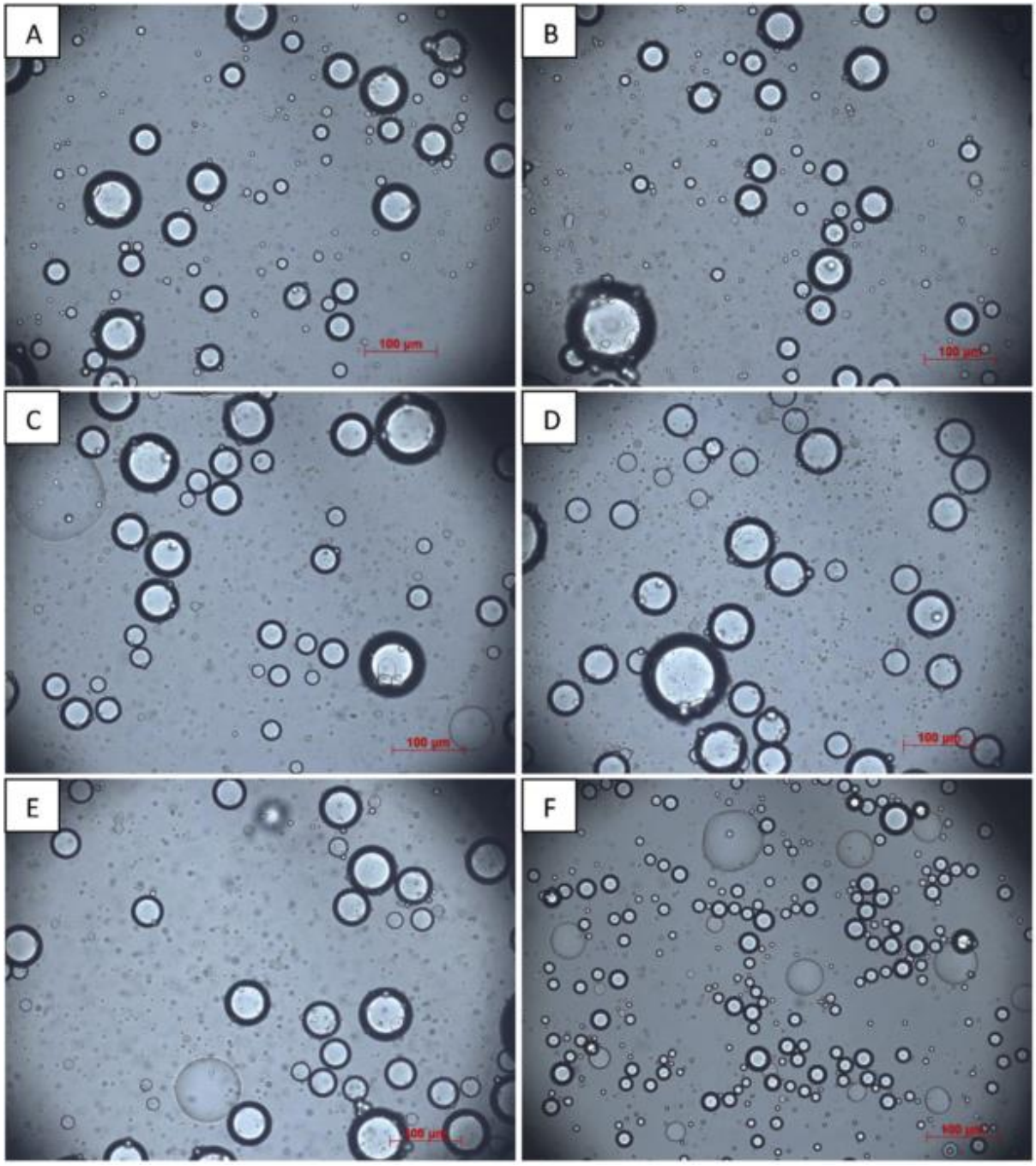

Figure 3.6. Optical microscope images of emulsions prepared at pH 3.0 using 1% plain zein colloidal particles (A), 1% zein/NaCas nanocomplexes with the zein:NaCas ratio of 10:1 (B), 10:2 (C), 10:3 (D), 10:4 (E), and plain NaCas (F).

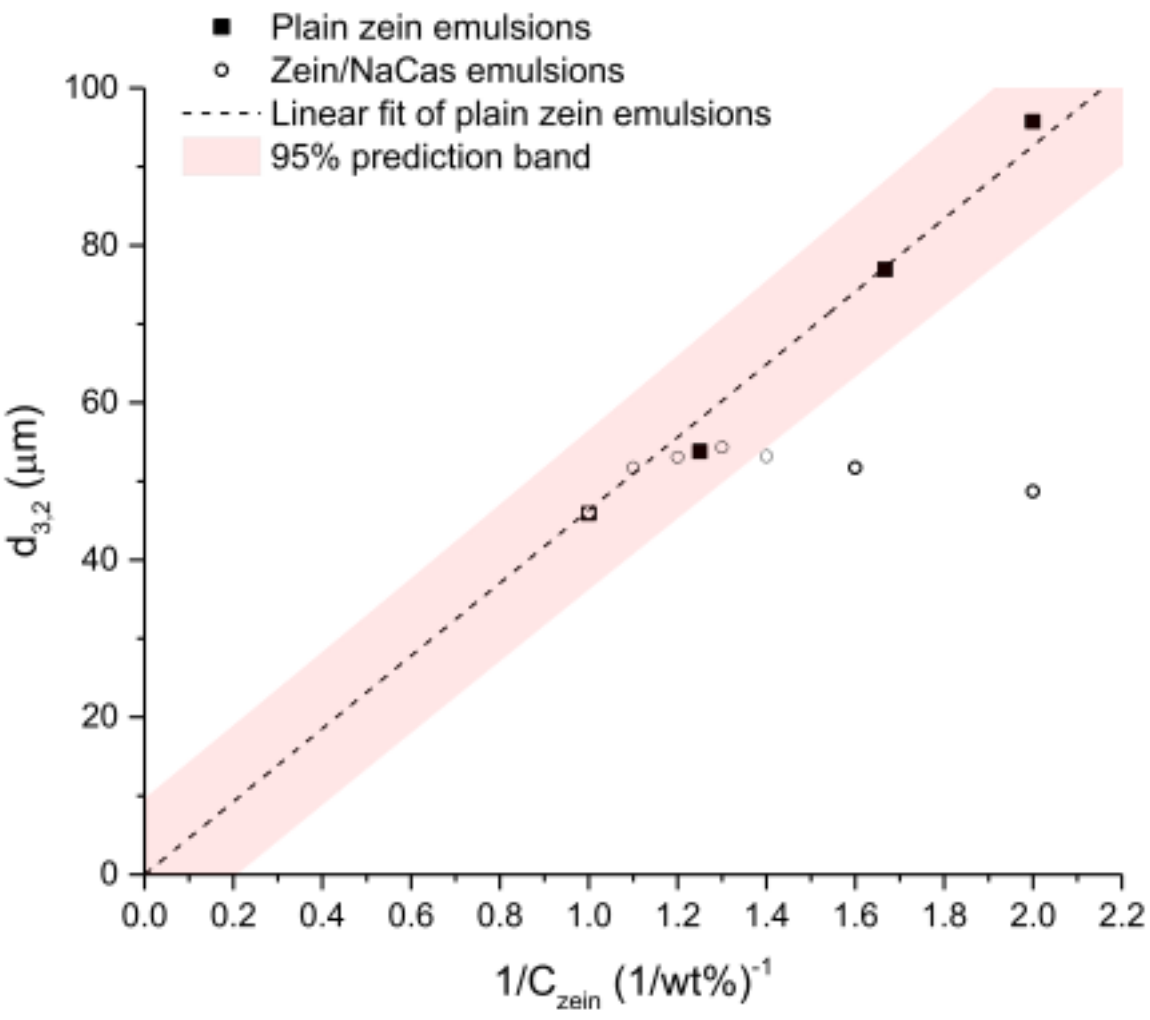

Figure 3.7. Emulsion droplet mean diameter, d3,2 (mm), as a function of the inverse initial concentration of zein (wt%)?1. The linear regression line with 95% prediction band was derived using plain zein Pickering emulsions with different zein concentration

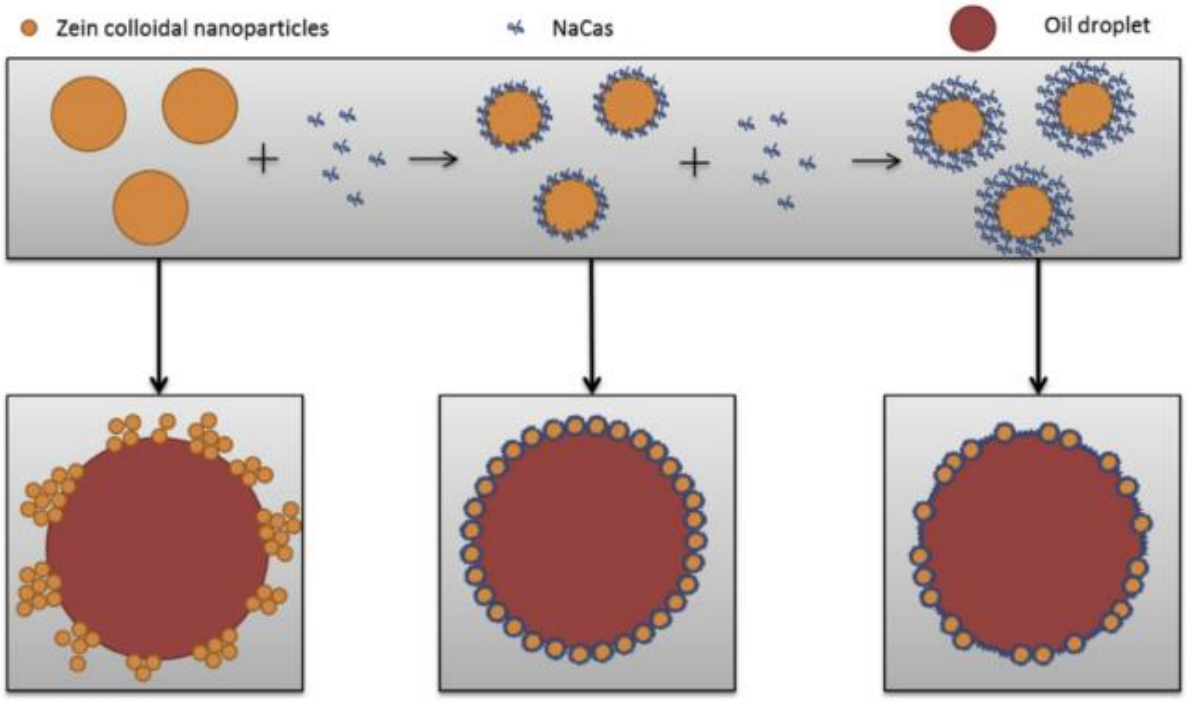

Figure 3.8. Schematic diagram of different interfacial arrangements at various zein:NaCas ratios.

3.7 References

Alargova RG, Paunov VN, Velev OD. 2006. Formation of polymer microrods in shear flow by emulsification - Solvent attrition mechanism. Langmuir 22:765–774.

Binks BP, Rodrigues JA, Frith WJ. 2007. Synergistic interaction in emulsions stabilized by a mixture of silica nanoparticles and cationic surfactant. Langmuir [Internet] 23:3626–36. Available from: http://pubs.acs.org/doi/abs/10.1021/la0634600

Chen H, Zhang Y, Zhong Q. 2015. Physical and antimicrobial properties of spray-dried zein–casein nanocapsules with co-encapsulated eugenol and thymol. J. Food Eng. [Internet] 144:93–102. Available from: http://linkinghub.elsevier.com/retrieve/pii/S026087741400329X

Chen H, Zhong Q. 2014. Processes improving the dispersibility of spray-dried zein nanoparticles using sodium caseinate. Food Hydrocoll. [Internet] 35:358–366. Available from: http://dx.doi.org/10.1016/j.foodhyd.2013.06.012

Destribats M, Rouvet M, Gehin-Delval C, Schmitt C, Binks BP. 2014. Emulsions stabilised by whey protein microgel particles: towards food-grade Pickering emulsions. Soft Matter [Internet] 10:6941–54. Available from: http://www.ncbi.nlm.nih.gov/pubmed/24675994

Dickinson E. 2010. Food emulsions and foams: Stabilization by particles. Curr. Opin. Colloid Interface Sci. [Internet] 15:40–49. Available from: http://linkinghub.elsevier.com/retrieve/pii/S1359029409001010

Dickinson E. 2011. Mixed biopolymers at interfaces: Competitive adsorption and multilayer structures. Food Hydrocoll. [Internet] 25:1966–1983. Available from: http://dx.doi.org/10.1016/j.foodhyd.2010.12.001

Dickinson E. 2012. Use of nanoparticles and microparticles in the formation and stabilization of food emulsions. Trends Food Sci. Technol. [Internet] 24:4–12. Available from: http://linkinghub.elsevier.com/retrieve/pii/S0924224411001981

Dickinson E. 2015. Structuring of colloidal particles at interfaces and the relationship to food emulsion and foam stability. J. Colloid Interface Sci. [Internet] 449:38–45. Available from: http://linkinghub.elsevier.com/retrieve/pii/S0021979714007292

Dickinson E, Golding M. 1997. Depletion flocculation of emulsions containing unadsorbed sodium caseinate. Food Hydrocoll. [Internet] 11:13–18. Available from: http://dx.doi.org/10.1016/S0268-005X(97)80005-7

Evers CHJ, Andersson T, Lund M, Skepö M. 2012. Adsorption of unstructured protein β-casein to hydrophobic and charged surfaces. Langmuir 28:11843–11849.

de Folter JWJ, van Ruijven MWM, Velikov KP. 2012. Oil-in-water Pickering emulsions stabilized by colloidal particles from the water-insoluble protein zein. Soft Matter [Internet] 8:6807. Available from: http://xlink.rsc.org/?DOI=c2sm07417f

Gao Z-M, Yang X-Q, Wu N-N, Wang L-J, Wang J-M, Guo J, and others. 2014. Protein-based pickering emulsion and oil gel prepared by complexes of zein colloidal particles and stearate. J. Agric. Food Chem. [Internet] 62:2672–8. Available from: http://www.ncbi.nlm.nih.gov/pubmed/24621373

Ghouchi Eskandar N, Simovic S, Prestidge CA. 2007. Synergistic effect of silica nanoparticles and charged surfactants in the formation and stability of submicron oil-in-water emulsions. Phys. Chem. Chem. Phys. [Internet] 9:6426. Available from: http://www.ncbi.nlm.nih.gov/pubmed/18060160

Golemanov K, Tcholakova S, Kralchevsky P a., Ananthapadmanabhan KP, Lips a. 2006. Latex-particle-stabilized emulsions of anti-bancroft type. Langmuir 22:4968–4977.

Li KK, Zhang X, Huang Q, Yin SW, Yang XQ, Wen QB, and others. 2014. Continuous preparation of zein colloidal particles by Flash NanoPrecipitation (FNP). J. Food Eng. [Internet] 127:103–110. Available from: http://dx.doi.org/10.1016/j.jfoodeng.2013.12.001

Liang H-N, Tang C. 2014. Pea protein exhibits a novel Pickering stabilization for oil-in-water emulsions at pH 3.0. LWT - Food Sci. Technol. [Internet] 58:463–469. Available from: http://linkinghub.elsevier.com/retrieve/pii/S002364381400173X

Liu F, Tang C-H. 2013. Soy protein nanoparticle aggregates as pickering stabilizers for oil-in-water emulsions. J. Agric. Food Chem. [Internet] 61:8888–98. Available from: http://www.ncbi.nlm.nih.gov/pubmed/23977961

Liu F, Tang C-H. 2015. Soy glycinin as food-grade Pickering stabilizers: Part. I. Structural characteristics, emulsifying properties and adsorption/arrangement at interface. Food Hydrocoll. [Internet]:1–14. Available from: http://linkinghub.elsevier.com/retrieve/pii/S0268005X15001897

Liu F, Tang CH. 2014. Emulsifying properties of soy protein nanoparticles: Influence of the protein concentration and/or emulsification process. J. Agric. Food Chem. [Internet]

62:2644–2654. Available from: http://pubs.acs.org/doi/abs/10.1021/jf405348k

McClements DJ. 2012. Advances in fabrication of emulsions with enhanced functionality using structural design principles. Curr. Opin. Colloid Interface Sci. [Internet] 17:235–245. Available from: http://linkinghub.elsevier.com/retrieve/pii/S1359029412000702

Nel AE, Mädler L, Velegol D, Xia T, Hoek EM V, Somasundaran P, and others. 2009. Understanding biophysicochemical interactions at the nano-bio interface. Nat. Mater. [Internet] 8:543–557. Available from: http://dx.doi.org/10.1038/nmat2442

Nesterenko A, Drelich A, Lu H, Clausse D, Pezron I. 2014. Influence of a mixed particle/surfactant emulsifier system on water-in-oil emulsion stability. Colloids Surfaces A Physicochem. Eng. Asp. [Internet] 457:49–57. Available from: http://linkinghub.elsevier.com/retrieve/pii/S0927775714004944

Niu F, Zhou J, Niu D, Wang C, Liu Y, Su Y, and others. 2015. Food Hydrocolloids Synergistic effects of ovalbumin / gum arabic complexes on the stability of emulsions exposed to environmental stress. Food Hydrocoll. [Internet] 47:14–20. Available from: http://dx.doi.org/10.1016/j.foodhyd.2015.01.002

Patel AR, Bouwens ECM, Velikov KP. 2010. Sodium caseinate stabilized zein colloidal particles. J. Agric. Food Chem. [Internet] 58:12497–503. Available from: http://www.ncbi.nlm.nih.gov/pubmed/21077613

Qi F, Wu J, Sun G, Nan F, Ngai T, Ma G. 2014. Systematic studies of Pickering emulsions stabilized by uniform-sized PLGA particles: preparation and stabilization mechanism. J. Mater. Chem. B [Internet] 2:7605–7611. Available from: http://dx.doi.org/10.1039/C4TB01165A

San-Miguel A, Behrens SH. 2012. Influence of nanoscale particle roughness on the stability of pickering emulsions. Langmuir 28:12038–12043.

Svensson O, Kurut A, Skepö M. 2014. Adsorption of β-casein to hydrophilic silica surfaces. Effect of pH and electrolyte. Food Hydrocoll. 36:332–338.

Tcholakova S, Denkov ND, Banner T. 2004. Role of surfactant type and concentration for the mean drop size during emulsification in turbulent flow. Langmuir 20:7444–7458.

Tcholakova S, Denkov ND, Ivanov IB, Campbell B. 2002. Coalescence in beta-Lactoglobulin-Stabilized Emulsions : Effects of Protein Adsorption and Drop Size. Langmuir 18:8960–8971.

Tcholakova S, Denkov ND, Ivanov IB, Campbell B. 2006. Coalescence stability of emulsions containing globular milk proteins. Adv. Colloid Interface Sci. 123–126:259–293.

Tcholakova S, Denkov ND, Lips A. 2008. Comparison of solid particles, globular proteins and surfactants as emulsifiers. Phys. Chem. Chem. Phys. [Internet] 10:1608–27. Available from: http://www.ncbi.nlm.nih.gov/pubmed/18060160

Tcholakova S, Denkov ND, Sidzhakova D, Ivanov IB, Campbell B. 2003. Interrelation between drop size and protein adsorption at various emulsification conditions. Langmuir 19:5640–5649.

Thomar P, Nicolai T. 2015. Dissociation of native casein micelles induced by sodium caseinate. Food Hydrocoll. [Internet]. Available from: http://dx.doi.org/10.1016/j.foodhyd.2015.03.016

Tikekar R V., Pan Y, Nitin N. 2013. Fate of curcumin encapsulated in silica nanoparticle stabilized Pickering emulsion during storage and simulated digestion. Food Res. Int. [Internet] 51:370–377. Available from: http://dx.doi.org/10.1016/j.foodres.2012.12.027

Wang L-J, Hu Y-Q, Yin S-W, Yang X-Q, Lai F-R, Wang S-Q. 2015. Fabrication and Characterization of Antioxidant Pickering Emulsions Stabilized by Zein/Chitosan Complex Particles (ZCPs). J. Agric. Food Chem. [Internet] 63:2514–2524. Available from: http://pubs.acs.org/doi/abs/10.1021/jf505227a

Wang LJ, Yin YC, Yin SW, Yang XQ, Shi WJ, Tang CH, and others. 2013. Development of novel zein-sodium caseinate nanoparticle (ZP)-stabilized emulsion films for improved water barrier properties via emulsion/solvent evaporation. J. Agric. Food Chem. [Internet] 61:11089–11097. Available from: http://pubs.acs.org/doi/full/10.1021/jf4029943

Wang Y, Padua GW. 2012. Nanoscale characterization of zein self-assembly. Langmuir 28:2429–2435.

Wu J, Shi M, Li W, Zhao L, Wang Z, Yan X, and others. 2015. Pickering emulsions stabilized by whey protein nanoparticles prepared by thermal cross-linking. Colloids Surfaces B Biointerfaces [Internet] 127:96–104. Available from: http://linkinghub.elsevier.com/retrieve/pii/S0927776515000363

Ye A. 2008. Interfacial composition and stability of emulsions made with mixtures of commercial sodium caseinate and whey protein concentrate. Food Chem. 110:946–952.

Zhang Y, Niu Y, Luo Y, Ge M, Yang T, Yu L, and others. 2014. Fabrication, characterization

and antimicrobial activities of thymolloaded zein nanoparticles stabilized by sodium caseinate-chitosan hydrochloride double layers. Food Chem. [Internet] 142:269–275. Available from: http://dx.doi.org/10.1016/j.foodchem.2013.07.058

Zhong Q, Jin M. 2009. Zein nanoparticles produced by liquid–liquid dispersion. Food Hydrocoll. [Internet] 23:2380–2387. Available from: http://linkinghub.elsevier.com/retrieve/pii/S0268005X09001374

CHAPTER 4

Microfluidic fabrication of hollow protein microcapsules for rate-controlled release[2]

4.1 Abstract

Droplet-based microfluidics is an emerging technique that is capable of producing sophisticated supramolecular microcapsules within one-step. However, food materials, due to their physical and chemical complexity, have limited success with microfluidic processes. The objective of this work is to produce food-grade protein microcapsules in a microfluidic system and to control their structural properties by adjusting formulation and flow rates. In this study, a T-junction microfluidic chip was used to create an interface for zein to self-assemble, and therefore form microcapsules with tunable particle size, pore distribution, and permeability. Our SEM and CLSM results show that the particle size and the number of pores increased with the flow rate of dispersing phase, while the pore size decreased with the flow rate of dispersing phase. In order to quantify release profiles, release half-life (t_{50}) was used as an indicator for the particle permeability. A wide range of t_{50}, from 3 to 62 minutes was achieved, by changing zein concentration and the flow rate of dispersing phase. Using Rhodamine B as an encapsulant, the release rate was positively correlated with the zein concentration and the flow rate of the dispersing phase. Finally, a response surface analysis of formulation and flow rate was applied to aid to design a carrier with desirable release rate.

Keywords

Microfluidics, zein, controlled release, self-assembly, internal phase separation

[2] ***The contents of this section have been published in: Feng, Y., & Lee, Y. (2017). Microfluidic fabrication of hollow protein microcapsules for rate-controlled release. RSC Advances, 7(78), 49455-49462. with the reprint permission from the publisher.***

4.2 Introduction

The fabrication of microcapsules as a carrier for stabilizing and delivering core materials have been extensively studied and widely applied in biomedical, food, cosmetic, agricultural and many other industries(Gouin 2004; Kaufman and others 2015). Recently, controlling the release profile of a core from microcapsules is gaining increased attention, and one of the most well-known approaches is to use colloidosmes. Colloidosomes are microcapsules whose shells are consisted of densely packed colloidal particles as building blocks (Dinsmore and others 2002; Lee and Weitz 2008; Thompson and others 2014). The primary features of colloidosomes include the integrity of microcapsule during release, controllable permeability, stimulus-triggering ability and physical stability, which make colloidosomes desirable for releasing pharmaceuticals, bioactive compounds, and fragrances in a controlled manner (Lee and Weitz 2008; San Miguel and others 2010). The conventional approaches to assembling colloidosomes possess several limitations such as complexity, low-efficiency, lack of uniformity, and requirement of toxic solvents during the process (Lee and Weitz 2008; Thompson and others 2014). Therefore, it is of great interest to develop an alternative strategy that is simple and environmental-friendly while features similar advantages such as controllable release rate.

Droplet-based microfluidics platform is an emerging technique that has become a topic of interest for analytical (e.g. cell analysis, DNA assays, high-throughput screening)(Mark and others 2010) and synthetic (e.g. encapsulation, polymerization, anti-solvent nanoparticle fabrication)(Headen and others 2014; Kim and others 2015; Olenskyj and others 2017) applications. For encapsulation applications, microfluidic platform provides precise particle size control over a wide range, which is vital for ensuring product homogeneity(Headen and others 2014). Microfluidic platform has been reported as a single-step process for fabricating many sophisticated supramolecular microcapsules, for example, non-spherical particles(Shum and others 2010), porous microcapsules(Zhang and others 2012), alginate microspheres(Workman and others 2008), dendritic microcapsules (Zheng and others 2014), cross-linked protein capsules(Zhou and others 2014), and biological microgels(Zhang and others 2007). Microfluidic chip has also been deployed to trigger precisely controlled interfacial reactions, for fabricating complex and multiple emulsions(Zhao and Middelberg 2009; Zhao and Middelberg 2013). However, most of these approaches require crosslinking

agents, UV treatment, and polymer precursors, which may be toxic and potentially cytotoxic. These limitations are especially unfavorable for encapsulating live cells, as well as sensitive pharmaceuticals and nutraceuticals(Headen and others 2014). Furthermore, there have been very few successes in using biological materials in microfluidic processes such as proteins, which could be prone to clog the microfluidic channels.

Zein is a storage protein from corn that is insoluble in water but capable of self-assembly to form many types of microstructures such as films(Y. Zhang and others 2015), nanoparticles(Pan and Zhong 2016a; Pan and Zhong 2016b), or Pickering emulsions(Feng and Lee 2016). Its distinct amino acid composition and rigidity in the solid state make it a potential food-grade wall material for fabricating diffusion-driven controlled-release systems. To date, self-assembly of zein could only be achieved with uncontrolled or limited-controlled manners (e.g., evaporation induced self-assembly(Wang and Padua 2012), anti-solvent self-assembly(Zhong and Jin 2009)). However, recent advances made it possible to direct particle assembly using microfluidic platform(Brugarolas and others 2013). Many studies had explored the application of zein as delivery carriers, although several limitations were reported as well (Luo and others 2011; Chen and Zhong 2015; Hu and others 2016). One inherent limitation is that current zein-based delivery systems are only able to carry hydrophobic compounds, in which the encapsulation was achieved during a co-precipitation of zein and encapsulant in water. Therefore, the encapsulant has to be insoluble in water but soluble in 60%-90% ethanol. The second limitation is associated with particle size control that, only submicron (100-300 nm) zein nanoparticles were able to be generated (Zhong and Jin 2009). Small particles generally release encapsulated compounds rapidly due to their high surface-volume ratios and instant particle disintegration in the gastro-intestinal (GI) tract, thus are not feasible for a sustained release (Golomb and others 1990). In this study, we report a facile method to fabricate hollow microcapsules with tunable release rates, using a food-grade protein, zein. To the author's knowledge, this is the first approach creating an interface to direct zein self-assembly and form a rigid shell. A water soluble dye Rhodamine B was used as a tracer to indicate the permeability of microcapsule and analyze the release rate.

4.3 Materials and methods

4.3.1 Materials

Zein (Z3625, Sigma-Aldrich, St. Louis, MO) dissolved in 70% (v/v) ethanol (200 Proof, Decon Laboratories, King of Prussia, PA) was used as the dispersing phase. Tributyrin (W222305, Sigma-Aldrich, St. Louis, MO) containing 2% (w/v) soy lecithin (MP Biomedicals Inc, Solon, OH) was used as the continuous phase. Rhodamine B (R6626, Sigma-Aldrich, St. Louis, MO) was added into the dispersing phase at 2 mg/ml, to assess the rate of release. Hexane (Macron Fine Chemicals, Center Valley, PA) was used to wash the microcapsules. No. 42 (pore size 2.5 μm) Whatman filter paper (Whatman Inc., Florham Park, NJ) was used to collect final products.

4.3.2 Microfluidic fabrication

The dispersing phase was prepared by dissolving various amount (2%, 4% and 6% w/v) of zein into an ethanol-water binary system containing 70% (v/v) ethanol. The continuous phase was prepared by mixing 2% (w/v) of soy lecithin with tributyrin by stirring at 250 rpm for overnight, followed by centrifugation at 2000 g for 10 min to remove impurities. Hollow zein microcapsules were then produced in a 100 μm T-junction microfluidic chip (Dolomite, UK) through internal phase separation and the mechanism is shown in Figure 4.1. The samples prepared in this study are listed in Table 4.1. Three flow rate combinations were chosen for this study based on our preliminary study. Flow rates were controlled using a Harvard Model 11 Elite syringe pump (Harvard Apparatus Inc., Holliston, MA). An amount of 2 mg/ml Rhodamine B (Sigma-Aldrich, St. Louis, MO) was added into the dispersing phase as a release model indicator. Once collected, the capsules were immediately washed with hexane for three times on a filter paper with vacuum. The final microcapsules were obtained by transferring the filtered samples into a convective oven to remove excessive water at 30°C for 6 hours.

4.3.3 Characterization of microcapsules

Scanning electron microscopy (SEM).

The surface morphology of final products was imaged using a Quanta 450 FEG environmental scanning electron microscope (ESEM, FEI Company, Hillsboro OR) located in Beckman Institute. The blocks were mounted on SEM stubs and coated with 60 nm of gold-palladium using a Desk-II turbo sputter coater (Denton Vacuum,

Moorestown, NJ). Flash-Dry colloidal silver paint (cat. no. 04998-AB; SPI Supplies, West Chester PA) was applied to the blocks to ensure proper grounding. The embedded particles were then imaged using a Quanta 450 FEG environmental scanning electron microscope (ESEM; FEI Company, Hillsboro OR). An image analysis was then performed using Image-Pro Plus 7.0 software (Media Cybernetics, MD, USA) for calculating the particle size of each samples.

Confocal laser scanning microscopy (CLSM).

A CLSM was used to visualize the internal structure of the microcapsules. Freshly collected microcapsule suspensions (1 ml) were stained with 40 μL of Nile blue (0.1%) for 2 h. A Zeiss LSM 700 confocal mi- croscope (Zeiss, Germany) was operated using the excitation wavelength of 488 nm for the Nile blue dye to visualize the emulsions. Images were taken at a magnification of 20x and further processed using the instrumental software.

X-ray diffraction (XRD).

The XRD patterns were assessed using a diffractometer (D5000, Siemens) with Cu-Kα radiation (λ=1.5406 Å) and 0.2° step scan from 5 to 35° in 2θ angle. The scanning rate was set at 1°/min. The d-spacing for a given scattering angle, 2θ, was calculation with Bragg's law (1).

$$d = \frac{\lambda}{2\,sin\theta} \quad (1)$$

Where λ is the wavelength of the Cu-Kα radiation.

Circular dichroism spectroscopy (CD).

The CD spectra were recorded with a JASCO J-715 spectropolarimeter (Jasco Inc., Easton, MD). Samples were placed in a quarts cell with a 1 cm path length. The measurement was conducted over the range of 200-250 nm at 25°C, with the scanning speed of 50nm/min, and the resolution of 1 nm. The content of α-helix, β-sheet, and random coil was calculated using the BeStSel software (Micsonai and others 2015), which could be accessed online at http://bestsel.elte.hu. The Savitsky-Golay smoothing algorithm was used, with a polynomial order of 3 and a smoothing window of 20 points, according to the literature (Greenfield 2006).

4.3.4 Release profiles

Release curves.

To study the release profile, approximately 5mg of microcapsules were dispersed into 50 ml of deionized (DI) water with constant stirring at 250 rpm to release the water soluble dye, Rhodamine B. In total, a number of twelve measurements were taken at 1, 3, 5, 10, 20, 30, 45, 60, 120, 180, 360, and 1440 min, respectively, to evaluate the rate of release by measuring the dye concentration in water. For each measurement, 0.5 ml of the dispersion was removed using a 3 ml dispersible syringe (Exelint International Co., Los Angeles, CA), and the aquilot was then filtered using a 4 mm syringe filter with pore size 0.45 μm (Restek Corp., Bellefonte, PA), to avoid potential contamination by the microcapsules. An equivalent volume of DI water was supplemented (Chen and others 2015) upon the removal of the sample. The fluorescence intensity of the aliquot was measured using a SpectraMax M2e microplate reader (Molecular Devices, Sunnyvale, CA) in triplicate. An excitation wavelength and emission wavelength were set at 420 nm and 565 nm, respectively (Wang and others 2015). The fraction of cumulative release versus time was normalized and plotted with the assumption that complete release is achieved at 24 hours.

Release curve fitting and release half-lives (t50).

To analyze the release kinetics, Korsmeyer-Peppas model was used to fit the release curve ($0 \leq y \leq 0.6$)(Korsmeyer and others 1983) using Matlab software R2014a (The Mathworks Inc., Natick, MA), and the fitting equation is shown below as Equation (2).

$$\frac{M_t}{M_\infty} = kt^n \tag{2}$$

Where M_t/M_∞ is the fractional release of Rhodamine B, t is the release time, k is a kinetic constant characteristic, and n is an exponent which characterizes the mechanism of release of the tracer. Release half-lives (t50) were then derived from the fitting equation. The variation of release half-lives with processing conditions were subjected to statistical analysis using response surface methodology by Matlab.

4.4 Results and discussion

4.4.1 Mechanisms of microcapsule formation

Figure 4.1 is a schematic diagram displaying the formation of hollow zein microcapsules in a T-junction microfluidic chip. A 70% (v/v) ethanol solution containing zein and Rhodamine B was introduced to the microfluidic channel as the dispersing phase, and the continuous phase is composed of tributyrin containing 2% (w/v) soy lecithin as an emulsifier. Upon the mixing at the joint, a jetting regime was observed where the dispersing phase maintains parallel flow before breaking up into droplets within the flow rates tested in this study. The formation of different regimes is determined by two competing forces, viscous dragging force, and surface tension(Utada and others 2007; Muijlwijk and others 2016). Herein, we used the jetting regime to generate particles considering its high yield and less risk of clogging, at the expense of losing a certain degree of mono-dispersity in particle size compared to the dripping regime.

Ethanol in the dispersing phase is miscible with tributyrin in the continuous phase, while water is not. In this study, the flow rate of continuous phase was much higher (more than 30 times) than the flow rate of dispersing phase, such that the ethanol in the dispersing phase would constantly diffuse into the continuous phase due to the concentration gradient. Once the dispersing droplets dispatch from the parallel flow, a greater interface area is created which will further accelerate ethanol migration. At the same time, zein self-assembly is triggered by the continuous decrease of ethanol concentration inside the droplet. The formation of wall starts at the droplet interface, where the ethanol concentration is lower than the center of the droplet because of the ethanol flux. Eventually, the liquid remaining in the droplet will be mostly water, and zein becomes solid as the wall material. The self-assembly of zein is a complex process, which involves a transformation from α-helices to β-sheets, followed by side-by-side packing of β-sheets to form a rigid structure(Wang and Padua 2012). Typically, this process is induced by evaporation of ethanol to produce film structure. In this work, an oil-water interface was created to direct zein self-assembly in droplet microfluidics chips. The self-assembly in the internal phase separation process was verified by CD spectroscopy and XRD analysis. The CD spectrum presented in the Figure 4.2 compared the secondary structure of raw zein and microfluidic treated zein, using sample 5 as an example. The diminishment of α-helix and formation of β-sheet was observed, which indicates that self-assembly of zein could occur in a short time, on the scale of a few seconds. Secondary structure is an important property for the microcapsules, and it

might also affect release profiles, though no studies have been reported yet. In terms of the secondary structure formation of zein, it is highly related to the residence time of zein self-assembly. Typically the time needed to make a difference for zein is in the scale hours (Wang and Padua 2012). However, the residence time of microfluidic process is short, which is usually in the scale of seconds. So it was expected to have that the similar secondary structures between the particles in this study. In order to verify, three samples with different zein concentrations and dispersing phase flow rates were selected for CD spectrums. As expected, the differences among their secondary structures are minor. More details could be found in the supplementary information.

The XRD patterns shown in the Figure 4.3 also compared the structure between raw zein and zein microcapsules (sample 5). For both samples, there are two distinctive peaks exhibiting at the same 2θ angles, which are close to 9° and 21°. Based on the d-spacing equation (1), the characteristic d-spacing values could be calculated as 9.8 Å and 4.2 Å, respectively. According to the literature, these two characteristic d-spacing values have been clearly interpreted. The smaller d-spacing (4.2 Å) is related to the back distance within the α-helix, whereas the longer d-spacing (9.8 Å) comes from the lateral α-helix packing(Wang and others 2005). The ratio between these two peaks is an indication of the degree of α-helix packing (Wang and others 2005; Liu and others 2016). Physical and chemical changes, such as thermal treatment and the anti-solvent process as in this study, could induce secondary structural transformation. One notable and common transition is the helix-to-coil transition(Z. Zhang and others 2015), which we also found in this study. Since unwinding of α-helix is a necessary step in the helix-to-coil transition, therefore the peak ratio evolution before and after microfluidic treatment is an important sign of helix-to-coil transition and secondary structural transformation. In this study, it was found that the structure of lateral α-helix packing decreased in zein microcapsules, indicating the occurrence of structural transformation (Figure 4.3).

4.4.2 Morphology and Internal structures of zein microcapsules

The morphology of the dried particles at various zein concentrations and flow rate combinations are shown in Figure 4.4. One of the promising features of a microfluidic device is that the droplet size can be finely tuned by adjusting the flow rates of dispersing and continuous phases(Utada and others 2007). An image analysis was performed to calculate the particle size of microcapsules, and the results are shown in

the figure 4.5. A trend was identified that the size of the microcapsule increased with increasing the flow rate of dispersing phase, while zein concentration had less impact. Flow rate ratio is one of the predominant factors governing the droplet size, which has been described in a previous study(Muijlwijk and others 2016). On the other hand, zein concentration in the dispersing phase determined the solid content in the droplet, and the droplets with greater amount of zein are more resistant against shrinking during ethanol diffusion, which also resulted in larger microcapsule size.

Precise control over particle size generally correlates with enhanced control of the rate of release of an encapsulant. It was observed from the SEM images that the particle size was relatively uniform at low dispersing flow rates (0.1 and 0.2 ml/hr), but a larger variation of particle size was observed when the flow rate of dispersing phase reached 0.3 ml/hr. A probable reason is that the parallel flow extended too far in the microfluidic channel when the flow rate of dispersing phase increased. Therefore the detachment occurs at later time, leaving a short residence time for zein to self-assemble. Without a completely hardened droplet surface, microcapsules may coalesce in the tubing or collector, and result in non-uniform particle size. There are two other reasons that might also cause the polydispersity of proteins capsules in this study. First, zein is a biologically originated material, which is naturally inhomogeneous. Zein contains α-zein, β-zein, γ-zein and δ-zein, and they have tendency to form micelle or nanoaggregates in the solution and therefore alter local concentration of each composition(Kim and Xu 2008). Another reason could be related to the morphological change during drying process. When the water is removed from core, there could be different degrees of shrinkage which may result in different shape and size. For example, bowl-like structures and wrinkled structures have been found, depending on their hollow core distribution patterns.

Figure 4.6 displays the internal structure of zein microcapsules captured using CLSM. The images show that the internal structure of microcapsules is hollow, and the number of hollow cores varied from single core to multiple cores, by simply adjusting the flow rate of dispersing phase. At lower flow rate of the dispersing phase it formed zein microcapsules with less number of hollow cores, while a higher dispersing flow rate tended to form increased number of hollow cores. The differences in the number of hollow cores could be attributed to droplet size, which could affect the rate of ethanol diffusion during internal phase separation process. When the droplet size was small,

ethanol could be readily extracted into the continuous phase, tributyrin, leaving a large but single hollow core, while the slow diffusion of ethanol to the continuous phases is expected in the case of large droplets. The formation of internal structure is difficult to predict, due to the complexity of two competing processes, ethanol diffusion and zein self-assembly. The rate of either process could have a significant impact on the other, for example, the formation of zein network could decrease the rate of ethanol diffusion. Therefore, the general conclusion of a positive correlation between the flow rate of dispersing phase and the number of hollow cores may not be drawn. However, this method did provide a facile approach to tune the internal structure of microcapsules.

4.4.3 Release profiles

Figure 4.7(a) shows the release profiles and fitted curves of all samples tested in this study. The release test was carried out for 24 hours, and approximately 60% of Rhodamine was recovered. This number is reasonable, because Rhodamine B has greater affinity to ethanol than water and a considerable fraction of Rhodamine B was diffused along with ethanol. A curve fitting indicates that the release was driven by both diffusion and case II transportation, due to the occurance of strain retardation during the hydration and swelling of microcaspules.

The samples produced with 2% zein released the dye fairly fast, probably due to a formation of thinner wall than the samples with higher zein concentration. Increasing zein concentration to 4% was able to prolong the release while increasing zein concentration to 6% did not induce further delay of the release. The cross-section images indicated that the difference in pore size between 4% and 6% zein samples might not be significant, so it is reasonable to conclude that further increase of zein concentration may not further modify the release profile. On the other hand, increasing the flow rate of the dispersing phase could also prolong the release. It has been discussed above that the larger size of microcapsules was generated at higher dispersing flow rates. Usually, larger particles possess smaller surface to volume ratios, so the release of the dye was hindered as well. Another reason could be associated with the structure of microcapsules. Those microcapsules with single large cores could release core material rather faster when compared to those microcapsules with multiple small pores, which could be attributed to the differences in wall thickness. For the microcapsules with single large cores, the wall is thin which favors fast diffusion. However, for those microcapsules with porous structure with multiple small cores, the pores embedded in

the center have relatively thick and multiple walls to pass through during diffusion. Similar finding and mechanism were also reported in a previous study with quantifications (Mehta and others 2000). When releasing drugs in *in-vitro* models, the rate of release is more complicated and also depends on other factors such as degradation of microcapsules(Klose and others 2006). Therefore, further development and optimization is necessary to engineer the microcapsule for applications such as gastro-intestinal delivery. Response surface is a robust methodology to study multivariable experiment and to find the experimental region that would generate desirable results(Hou and Regenstein 2006). Figure 4.7(b) shows a response surface that correlates the release half-lives (t_{50}) with processing conditions ($R^2 = 0.852$). Based on the response surface prediction, a wide range of t_{50}, from 3 minutes to 62 minutes, was achieved by adjusting zein concentrations and the flow rate ratios. Microcapsules that capable of sustained release could be used as intestinal delivery carriers for enhanced bioavailability, or encapsulating antimicrobial components and fragrances for extended efficacy(Shi and Tan 2002; Sarkar and others 2016). On the other hand, microcapsules with boost release properties could be used for flavor compounds, in order to rapidly release flavors during oral processing while to improve flavor stability during storage(Yoshii and others 2001).

4.5 Conclusions

In this study, we demonstrated a facile approach to fabricating hollow protein microcapsules in a T-junction microfluidic chip. It was a single-step process that features great biocompatibility that all the materials involved were non-hazardous. The generation of droplets in the microfluidic chip allowed the creation of an interface to direct zein self-assembly and hence the formation of microcapsules. By adjusting zein concentration in the dispersing phase and flow rates during processing, the microcapsules with various particle size, internal structure and permeability could be prepared, which will allow designing microcapsules that are versatile for various applications. This type of microcapsules can be an alternative for replacing colloidosomes. It is easier, safer and more cost effective to produce than colloidosomes. Furthermore, this study also presented a great potential of zein, as a food-grade protein, which can be incorporated for expanded applications.

4.6 Tables and figures

Table 4.1. Summary of sample code and formulation

Sample No.	Zein% (w/v)	Dispersing phase flow rate (ml/hr)	Continuous phase flow rate (ml/hr)	Flow rate ratios (continuous/dispersing)	Rhodamine B(mg/ml)	pH
1	2%	0.1	10	100	2	3.0
2	2%	0.2	10	50	2	3.0
3	2%	0.3	10	33.3	2	3.0
4	4%	0.1	10	100	2	3.0
5	4%	0.2	10	50	2	3.0
6	4%	0.3	10	33.3	2	3.0
7	6%	0.1	10	100	2	3.0
8	6%	0.2	10	50	2	3.0
9	6%	0.3	10	33.3	2	3.0

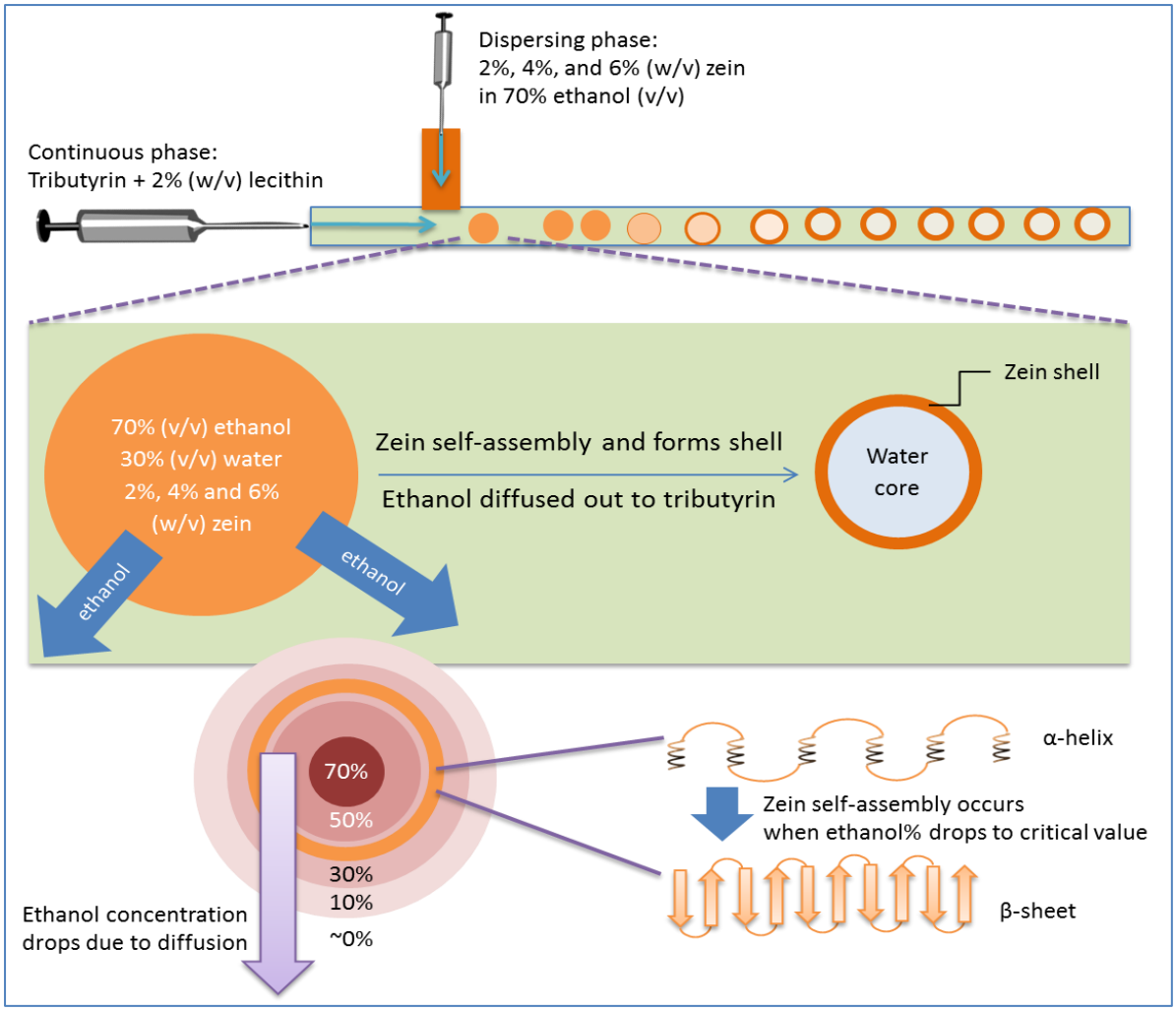

Figure 4.1. Schematic diagram illustrating the mechanism of the formation of hollow zein microcapsule in a microfluidic chip. An oil-water interface is created to initiate zein self-assembly followed by internal phase separation

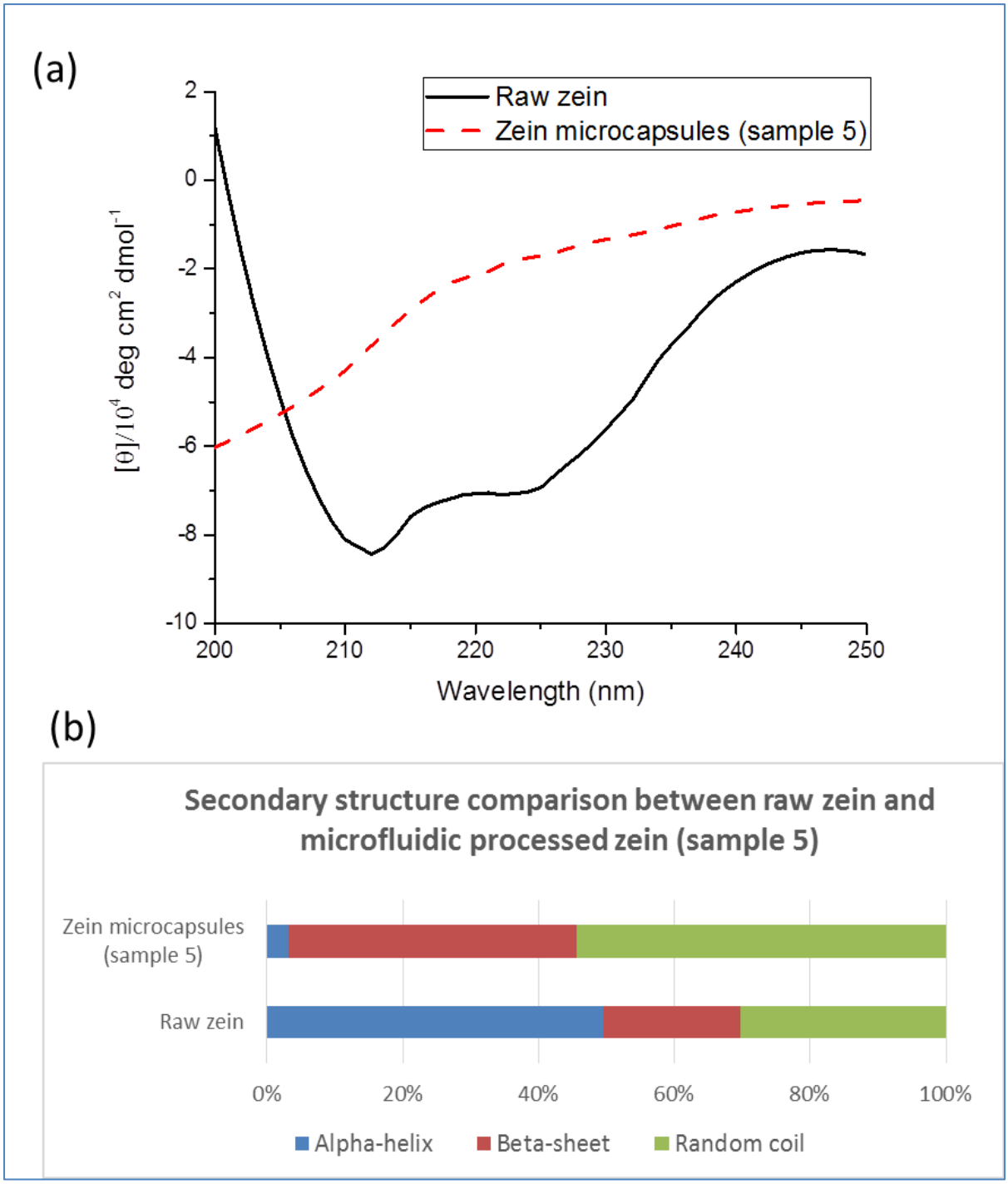

Figure 4.2. (a) CD spectra of raw zein and zein microcapsules. (b) the secondary protein structure of raw zein and zein microcapsules

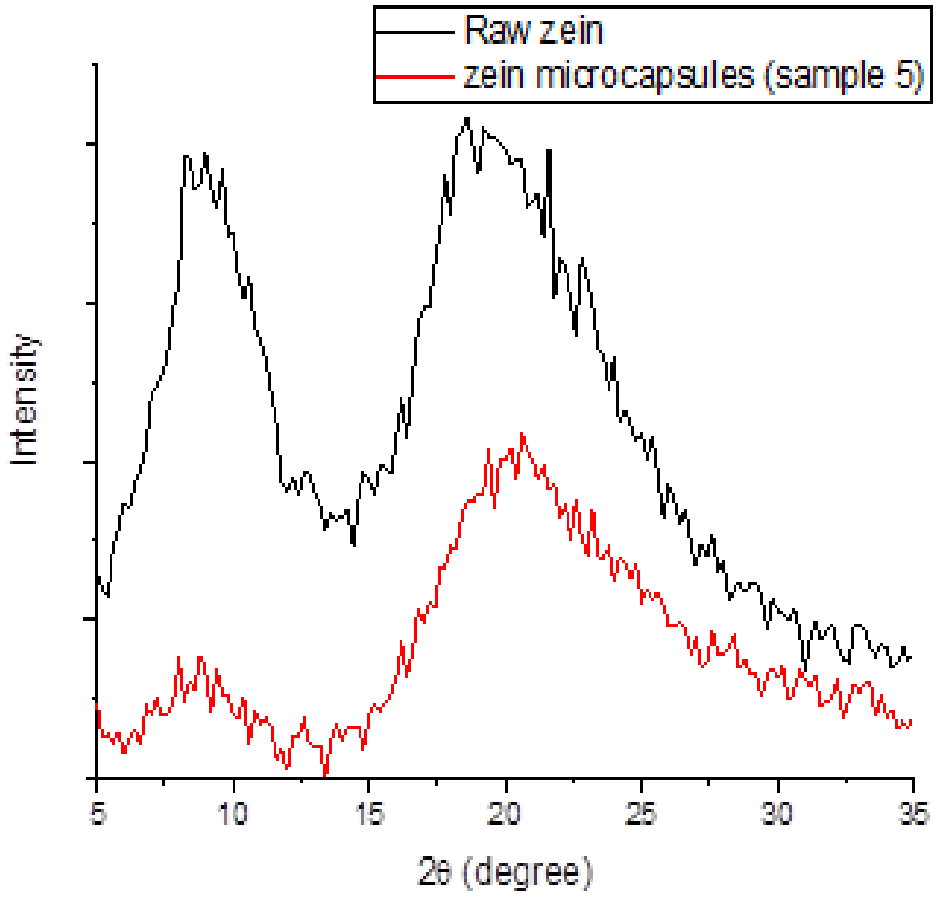

Figure 4.3. X-ray diffraction (XRD) patterns of raw zein and zein microcapsules

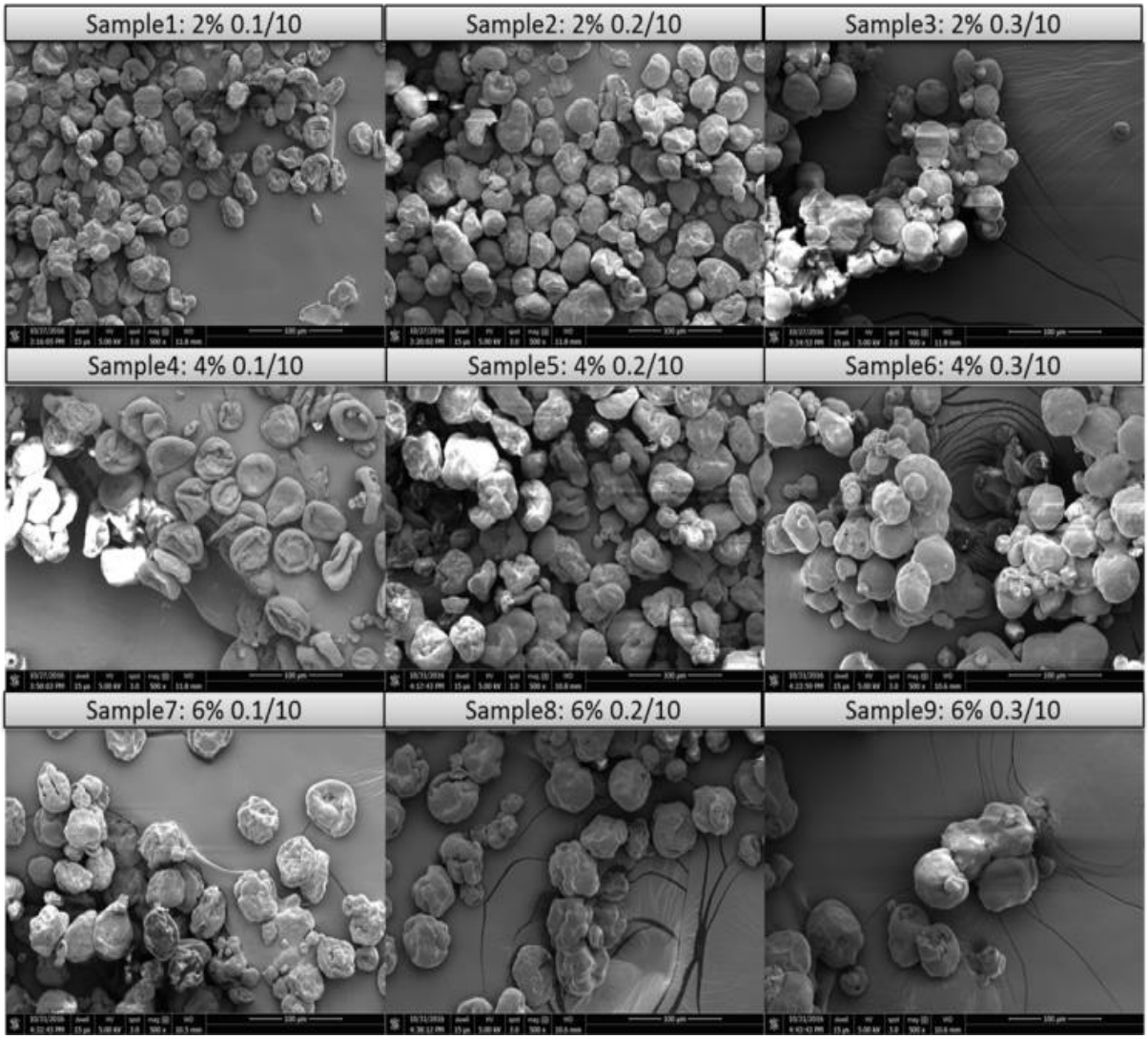

Figure 4.4. The morphology of hollow zein microcapsules produced at different concentration of zein and flow rate combinations. Sample code: zein% dispersing phase flow rate (ml/hr)/continuous phase flow rate (ml/hr). The scale bar for each image is 100 μm.

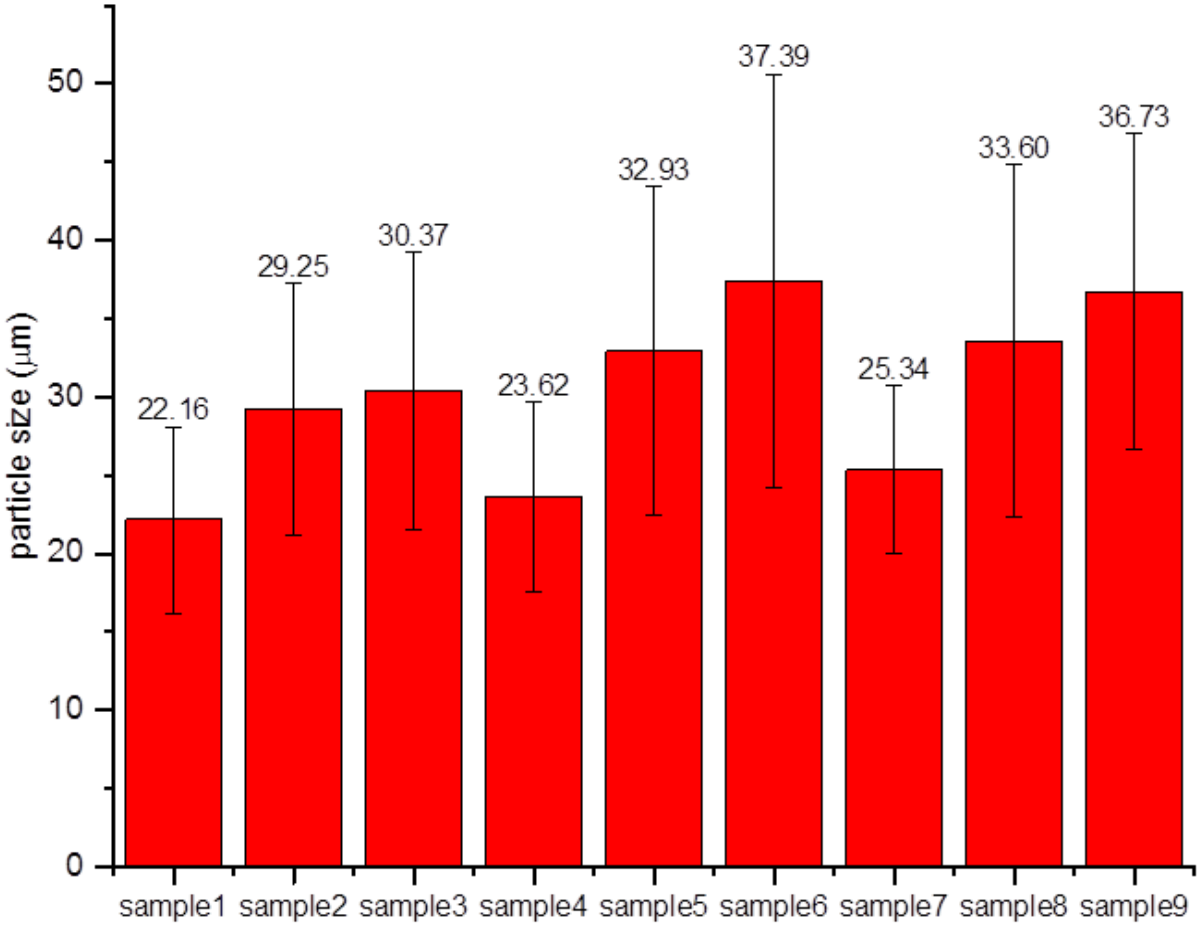

Figure 4.5. Mean particle size of microcapsules using image analysis on SEM images

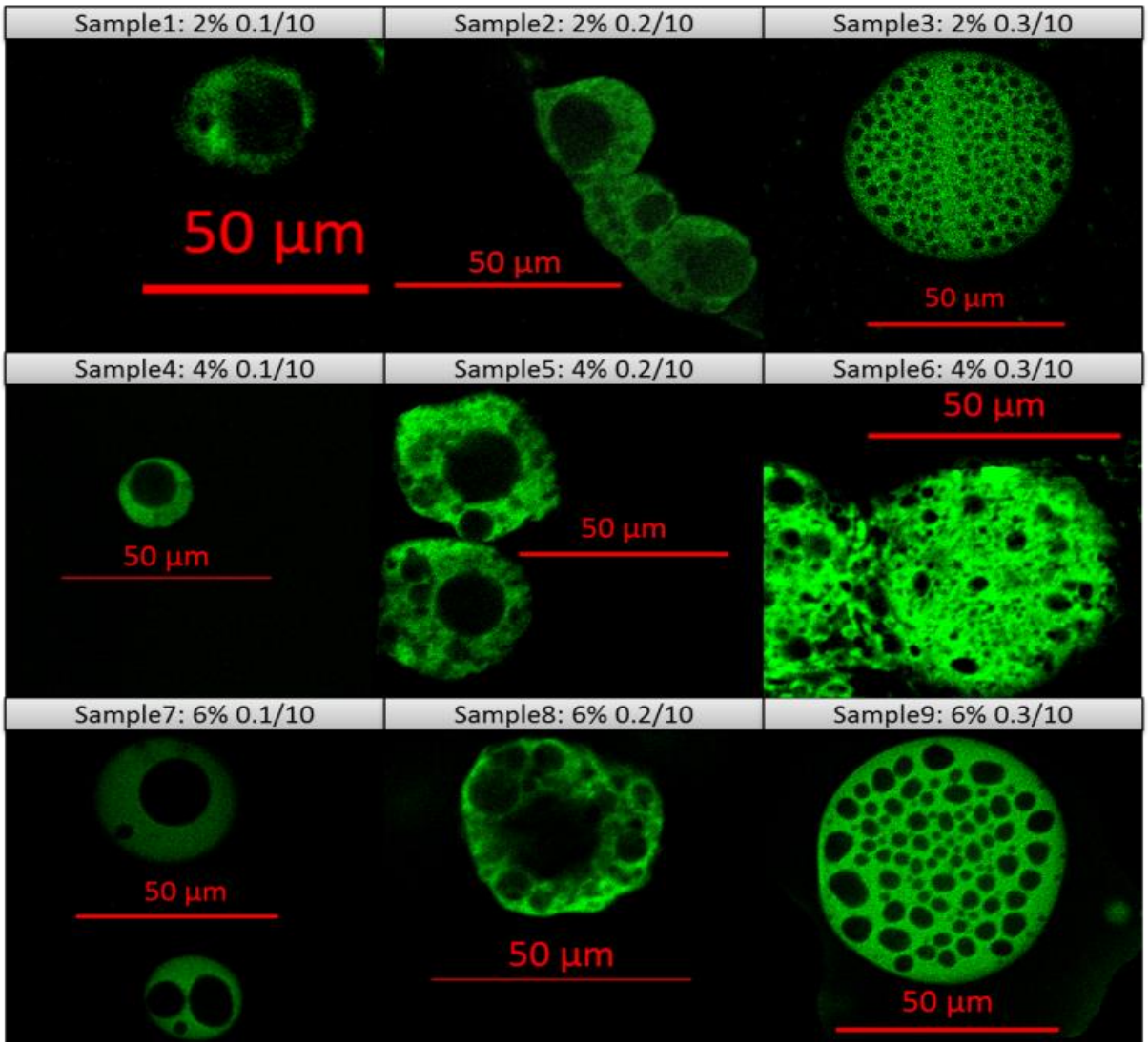

Figure 4.6. The internal structure of hollow zein microcapsules produced at different concentration of zein and flow rate combinations. Sample code: zein% dispersing phase flow rate (ml/hr)/continuous phase flow rate (ml/hr). The scale bar for each image is 50 µm.

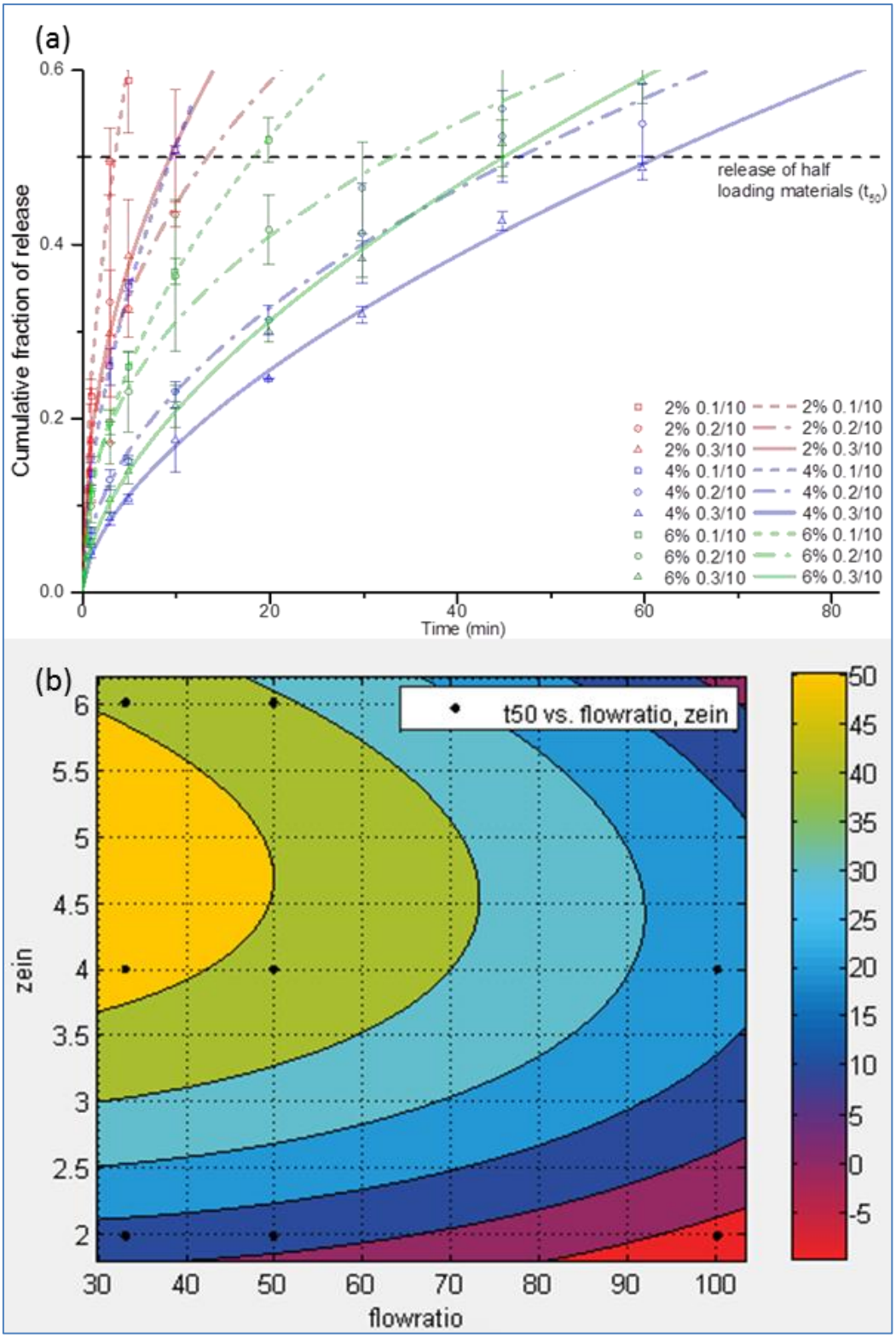

Figure 4.7. Release performance of zein microcapsules prepared at different conditions. (a) The combined release curves of all nine samples, displaying normalized fractional release versus release time (min) and fitting curves. Sample code: zein% dispersing phase flow rate (ml/hr)/continuous phase flow rate (ml/hr). (b) The response surface plot of release half-life time, as a function of zein concentration (%, w/v) and flow rate ratio.

4.7 References

Brugarolas T, Tu FQ, Lee D. 2013. Directed assembly of particles using microfluidic droplets and bubbles. Soft Matter [Internet] 9:9046–9058. Available from: http://pubs.rsc.org/en/content/articlepdf/2013/sm/c3sm50888a

Chen H, Zhang Y, Zhong Q. 2015. Physical and antimicrobial properties of spray-dried zein–casein nanocapsules with co-encapsulated eugenol and thymol. J. Food Eng. [Internet] 144:93–102. Available from: http://linkinghub.elsevier.com/retrieve/pii/S026087741400329X

Chen H, Zhong Q. 2015. A novel method of preparing stable zein nanoparticle dispersions for encapsulation of peppermint oil. Food Hydrocoll. [Internet] 43:593–602. Available from: http://linkinghub.elsevier.com/retrieve/pii/S0268005X14002616

Dinsmore a D, Hsu MF, Nikolaides MG, Marquez M, Bausch a R, Weitz D a. 2002. Colloidosomes: Selectively Permeable Capsules Composed of Colloidal Particles. Science (80-.). [Internet] 298:1006–1009. Available from: http://www.sciencemag.org/cgi/doi/10.1126/science.1074868

Feng Y, Lee Y. 2016. Surface modification of zein colloidal particles with sodium caseinate to stabilize oil-in-water pickering emulsion. Food Hydrocoll. [Internet] 56:292–302. Available from: http://linkinghub.elsevier.com/retrieve/pii/S0268005X15301971

Golomb G, Fisher P, Rahamim E. 1990. The relationship between drug release rate, particle size and swelling of silicone matrices. J. Control. Release [Internet] 12:121–132. Available from: http://linkinghub.elsevier.com/retrieve/pii/016836599090088B

Gouin S. 2004. Microencapsulation: Industrial appraisal of existing technologies and trends. Trends Food Sci. Technol. 15:330–347.

Greenfield NJ. 2006. Using circular dichroism spectra to estimate protein secondary structure. Nat. Protoc. [Internet] 1:2876–2890. Available from: http://www.nature.com/nprot/journal/v1/n6/abs/nprot.2006.202.html

Headen DM, Aubry G, Lu H, García AJ. 2014. Microfluidic-Based Generation of Size-Controlled, Biofunctionalized Synthetic Polymer Microgels for Cell Encapsulation. Adv. Mater. [Internet] 26:3003–3008. Available from: http://doi.wiley.com/10.1002/adma.201304880

Hou PZ, Regenstein J. 2006. Optimization of Extraction Conditions for Pollock Skin Gelatin.

J. Food Sci. [Internet] 69:C393–C398. Available from: http://doi.wiley.com/10.1111/j.1365-2621.2004.tb10704.x

Hu S, Wang T, Fernandez ML, Luo Y. 2016. Development of tannic acid cross-linked hollow zein nanoparticles as potential oral delivery vehicles for curcumin. Food Hydrocoll. [Internet] 61:821–831. Available from: http://linkinghub.elsevier.com/retrieve/pii/S0268005X16302946

Kaufman G, Nejati S, Sarfati R, Boltyanskiy R, Loewenberg M, Dufresne ER, and others. 2015. Soft microcapsules with highly plastic shells formed by interfacial polyelectrolyte–nanoparticle complexation. Soft Matter [Internet] 11:7478–7482. Available from: http://xlink.rsc.org/?DOI=C5SM00973A

Kim B, Jeon TY, Oh Y-K, Kim S-H. 2015. Microfluidic Production of Semipermeable Microcapsules by Polymerization-Induced Phase Separation. Langmuir [Internet] 31:6027–6034. Available from: http://pubs.acs.org/doi/abs/10.1021/acs.langmuir.5b01129

Kim S, Xu J. 2008. Aggregate formation of zein and its structural inversion in aqueous ethanol. J. Cereal Sci. 47:1–5.

Klose D, Siepmann F, Elkharraz K, Krenzlin S, Siepmann J. 2006. How porosity and size affect the drug release mechanisms from PLGA-based microparticles. Int. J. Pharm. 314:198–206.

Korsmeyer RW, Gurny R, Doelker E, Buri P, Peppas NA. 1983. Mechanisms of solute release from porous hydrophilic polymers. Int. J. Pharm. 15:25–35.

Lee D, Weitz D a. 2008. Double emulsion-templated nanoparticle colloidosomes with selective permeability. Adv. Mater. 20:3498–3503.

Liu G, Wei D, Wang H, Hu Y, Jiang Y. 2016. Self-assembly of zein microspheres with controllable particle size and narrow distribution using a novel built-in ultrasonic dialysis process. Chem. Eng. J. [Internet] 284:1094–1105. Available from: http://dx.doi.org/10.1016/j.cej.2015.09.067

Luo Y, Zhang B, Whent M, Yu LL, Wang Q. 2011. Preparation and characterization of zein/chitosan complex for encapsulation of α-tocopherol, and its in vitro controlled release study. Colloids Surfaces B Biointerfaces [Internet] 85:145–152. Available from: http://www.ncbi.nlm.nih.gov/pubmed/21440424

Mark D, Haeberle S, Roth G, von Stetten F, Zengerle R. 2010. Microfluidic lab-on-a-chip platforms: requirements, characteristics and applications. Chem. Soc. Rev. [Internet] 39:1153. Available from: http://xlink.rsc.org/?DOI=b820557b

Mehta K a, Kislalioglu MS, Phuapradit W, Malick AW, Shah NH. 2000. Effect of formulation and process variables on porosity parameters and release rates from a multi unit erosion matrix of a poorly soluble drug. J. Control. Release [Internet] 63:201–211. Available from: http://linkinghub.elsevier.com/retrieve/pii/S0168365999001935

Micsonai A, Wien F, Kernya L, Lee Y-H, Goto Y, Réfrégiers M, and others. 2015. Accurate secondary structure prediction and fold recognition for circular dichroism spectroscopy. Proc. Natl. Acad. Sci. [Internet] 112:E3095–E3103. Available from: http://www.pnas.org/lookup/doi/10.1073/pnas.1500851112

Muijlwijk K, Berton-carabin C, Schroën K. 2016. Cross-flow microfluidic emulsification from a food perspective. Trend food Sci. Technol. 49:51–63.

Olenskyj AG, Feng Y, Lee Y. 2017. Continuous microfluidic production of zein nanoparticles and correlation of particle size with physical parameters determined using CFD simulation. J. Food Eng. [Internet] 211:50–59. Available from: http://linkinghub.elsevier.com/retrieve/pii/S0260877417301668

Pan K, Zhong Q. 2016a. Organic Nanoparticles in Foods: Fabrication, Characterization, and Utilization. Annu. Rev. Food Sci. Technol. [Internet] 7:245–266. Available from: http://www.annualreviews.org/doi/10.1146/annurev-food-041715-033215

Pan K, Zhong Q. 2016b. Low energy, organic solvent-free co-assembly of zein and caseinate to prepare stable dispersions. Food Hydrocoll. [Internet] 52:600–606. Available from: http://www.sciencedirect.com/science/article/pii/S0268005X1530059X

San Miguel A, Scrimgeour J, Curtis JE, Behrens SH. 2010. Smart colloidosomes with a dissolution trigger. Soft Matter 6:3163.

Sarkar P, Bhunia AK, Yao Y. 2016. Emulsion Stabilized with Starch Octenyl Succinate Prolongs Nisin Activity Against Listeria Monocytogenes in a Cantaloupe Juice Model. J. Food Sci. [Internet] 81:M2982–M2987. Available from: http://10.0.4.87/1750-3841.13550%0Ahttp://search.ebscohost.com/login.aspx?direct=true&AuthType=ip,url,cookie,uid&db=aph&AN=120039438&site=ehost-live&scope=site

Shi X-Y, Tan T-W. 2002. Preparation of chitosan/ethylcellulose complex microcapsule and its

application in controlled release of Vitamin D2. Biomaterials [Internet] 23:4469–4473. Available from: http://linkinghub.elsevier.com/retrieve/pii/S0142961202001655

Shum HC, Abate AR, Lee D, Studart AR, Wang B, Chen CH, and others. 2010. Droplet microfluidics for fabrication of non-spherical particles. Macromol. Rapid Commun. 31:108–118.

Thompson KL, Williams M, Armes SP. 2014. Colloidosomes: Synthesis, properties and applications. J. Colloid Interface Sci. [Internet] 447:217–228. Available from: http://linkinghub.elsevier.com/retrieve/pii/S0021979714009187

Utada AS, Fernandez-Nieves A, Stone HA, Weitz DA. 2007. Dripping to Jetting Transitions in Coflowing Liquid Streams. Phys. Rev. Lett. [Internet] 99:94502. Available from: http://link.aps.org/doi/10.1103/PhysRevLett.99.094502

Wang X, Li Z, Yang Y, Gong X, Liao Y, Xie X. 2015. Photomechanically controlled encapsulation and release from ph-responsive and photoresponsive microcapsules. Langmuir 31:5456–5463.

Wang Y, Lopes Filho F, Geil P, Padua GW. 2005. Effects of processing on the structure of zein/oleic acid films investigated by X-ray diffraction. Macromol. Biosci. 5:1200–1208.

Wang Y, Padua GW. 2012. Nanoscale characterization of zein self-assembly. Langmuir 28:2429–2435.

Workman VL, Dunnett SB, Kille P, Palmer DD. 2008. On-chip alginate microencapsulation of functional cells. Macromol. Rapid Commun. 29:165–170.

Yoshii H, Soottitantawat A, Liu XD, Atarashi T, Furuta T, Aishima S, and others. 2001. Flavor release from spray-dried maltodextrin/gum arabic or soy matrices as a function of storage relative humidity. Innov. Food Sci. Emerg. Technol. 2:55–61.

Zhang H, Tumarkin E, Sullan RMA, Walker GC, Kumacheva E. 2007. Exploring microfluidic routes to microgels of biological polymers. Macromol. Rapid Commun. 28:527–538.

Zhang J, Coulston RJ, Jones ST, Geng J, Scherman O a, Abell C. 2012. One-Step Fabrication of Supramolecular Microcapsules from Microfluidic Droplets. Science (80-.). [Internet] 335:690–694. Available from: http://www.ncbi.nlm.nih.gov/pubmed/22323815

Zhang Y, Cui L, Che X, Zhang H, Shi N, Li C, and others. 2015. Zein-based films and their usage for controlled delivery: Origin, classes and current landscape. J. Control. Release [Internet] 206:203–219. Available from: http://dx.doi.org/10.1016/j.jconrel.2015.03.030

Zhang Z, Zhang R, Tong Q, Decker EA, McClements DJ. 2015. Food-grade filled hydrogels for oral delivery of lipophilic active ingredients: Temperature-triggered release microgels. Food Res. Int. [Internet] 69:274–280. Available from: http://dx.doi.org/10.1016/j.foodres.2015.01.004

Zhao CX, Middelberg APJ. 2009. Microfluidic mass-transfer control for the simple formation of complex multiple emulsions. Angew. Chemie - Int. Ed. 48:7208–7211.

Zhao CX, Middelberg APJ. 2013. One-step fabrication of titania hollow spheres by controlled interfacial reaction in a droplet-based microfluidic system. Microfluid. Nanofluidics 14:703–709.

Zheng Y, Yu Z, Parker RM, Wu Y, Abell C, Scherman O a. 2014. Interfacial assembly of dendritic microcapsules with host–guest chemistry. Nat. Commun. [Internet] 5:5772. Available from: http://www.nature.com/doifinder/10.1038/ncomms6772

Zhong Q, Jin M. 2009. Zein nanoparticles produced by liquid-liquid dispersion. Food Hydrocoll. 23:2380–2387.

Zhou J, Hyun DC, Liu H, Wu H, Xia Y. 2014. Protein capsules with cross-linked, semipermeable, and enzyme-degradable surface barriers for controlled release. Macromol. Rapid Commun. 35:1436–1442.

CHAPTER 5

Tuning engineering properties of protein microcapsules in microfluidic chips

5.1 Abstract

Engineering microcapsule properties are crucial to ensure their functionalities for various applications. Among the engineering properties of microcapsules, mechanical properties and surface morphology are particularly of great interest. However, the studies on engineering properties of microcapsules from biomaterials especially food materials are limited. This study proposed a facile approach to investigate and modify the morphological and nanomechanical properties of zein microcapsules, which is a protein derived from corn as a byproduct of biofuel. Internal phase separation method was used to generate zein microcapsules and three types of acids (phytic acid, citric acid and succinic acid) were added at two concentrations (10mM and 20mM) to modify the properties of microcapsules. The mechanical properties of microcapsules were then characterized with nanoindentation technique, and the morphological properties were analyzed with image analysis. The incorporation of phytic acid significantly increased the degree of wrinkling and viscoplasticity of the micropcapsules. Further characterization with circular dichroism (CD) and wide angle X-ray scattering (WAXS) suggests that less ordered zein structure was formed in the phytic acid than in the other two acids or without acid.

Keywords

Microfluidics, nanoindentation, wrinkle, nanomechanicals, zein, microcapsule

5.2 Introduction

Microencapsulation is an imperative technology and has already become an important processing technique in many industries (Shchukina and Shchukin 2012; Neubauer and others 2014). Recently, the applications of microencapsulation are becoming diverse, covering a broad range of fields from biology, chemistry to food and nutrition. Some of those emerging applications of microencapsulation include DNA synthesis and purification (Cavalieri and others 2009), triggered and rate controlled release for accurate drug delivery (Hoare and Kohane 2008; Chen and Subirade 2009; Lin and others 2011; Long and others 2013; Brugarolas and others 2014; Neubauer and others 2014; Thompson and others 2014; Ghaemi and others 2016; Ina and others 2016; Hussain and others 2017) enzyme immobilization (Qu and others 2015), biosensor assembly (Cosnier and others 2000), self-healing materials (Lv and others 2016), and even tissue engineering (Paliwal and Palakurthi 2014). To fulfill the various demands, engineering microcapsule properties are becoming crucial to ensure their proper functionalities for specific applications. In previous studies, among many engineering properties, morphology and mechanical properties have been recognized as the most important and widely studied(Sokolovskyy and others; Li and others 2016; Hussain and others 2017; Olenskyj and others 2017). To date, those successes in modifying microcapsule properties were mostly achieved with synthetic polymers and inorganic materials, while very few with biologically derived materials.

Zein is a prolamine derived from corn. According to its unique amino acid profile, zein contains more than half hydrophobic amino acid residues and behaves as a amphiphilic molecule in solutions (Wang and Padua 2010). The amphiphicity of zein enables it's self-assembly at featured conditions such as anti-solvent processes, which consequently drive the formation of zein film (Wang and Padua 2012) and nanoparticles (Zhong and Jin 2009; Feng and Lee 2016; Olenskyj and others 2017). In previous studies, the film-forming process was mostly triggered by ethanol evaporation or instant dilution induced by mixing, where the control over film structure was limited. Although zein film and nanoparticles produced by anti-solvent methods have been applied as delivery carriers for core materials (Patel and others 2010; Zhang and others 2015; Kashiri and others 2016; Pan and Zhong 2016), there is still lack of control over zein self-assembly, which is associated with the consistency, feasibility and versatility of zein-based delivery systems. Internal phase separation is a controlled phase separation method for preparing core-shell microcapsules usually driven by anti-solvent process (Loxley and Vincent 1998; Atkin and others 2004), which has also been applied

successfully to form zein microcapsules in our previous study using a microfluidic device (Feng and Lee 2017).

Conventional pathways for generating microcapsules are top-down processes, which usually involve energy intensive process such as a high shear or pressure induced homogenization and feature mass production (Mijatovic and others 2005). On the other hand, top-down processes are associated with mechanical attritions that require intensive energy cost, and possess the limited control of particle sizes, shape, surface, and mechanical properties(Hu and others 2008; Ali and others 2009). Therefore, it is of great interest to employ a bottom-up process as a platform to control and tune the engineering properties microcapsules. Precise control over microcapsule fabrication is especially important for developing strategies to modify their properties. In the past a few years, microfluidic droplet system has emerged as a bottom-up approach to synthesize particles homogeneously(Subramaniam and others 2005; Amici and others 2008). Although the yield of microfluidic process is very low, many strategies have been proposed to scale up parallel droplet microfluidics for mass production (Teh and others 2008).

Among the engineering properties of microcapsules, mechanical properties and surface morphology are particularly of great interest. In many different fields of application, mechanical properties of microcapsules play a variety of roles such as maintaining structural integrity, triggering core release and regulating release kinetics (Delcea and others 2010; Neubauer and others 2014). Due to the small size of microcapsules, characterizing their mechanical properties is challenging, and therefore considerable efforts have been made for developing methodologies (Berthoud and others 1999; Ebenstein and Pruitt 2006; Beake and others 2007; Brugarolas and others 2014; Neubauer and others 2014). Likewise, surface morphology is also a vital property of microcapsules. Recently, artificially wrinkled particles have been extensively studied for controlled drug delivery, absorbent materials, inkjet recording, aerodynmamics enhancement, and cell attachment (Neubauer and others 2014; Ina and others 2016; Li and others 2016; Hussain and others 2017). In order to meet the expanding and diversifying demand, customizing the engineering properties of microcapsules is becoming more important (Chan and Chew 2003). In this study, we present an approach to producing microcapsules with tunable mechanical and wrinkling properties, using a food grade material, zein.

5.3 Materials and methodology

5.3.1 Materials

Zein (Z3625, Sigma-Aldrich, St. Louis, MO) dissolved in 70% (v/v) ethanol (200 Proof, Decon Laboratories, King of Prussia, PA) was used as the dispersing phase. Tributyrin (W222305, Sigma-Aldrich, St. Louis, MO) containing 2% (w/v) soy lecithin (MP Biomedicals Inc, Solon, OH) was used as the continuous phase. Rhodamine B (R6626, Sigma-Aldrich, St. Louis, MO) was added into the dispersing phase at 2 mg/ml, to assess the rate of release. Hexane (Macron Fine Chemicals, Center Valley, PA) was used to wash the microcapsules. No. 42 (pore size 2.5 μm) Whatman filter paper (Whatman Inc., Florham Park, NJ) was used to collect final microcapsules. Phytic acid, citric acid and succinic acid were purchased from Sigma, St. Louis, MO.

5.3.2 Microfluidic fabrication

The dispersing phase was prepared by 4% (w/v) of zein into an ethanol-water binary system containing 70% (v/v) ethanol. Each sample contains 10 mM or 20 mM of phytic acid, citric acid or succinic acid. The continuous phase was prepared by mixing 2% (w/v) of soy lecithin with tributyrin by stirring at 250 rpm for overnight, followed by centrifugation at 200 g for 10 min to remove impurities. Hollow zein microcapsules were then produced in a 100 μm T-junction microfluidic chip (Dolomite, UK) through internal phase separation and the mechanism was described in our previous study (Feng and Lee 2017). The samples prepared in this study are listed in Table 5.1. The flow rates of dispersing phase and continuous phase were set at 0.2ml/hr and 10 ml/hr, respectively. Flow rates were controlled using a Harvard Model 11 Elite syringe pump (Harvard Apparatus Inc., Holliston, MA). Once collected, the capsules were immediately washed with hexane for three times on a filter paper with vacuum. The final microcapsules were obtained by transferring the filtered samples into a convective oven to remove excessive water at 30°C for 6 hours.

5.3.3 Characterization

Confocal Laser Scanning Morphology (CLSM)

A CLSM was used to visualize the internal structure of the microcapsules. Freshly collected microcapsule suspensions (1 ml) were stained with 40 μL of Nile blue (0.1%) for 2 h. A Zeiss LSM 700 confocal mi- croscope (Zeiss, Germany) was operated using the excitation wavelength of 488 nm for the Nile blue dye to visualize the emulsions. Images were taken at a magnification of 20x and further processed using the instrumental software.

Scanning Electron Microscopy (SEM)

The surface morphology of final microcapsules was imaged using a SEM (S-4700, Hitachi Company, Japan). The blocks were mounted on SEM stubs and coated with 60 nm of gold-palladium using a Desk-II turbo sputter coater (Denton Vacuum, Moorestown, NJ). Samples were adhered to a conductive carbon tape for imaging.

Degree of Wrinkling

The degree of wrinkling was assessed following a methodology described in previous literature with modifications(Ina and others 2016). Briefly, MATLAB (R2014a, The Mathworks Inc., Natic, MA) was used to analyze the CLSM morphology of microcapsules. The procedures for the MATLAB image analysis follows a previous study (Kuo and Lee 2014), including binary conversion, hole filling and bundary smoothing. Afterwards, the values of perimeter (P) and circumference (C) were derived based on the pixel information. The degree of wrinkling (DW) was then calculated as the ratio between P and C. Approximately fifty microcapsules were analyzed for each sample.

Mechanical properties

Mechanical properties of microcapsules were normally characterized using indentation methods and presented with parameters such as hardness, reduced modulus and Young's modulus (Lee and others 2012; Su and others 2012; Neubauer and others 2014; Ghaemi and others 2016; Sarrazin and others 2016). However, conventional indentation methods are not suitable for soft materials because of their visco-elastic and time-dependent nature (Ebenstein and Pruitt 2006; Neubauer and others 2014; Díez-Pascual and others 2015; Rath and others 2015). As such, several adaptions were developed as alternatives to take the time-dependent properties into account. In this experiment, creep indentation test was applied following previous studies (Beake and others 2007; Zellmer and others 2016).

Samples were mounted on magnetic AFM holders and placed in a desiccator overnight. The mechanical behavior of microcapsules was then probed using a nanoindenter (TI-950 Triboindenter, Hysitron Inc., Minneapolis, MN) and a Berkovich tip. For the indentation, the tip was load-controlled to 200 μN maximum load in 10 seconds (20 μN/s), followed by a 180 seconds holding period for creep testing. Load (σ) and displacement (δ) data at each time point were acquired and recoded at 200 points/s. Curves with the abnormal initial indentation depth (greater than 1 μm) were aborted, in which cases the slipping between the nanoindenter tip and the sample surface may occurred. At least five replications were performed on each sample.

Creep indentation results interpretation was described in previous studies, by data fitting in the equation proposed by Berthoud (Berthoud and others 1999)(2),

$$\frac{\delta-\delta_0}{\delta_0} = m_{eff}\ln(1+\frac{t}{\tau}) \quad (2)$$

where δ is the depth, δ_0 is the depth before creeping at 10s, t is the loading time, τ is minimum time needed to produce such a creep even, and m_{eff} represents the effective strain rate sensitivity or viscoplasticity (Berthoud and others 1999; Kermouche and others 2006; Beake and others 2007).

Small Angle X-Ray Scattering (SAXS) and Wide Angle X-Ray Scattering (WAXS)

WAXS data were collected with a Bruker General Area Detector Diffraction System (GADDS, Bruker AXS, Inc., Madison, WI). X-Rays were generated by a rotating anode generator with Cu target anode material. The X-ray wavelength was $K_{\alpha 1}$ =1.54 Å. The system was equipped with a four-circle diffractometer and a HiStar multiwire area detector. The distance between the sample and the detector was maintained at 8.52 cm. The system was operated at 40 kV and 60 mA. SAXS data were also collected with a HiStar area detector located 105.10 cm away from the sample.

Circular Dichroism (CD) spectra

The CD spectra were recorded with a JASCO J-715 spectropolarimeter (Jasco Inc., Easton, MD). Samples were placed in a quarts cell with a 1 cm path length. The measurement was conducted over the range of 200-250 nm at 25°C, with the scanning speed of 50nm/min, and the resolution of 1 nm. The content of α-helix, β-sheet, and random coil was calculated using the BeStSel software (Micsonai and others 2015), which could be accessed online at http://bestsel.elte.hu. The Savitsky-Golay smoothing algorithm was used, with a polynomial order of 3 and a smoothing window of 20 points, according to a previous study (Greenfield 2006).

5.3.4 Statistical analysis

All the measurements were conducted at least in triplicate. Data were analyzed using OriginPro 2015 software (OriginLab Corp., Northampton, MA) and Microsoft Excel 2010 (Microsoft Corp., Seattle, WA). Analysis of variance (ANOVA) and least significant difference (LSD) with Bonferroni correction were used to compare the means. The significance level was set at 0.05.

5.4 Results and discussion

5.4.1 Morphology

Figure 5.1 and Figure 5.2 are SEM and CLSM images that illustrate the morphology of zein microcapsules with three different additive acids. It is clear that all the samples are not spherical and their degree of wrinkling vary. The mechanism of the wrinkled particle formation through internal phase separation method has been discussed with a previous study (Loxley and Vincent 1998). The driving force for the wrinkle formation is the interior fluid diffusion induced shrinking during internal phase separation process. The principal reason that leads to the distinctive winking is due to the spontaneity of the shell formation and volume contraction processes, which is unique for internal phase separation. A mathematical expression shown below has been used to quantify the degree of contraction (eq. 1) (Ottewill and others 1996), which is the ratio between final microcapsule diameter (d_{mc}) to parent droplet diameter (d_e) dispersed from the microfluidic channel.

$$\frac{d_{mc}}{d_e} = \left(\frac{V_p + V_{ns}}{V_p + V_{ns} + V_s}\right)^{1/3} \quad (1)$$

where v_p is the volume of polymer, v_{ns} the volume of non-solvent, and vs the volume of good solvent in each droplet in the parent emulsion. In this study, the ratio between d_{mc} and d_e is about 0.7, indicating a 30% size reduction.

Comparing the microcapsules with different acid addition, it could be visually recognized that the surface of samples including phytic acid had the highest degree of wrinkling. According to the literature, the rate of shell formation plays an important role on the buckling (Loxley and Vincent 1998). In the case of fast shell formation, the shell is formed when the degree of contraction is low, where the further contraction causes extensive buckling. On the other hand, if the shell formed at a relatively late stage of contraction, the further size reduction would be limited and therefore cause less degree of wrinkling.

The distinctive feature of phytic acid samples is attributed to their high ionic strength, which hence give rise to strong interactions between phytic acid and proteins (Cheryan and Rackis 1980). This type of strong interaction between phytic acid and proteins could result in an immediate solidification of zein upon internal phase separation process, and readily form a shell structure which is subjected to extensive contraction when the ethanol inside the droplet diffuses out. The rapid solidification of zein could also lead to a less ordered arrangement of protein molecules.

5.4.2 Degree of wrinkling

In order to quantify the degree of wrinkling, CLSM images were taken for image analysis. Wrinkling is a three dimensional configuration, however, due to the limitations on imaging and analyzing 3-D images, most of image analysis was done based on two dimensional images, including the degree of wrinkling or index of sphericity analysis(Ionescu-Tirgoviste and others 2015; Ina and others 2016) that was applied in this study. Figure 5.2 displays the process for quantifying the degree of wrinkling. The original CLSM images were treated with MATLAB following standard image analysis procedures (Charpentier and others 2013) to obtain the 2-D degree of wrinkling results. The ratio between perimeter and circumference (P/C) (Ina and others 2016) was used to describe the degree of wrinkling.

Table 5.2 shows the degree of wrinkling results across all samples, and the results agreed with the visual observation from SEM images. When 10 mM of acids were incorporated in the formulas, the sample with phytic acid (MP1) is significantly more wrinkled than other acids. Citric acid and succinic acid are weak acids, and HCl was used to adjust the pH to 3.0. Therefore, the ionic strength for samples MC1, MC2, MS1, MS2, as well as M0 are approximately 1 mM. As a result, it would be understandable that increasing the acid concentration from 10mM to 20mM did not make significant differences. Different from citric acid and succinic acid, phytic acid contains six phosphate groups and twelve dissociable hydrogen ions. According to phytic acid titration test, approximately 60 mM of NaOH is needed to increase the pH of 10mM phytic acid to 3.0, where the ionic strength is about 60 mM (Roberts and others 2015). Protein aggregation is potentially enhanced due to the salting out effects. In addition to the ionic strength effect, types of specific ion also play an important role in the protein-protein interactions in a solution. According to the classical Hofmeister series (Okur and others 2017), phosphate ions are more tended to induce protein aggregation. In the case of phytic acid, due to the presence of six phosphate groups, the tendency of rapid solidification upon anti-solvent process is further promoted. Therefore, the early stage shell formation leads to extensive wall shrinkage during further contraction, and more wrinkled surfaces.

5.4.3 Mechanical properties

The mechanical properties of microcapsules were determined by nanoindentation creep test in this study. Previous approaches used normal indentation method to obtain Young's modulus, reduced modulus and hardness to characterize mechanical properties (Lee and others

2012; Su and others 2012). However, the classical indentation is not a feasible approach for soft materials, because it is challenging to measure modulus values in the magnitude of MPa or kPa (Díez-Pascual and others 2015). In addition, soft materials usually exhibit time-dependent properties. Therefore, it is of considerable importance to separate the influence of external effects and the non-linear viscous components (Ngan and Tang 2009). Viscoplasticity, is also known as strain rate sensitivity, was proposed to describe the non-recoverable viscoelastic deformation under a constant force (Berthoud and others 1999; Beake and others 2007; Díez-Pascual and others 2015). This parameter is crucial for dried microcapsules, for predicting their mechanical stability during storage or shear-induced processing.

Figure 5.4 shows the results of creeping curves from the nanoindentation test. The creep depth (δ-δ0) was normalized by the initial indentation depth δ0, to eliminate the effects of external factors such as indent location and indent angle (Berthoud and others 1999). As such, the normalized creep depth shows the creep sensitivity, which was then quantified by a unitless parameter, strain rate sensitivity or viscoplasticity (Meff). The typical viscoplasticity values are in the range of 0.04 to 0.1 for glassy polymers such as polystyrene (PS) and poly methyl methacrylate (PMMA) (Berthoud and others 1999). A larger m_{eff} value indicates an inelastic behavior of solids which is more prone to plastic deformation. Therefore, the samples MP1 and MP2 are more prone to plastic deformation during the creep stage, compared to other samples (Figure 5.4). The finding was further confirmed with the data fitting results shown in the table 5.3, using the equation (2). The viscoplasticity of MP1 and MP2 are significantly greater than other samples, indicating its susceptibility to plastic deformation under a constant force.

It is interesting that the viscoplasticity of samples with citric acid and succinic acid are not significantly different from M0, because small molecules such as citric acid and succinic acid are normally considered as plasticizers, which improve the plasticity by lowering glass transition temperature. According to the Fox-Flory equation (Fox and Flory 1950), the glass transition temperature is a function of average molecular weight M_n(Eq. 3).

$$T_g = T_{g,\infty} - \frac{K}{M_n} \quad (3)$$

Where $T_{g,\infty}$ is the maximum glass transition temperature that can be achieved, K is an empirical value and M_n is the average molecular weight. Although acids were added at very small concentration, the addition of 10mM or 20mM of small molecules would decrease the M_n significantly and affect the T_g, which further leads to an increased plastic property. However, the formation of zein structure in this study involves a self-assembly process and

acid-protein interactions, which is more complicated than a typical polymer structure due to the secondary structure evolution (Wang and others 2005; Wang and others 2008; Wang and Padua 2012). It was also reported that the structural orderliness, intermolecular bonding and the presence of α-helix could play important roles in mechanical properties (Knowles and Buehler 2011; Wang and others 2015).

5.4.4 Molecular arrangement

The molecular arrangement of selected samples (M0, MC1, MP1 and MS1) were characterized using circular dichroism (CD) spectrum, small-angle X-ray scattering (SAXS) and wide-angle X-ray scattering (WAXS). The SAXS results did not show significant differences (supplemental materials), indicating that there is no ordered structure in the scale of 2 nm to 70 nm. This result was different from a previous study, where zein self-assembly was induced by ethanol evaporation (Wang and Padua 2012). The residence time in the microfluidic process is probably too short for zein molecules to re-organize into a more ordered structure. The CD spectrum (Figure 5.5) suggests a substantial alteration in the secondary structure, from raw zein to microfluidic zein. Calculated by the BeStSel algorism (Micsonai and others 2015), raw zein contains about 47.17% α-helix, 24.87% β-sheet and 27.97% random coil. After internal phase separation, the amount of α-helix structure dropped to a single digit, because they were transformed into β-sheet and random coil during self-assembly. The results were consistent with the previous study (Wang and Padua 2012), except the greater fraction of random coil and less fraction of β-sheet were observed in this study. This difference is expected due to the short residence time of internal phase separation process, allowing limited time for the formation of more ordered structure. Table 5.4 compares the secondary structure among different samples. It was notable that the MP1 sample contains the least amount of α-helix and the highest fraction of random coil, indicating its less ordered structure compared other samples. According to the literature (Knowles and Buehler 2011; Wang and others 2015), the results explained the nanomechanics data where the samples with phytic acid are more prone to plastic deformation under constant force.

Figure 5.6 shows the WAXS patterns of zein microcapsules and raw zein. There are two distinctive peaks exhibiting at the same 2θ angles. According to the Bragg's law, the characteristic d-spacing values could be calculated as 9.9 Å and 4.4Å, respectively. The smaller d-spacing (~5 Å) is related to the backbone distance within the α-helix (Ottewill and others 1996; Lai and others 1999; Wang and others 2005), whereas the longer d-spacing (~9.9 Å) comes from the lateral α-helix packing (Lai and others 1999; Wang and others 2005). The

peak area ratio of raw zein powder in this study is around 0.237, which is close to the reported value of 0.25 in the literature (Wang and others 2005), as a validation for this method. The parameter of peak area ratio suggests the orderliness of α-helix packing. This ratio value was found to be smallest in the MP1 sample, indicating the least ordered packing of α-helix. The reason could be attributed to its high ionic strength and salting out effects, which lead to rapid solidification with limited structural reorganization. However, because of the small quantity of the total α-helix in the microcapsules, samples with high peak area ratios (M0 and MC1) did not display significantly enhanced mechanical stability as well.

5.5 Conclusions

In this study, zein microcapsules with different surface morphology and nanomechanical properties were formed in a droplet-based microfluidic system. Three acids were used as additives to alter the engineering properties of zein microcapsules. The data shows that incorporation of phytic acid significantly increased the degree of wrinkling and viscoplasticity of zein microcapsules, while the addition of citric acid and succinic acid did not result in a significant difference. It was also found that increasing the additive concentration from 10mM to 20mM did change the properties of all three acids. Further characterization of microcapsules suggest that the molecular structure of sample containing phytic acid is less ordered than other samples, which was composed of less amount and more randomly packed α-helix. Overall, this study provided a facile approach to tweak the engineering properties of microcapsules in a microfluidic process. Future work is needed to uncover the relations between nanoscale structure and macroscale properties, as well as the mechanisms of their interactions. More work is still needed to reveal the relation between molecular structure and nanomechanics.

5.6 Tables and figures

Table 5.1. A summary of sample code and formulations. M0 is zein microcapsules without acids, MC1 and MC2 are zein microcapsules with two concentrations of citric acid, MP1 and MP2 are zein microcapsules with two concentrations of phytic acid, MS1 and MS2 are zein microcapsules with two concentrations of succinic acid.

Sample code	Zein% (w/v)	Citric acid	Phytic acid	Succinic acid	pH
M0	4%				3.0
MC1	4%	10 mM			3.0
MC2	4%	20 mM			3.0
MP1	4%		10 mM		3.0
MP2	4%		20 mM		3.0
MS1	4%			10 mM	3.0
MS2	4%			20 mM	3.0

Table 5.2. Degree of wrinkling of samples with different amounts and types of acids, sample MC1 contains 10 mM citric acid, Sample MC2 contains 20 mM citric acid, sample MP1 contains 10 mM phytic acid, sample MP2 contains 20 mM phytic acid, sample MS1 contains 10 mM succinic acid and sample MS2 contains 20 mM succinic acid.

Sample code	M0	MC1	MC2	MP1	MP2	MS1	MS2
Degree of wrinkling	1.045^{b}	1.043^{b}	1.044^{b}	1.088^{a}	1.084^{a}	1.033^{b}	1.035^{b}

†Means showing a common letter are not significantly different across different samples ($\alpha = 0.05$).

Table 5.3. m_{eff} (viscoplasticity) results derived from data fitting. Sample MC1 contains 10 mM citric acid, Sample MC2 contains 20 mM citric acid, sample MP1 contains 10 mM phytic acid, sample MP2 contains 20 mM phytic acid, sample MS1 contains 10 mM succinic acid and sample MS2 contains 20 mM succinic acid.

Sample code	M0	MC1	MC2	MP1	MP2	MS1	MS2
Viscoplasticity (m_{eff})	0.0453^{b}	0.0459^{b}	0.0472^{b}	0.0772^{a}	0.0633^{a}	0.0466^{b}	0.0454^{b}

†Means showing a common letter are not significantly different across different samples ($\alpha = 0.05$).

Table 5.4. Distribution of protein secondary structures of microcapsules. Sample M0 is the control microcapsule without any acid additive. Sample MC1 contains 10 mM citric acid, sample MP1 contains 10 mM phytic acid, and sample MS1 contains 10 mM succinic acid.

	α-helix (%)	**β-sheet (%)**	**Random coil (%)**
M0	3.20[ab]	42.37	54.40
MP1	1.48[b]	40.40	58.14
MC1	4.56[a]	38.24	57.26
MS1	2.40[ab]	41.43	56.13

†Means showing a common letter are not significantly different across different samples (α = 0.05).

Table 5.5. WAXS d-spacings and peak area ratios for raw zein and zein microcapsules. Sample M0 is the control microcapsule without any acid additive. Sample MC1 contains 10 mM citric acid, sample MP1 contains 10 mM phytic acid, and sample MS1 contains 10 mM succinic acid.

Sample code	**d_1**	**d_2**	**Peak area ratio (A_2/A_1^*)**
Raw zein	4.5 Å	10.1 Å	0.237
M0	4.4 Å	10.2 Å	0.497
MC1	4.2 Å	9.9 Å	0.371
MP1	4.4 Å	9.8 Å	0.225
MS1	4.4 Å	9.8 Å	0.256

*A_1/A_2: ratio of the d_2 peak area and d_1 peak area

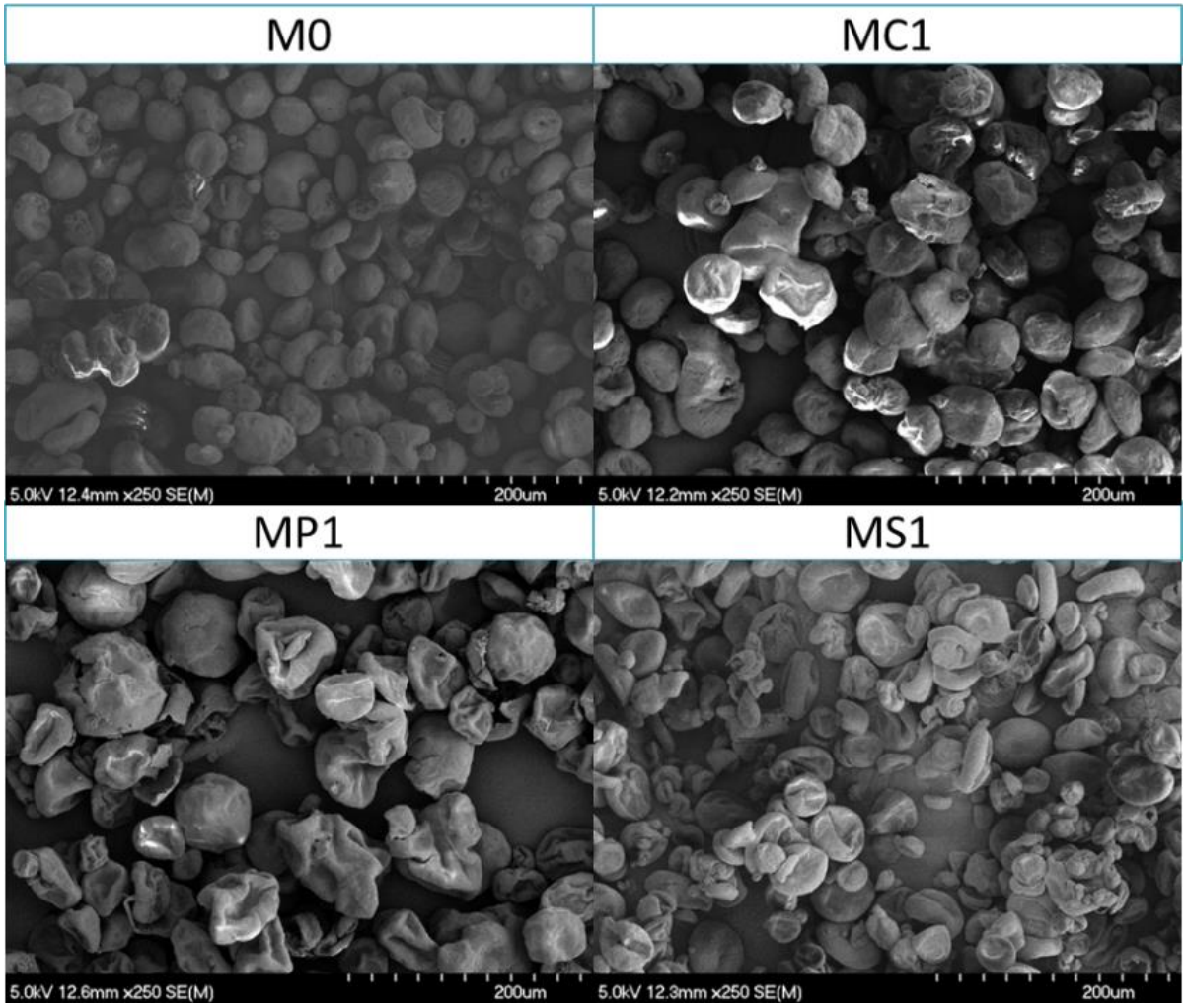

Figure 5.1. SEM images of zein microcapsules prepared using internal phase separation method. Three acids were used as additives for altering morphology. Sample M0 is the control microcapsule without any acid additive. Sample MC1 contains 10 mM citric acid, sample MP1 contains 10 mM phytic acid, and sample MS1 contains 10 mM succinic acid.

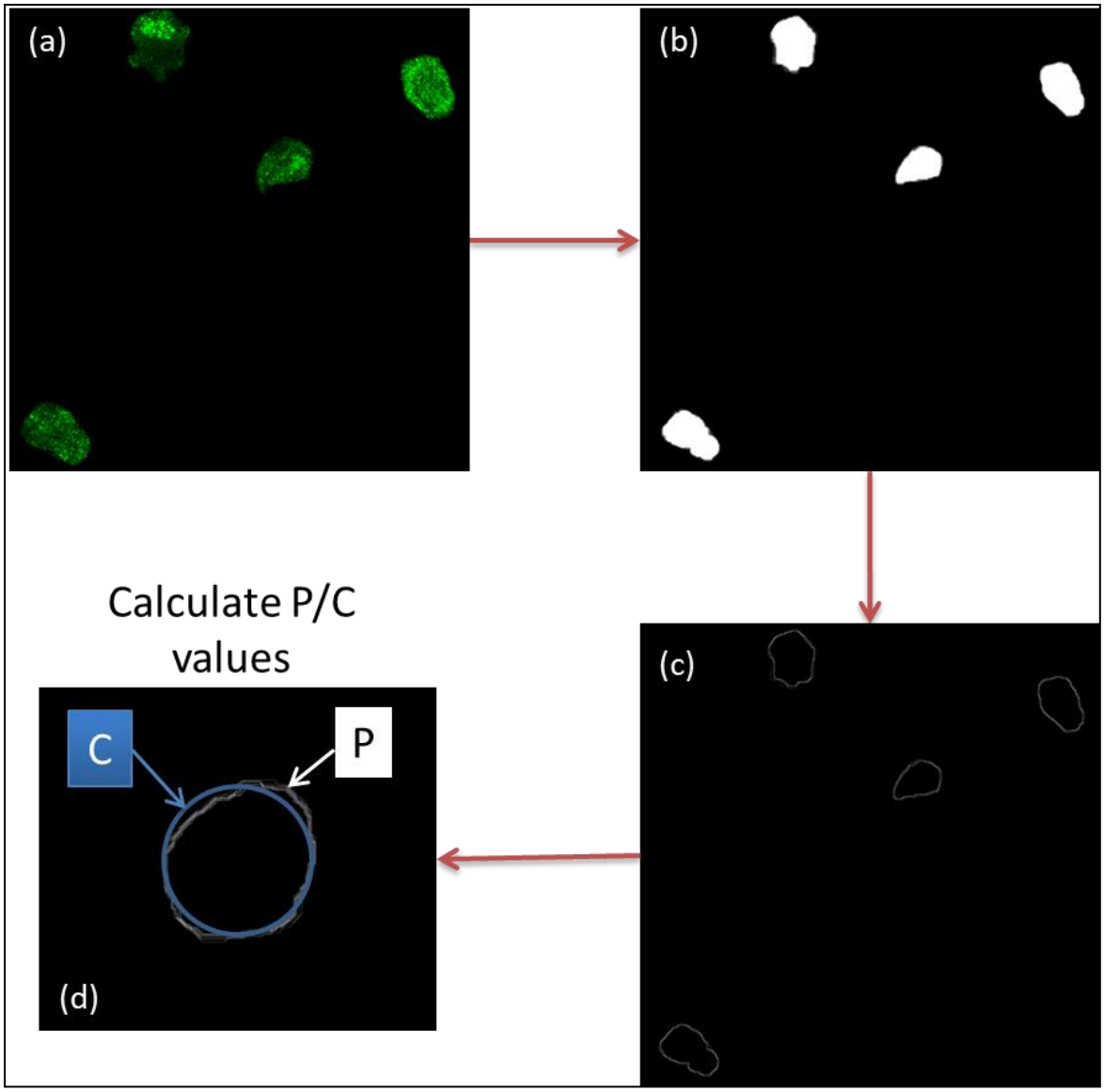

Figure 5.2. Procedures for deriving the P/C ratios from image analysis as an indicator for the degree of wrinkling. Figure (a) shows the original imaged from confocal laser scanning microscopy (CLSM), (b) shows a binary conversion of image, (c) is the identification and isolation, and (d) calculates the P/C ratios as the indicator of the degree of wrinkling.

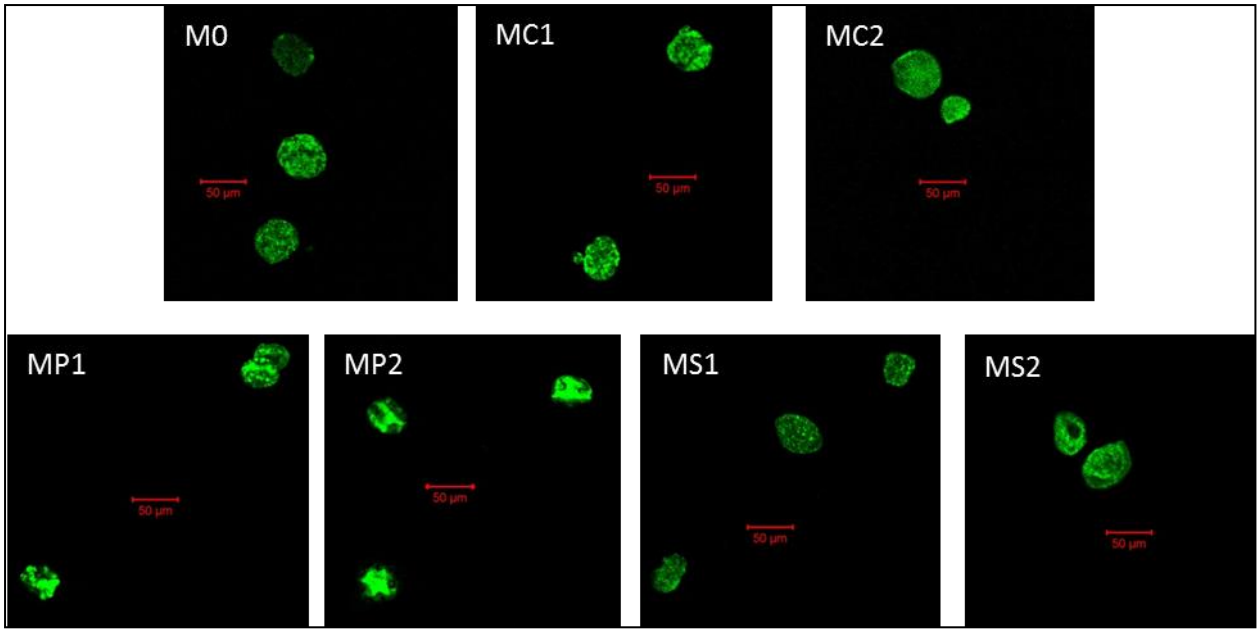

Figure 5.3. Confocal laser scanning microscopy (CLSM) images of samples, Sample M0 is the control microcapsule without any acid additive. Sample MC1 contains 10 mM citric acid, Sample MC2 contains 20 mM citric acid, sample MP1 contains 10 mM phytic acid, sample MP2 contains 20 mM phytic acid, sample MS1 contains 10 mM succinic acid and sample MS2 contains 20 mM succinic acid.

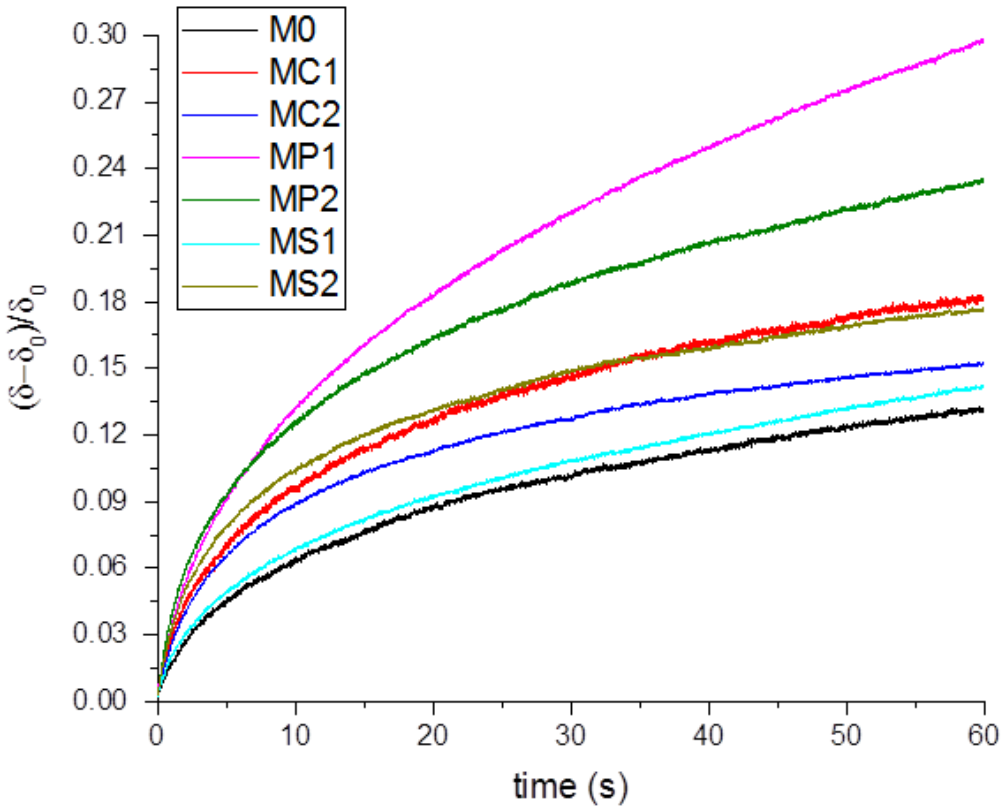

Figure 5.4. Normalized creep depth as a function of creep time. Sample MC1 contains 10 mM citric acid, Sample MC2 contains 20 mM citric acid, sample MP1 contains 10 mM phytic acid, sample MP2 contains 20 mM phytic acid, sample MS1 contains 10 mM succinic acid and sample MS2 contains 20 mM succinic acid.

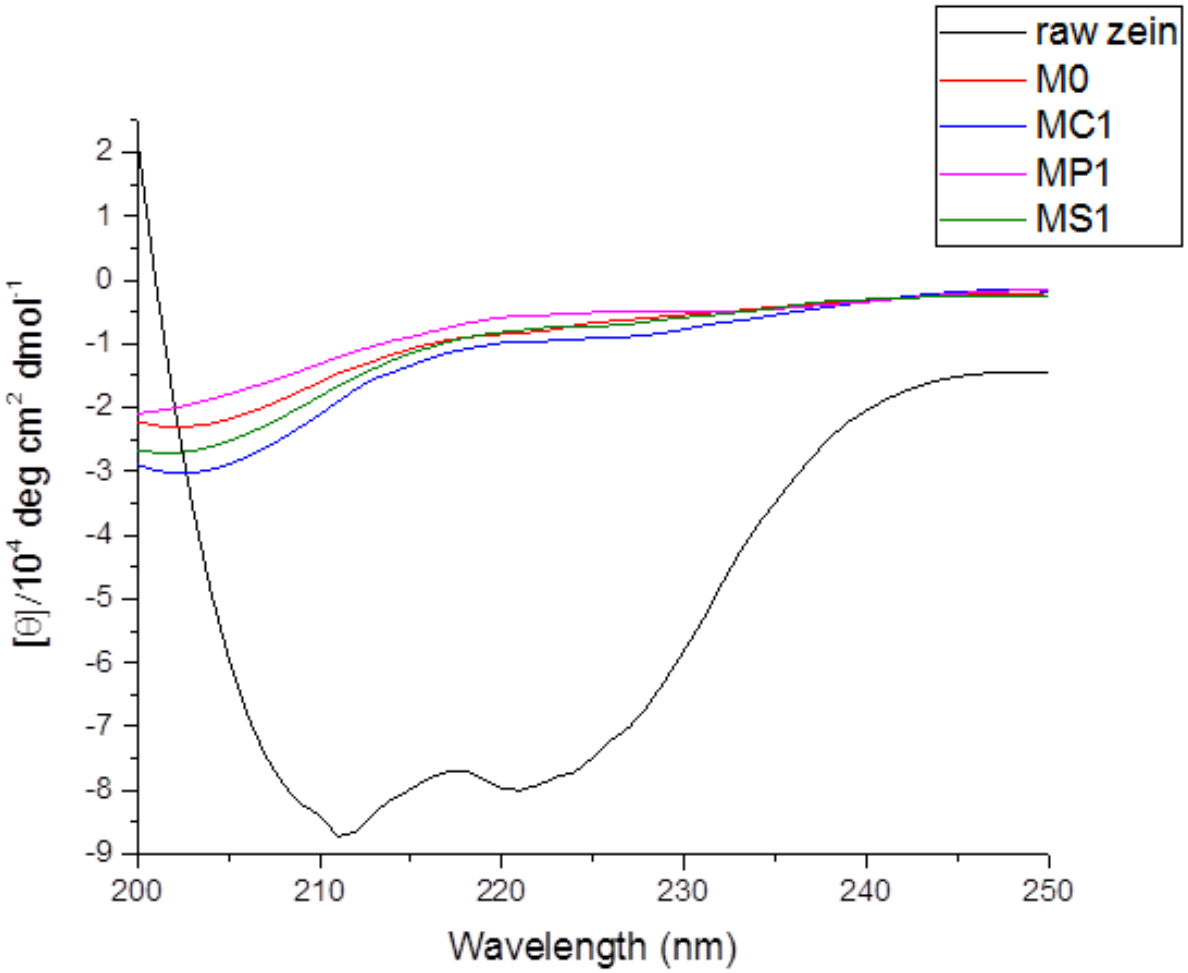

Figure 5.5. Circular dichroism (CD) spectrum of zein microcapsules and raw zein. Sample M0 is the control microcapsule without any acid additive. Sample MC1 contains 10 mM citric acid, sample MP1 contains 10 mM phytic acid, and sample MS1 contains 10 mM succinic acid.

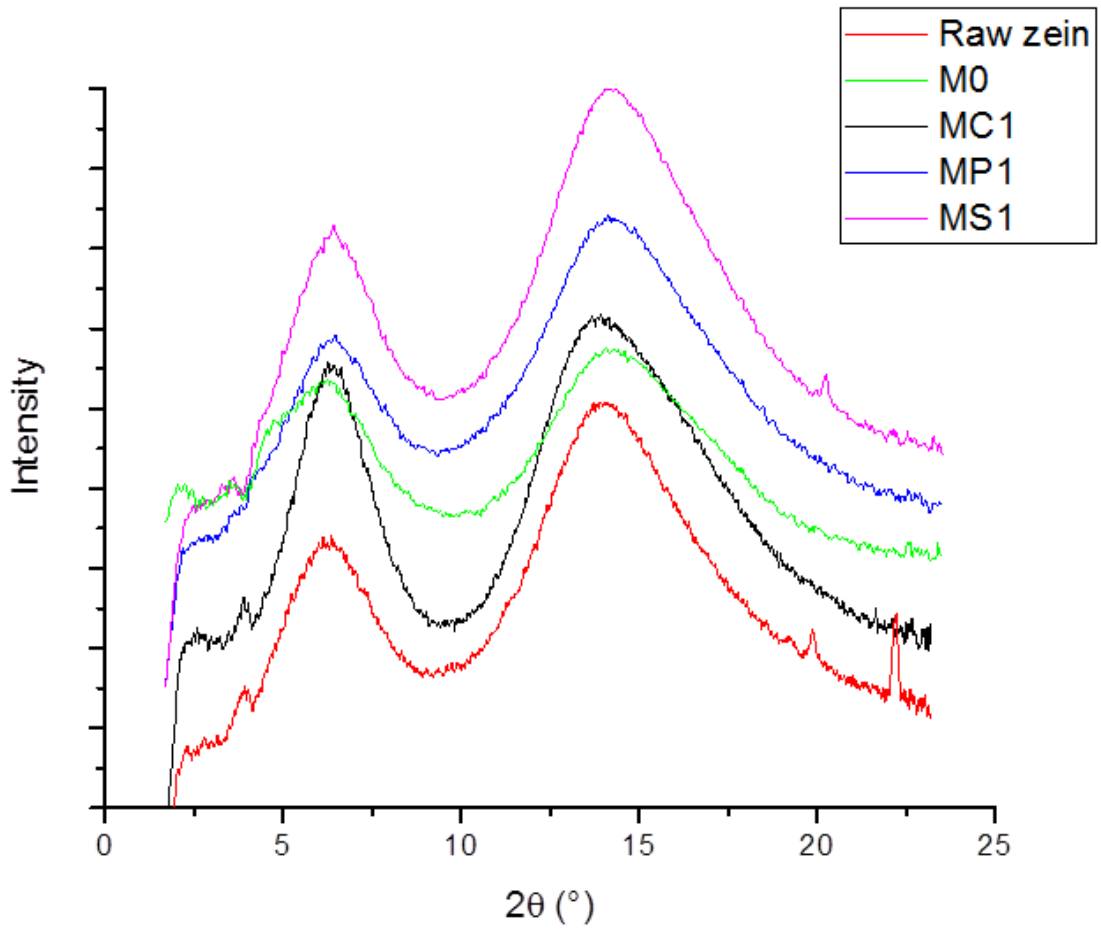

Figure 5.6. WAXS patterns of zein microcapsules and raw zein. Sample M0 is the control microcapsule without any acid additive. Sample MC1 contains 10 mM citric acid, sample MP1 contains 10 mM phytic acid, and sample MS1 contains 10 mM succinic acid.

5.7 References

Ali HSM, York P, Blagden N. 2009. Preparation of hydrocortisone nanosuspension through a bottom-up nanoprecipitation technique using microfluidic reactors. Int. J. Pharm. [Internet] 375:107–113. Available from: http://linkinghub.elsevier.com/retrieve/pii/S0378517309001732

Amici E, Tetradis-Meris G, de Torres CP, Jousse F. 2008. Alginate gelation in microfluidic channels. Food Hydrocoll. 22:97–104.

Atkin R, Davies P, Hardy J, Vincent B. 2004. Preparation of Aqueous Core/Polymer Shell Microcapsules by Internal Phase Separation. Macromolecules [Internet] 37:7979–7985. Available from: http://pubs.acs.org/doi/abs/10.1021/ma048902y

Beake BD, Bell GA, Brostow W, Chonkaew W. 2007. Nanoindentation creep and glass transition temperatures in polymers. Polym. Int. [Internet] 56:773–778. Available from: http://onlinelibrary.wiley.com/doi/10.1002/pi.2098/full

Berthoud P, Sell CG, Hiver JM. 1999. Elastic-plastic indentation creep of glassy poly(methyl methacrylate) and polystyrene: characterization using uniaxial compression and indentation tests. J. Phys. D. Appl. Phys. [Internet] 32:2923. Available from: http://stacks.iop.org/0022-3727/32/i=22/a=315

Brugarolas T, Gianola DS, Zhang L, Campbell GM, Bassani JL, Feng G, and others. 2014. Tailoring and understanding the mechanical properties of nanoparticle-shelled bubbles. ACS Appl. Mater. Interfaces 6:11558–11572.

Cavalieri F, Postma A, Lee L, Caruso F. 2009. Assembly and Functionalization of DNA ⁒ Polymer Microcapsules. Nano 3:234–240.

Chan H-K, Chew NYK. 2003. Novel alternative methods for the delivery of drugs for the treatment of asthma. Adv. Drug Deliv. Rev. [Internet] 55:793–805. Available from: http://www.sciencedirect.com/science/article/pii/S0169409X03000784

Charpentier I, Sarocchi D, Rodriguez Sedano LA. 2013. Particle shape analysis of volcanic clast samples with the Matlab tool MORPHEO. Comput. Geosci. [Internet] 51:172–181. Available from: http://dx.doi.org/10.1016/j.cageo.2012.07.015

Chen L, Subirade M. 2009. Elaboration and characterization of soy/zein protein microspheres for controlled nutraceutical delivery. Biomacromolecules 10:3327–3334.

Cheryan M, Rackis JJ. 1980. Phytic acid interactions in food systems. Available from: http://www.tandfonline.com/doi/abs/10.1080/10408398009527293

Cosnier S, Szunerits S, Marks RS, Novoa A, Puech L, Perez E, and others. 2000. A rapid and easy procedure of biosensor fabrication by micro-encapsulation of enzyme in hydrophilic synthetic latex films. Application to the amperometric determination of glucose. Electrochem. commun. 2:851–855.

Delcea M, Schmidt S, Palankar R, Fernandes PAL, Fery A, Möhwald H, and others. 2010. Mechanobiology: Correlation between mechanical stability of microcapsules studied by afm and impact of cell-induced stresses. Small 6:2858–2862.

Díez-Pascual AM, Gómez-Fatou M a., Ania F, Flores A. 2015. Nanoindentation in polymer nanocomposites. Prog. Mater. Sci. [Internet] 67:1–94. Available from: http://dx.doi.org/10.1016/j.pmatsci.2014.06.002

Ebenstein DM, Pruitt L a. 2006. Nanoindentation of biological materials. Nano Today 1:26–33.

Feng Y, Lee Y. 2016. Surface modification of zein colloidal particles with sodium caseinate to stabilize oil-in-water pickering emulsion. Food Hydrocoll. [Internet] 56:292–302. Available from: http://linkinghub.elsevier.com/retrieve/pii/S0268005X15301971

Feng Y, Lee Y. 2017. Microfluidic fabrication of hollow protein microcapsules for rate-controlled release. RSC Adv. [Internet] 7:49455–49462. Available from: http://xlink.rsc.org/?DOI=C7RA08645H

Fox TG, Flory PJ. 1950. Second-order transition temperatures and related properties of polystyrene. I. Influence of molecular weight. J. Appl. Phys. 21:581–591.

Ghaemi A, Philipp A, Bauer A, Last K, Fery A, Gekle S. 2016. Mechanical behaviour of micro-capsules and their rupture under compression. Chem. Eng. Sci. [Internet] 142:236–243. Available from: http://dx.doi.org/10.1016/j.ces.2015.11.002

Greenfield NJ. 2006. Using circular dichroism spectra to estimate protein secondary structure. Nat. Protoc. [Internet] 1:2876–2890. Available from: http://www.nature.com/nprot/journal/v1/n6/abs/nprot.2006.202.html

Hoare TR, Kohane DS. 2008. Hydrogels in drug delivery: Progress and challenges. Polymer (Guildf). [Internet] 49:1993–2007. Available from: http://dx.doi.org/10.1016/j.polymer.2008.01.027

Hu TT, Wang JX, Shen ZG, Chen JF. 2008. Engineering of drug nanoparticles by HGCP for pharmaceutical applications. Particuology 6:239–251.

Hussain M, Xie J, Hou Z, Shezad K, Xu J, Wang K, and others. 2017. Regulation of Drug Release by Tuning Surface Textures of Biodegradable Polymer Microparticles. ACS Appl. Mater. Interfaces [Internet]:acsami.7b02002. Available from: http://pubs.acs.org/doi/abs/10.1021/acsami.7b02002

Ina M, Zhushma AP, Lebedeva N V., Vatankhah-Varnoosfaderani M, Olson SD, Sheiko SS. 2016. The design of wrinkled microcapsules for enhancement of release rate. J. Colloid Interface Sci. [Internet] 478:296–302. Available from: http://dx.doi.org/10.1016/j.jcis.2016.06.022

Ionescu-Tirgoviste C, Gagniuc PA, Gubceac E, Mardare L, Popescu I, Dima S, and others. 2015. A 3D map of the islet routes throughout the healthy human pancreas. Sci. Rep. [Internet] 5:14634. Available from: http://www.ncbi.nlm.nih.gov/pubmed/26417671%5Cnhttp://www.pubmedcentral.nih.gov/articlerender.fcgi?artid=PMC4586491

Kashiri M, Cerisuelo JP, Domínguez I, López-Carballo G, Hernández-Muñoz P, Gavara R. 2016. Novel antimicrobial zein film for controlled release of lauroyl arginate (LAE). Food Hydrocoll. 61:547–554.

Kermouche G, Loubet JL, Bergheau JM. 2006. A new index to estimate the strain rate sensitivity of glassy polymers using conical/pyramidal indentation. Philos. Mag. 86:5667–5677.

Knowles TPJ, Buehler MJ. 2011. Nanomechanics of functional and pathological amyloid materials. Nat. Nanotechnol. [Internet] 6:469–479. Available from: http://www.ncbi.nlm.nih.gov/pubmed/21804553%5Cnhttp://dx.doi.org/10.1038/nnano.2011.102%5Cnhttp://www.nature.com/doifinder/10.1038/nnano.2011.102

Kuo WY, Lee Y. 2014. Temporal sodium release related to gel microstructural properties-implications for sodium reduction. J. Food Sci. 79:E2245–E2252.

Lai H-M, Geil PH, Padua GW. 1999. X-ray Diffraction Characterization of the Structure of Zein – Oleic Acid Films. J. Appl. Polym. Sci. [Internet] 71:1267–1281. Available from: http://dx.doi.org/10.1002/(SICI)1097-4628(19990222)71:8%3C1267::AID-APP7%3E3.0.CO%5Cn2-O

Lee J, Zhang M, Bhattacharyya D, Yuan YC, Jayaraman K, Mai YW. 2012. Micromechanical behavior of self-healing epoxy and hardener-loaded microcapsules by nanoindentation. Mater. Lett. [Internet] 76:62–65. Available from: http://dx.doi.org/10.1016/j.matlet.2012.02.052

Li M, Joung D, Hughes B, Waldman SD, Kozinski JA, Hwang DK. 2016. Wrinkling Non-Spherical Particles and Its Application in Cell Attachment Promotion. Sci. Rep. [Internet] 6:30463. Available from: http://www.nature.com/articles/srep30463

Lin N, Huang J, Chang PR, Feng L, Yu J. 2011. Effect of polysaccharide nanocrystals on structure, properties, and drug release kinetics of alginate-based microspheres. Colloids Surfaces B Biointerfaces [Internet] 85:270–279. Available from: http://dx.doi.org/10.1016/j.colsurfb.2011.02.039

Long Y, Song K, York D, Zhang Z, Preece JA. 2013. Engineering the mechanical and physical properties of organic-inorganic composite microcapsules. Colloids Surfaces A Physicochem. Eng. Asp. [Internet] 433:30–36. Available from: http://dx.doi.org/10.1016/j.colsurfa.2013.04.055

Loxley A, Vincent B. 1998. Preparation of Poly(methylmethacrylate) Microcapsules with Liquid Cores. J. Colloid Interface Sci. [Internet] 208:49–62. Available from: http://linkinghub.elsevier.com/retrieve/pii/S0021979798956983

Lv L, Schlangen E, Yang Z, Xing F. 2016. Micromechanical properties of a new polymeric microcapsule for self-healing cementitious materials. Materials (Basel). 9:1–16.

Micsonai A, Wien F, Kernya L, Lee Y-H, Goto Y, Réfrégiers M, and others. 2015. Accurate secondary structure prediction and fold recognition for circular dichroism spectroscopy. Proc. Natl. Acad. Sci. [Internet] 112:E3095–E3103. Available from: http://www.pnas.org/lookup/doi/10.1073/pnas.1500851112

Mijatovic D, Eijkel JCT, van den Berg a. 2005. Technologies for nanofluidic systems: top-down vs. bottom-up--a review. Lab Chip [Internet] 5:492–500. Available from: http://www.ncbi.nlm.nih.gov/pubmed/15856084

Neubauer MP, Poehlmann M, Fery A. 2014. Microcapsule mechanics: From stability to function. Adv. Colloid Interface Sci. [Internet] 207:65–80. Available from: http://dx.doi.org/10.1016/j.cis.2013.11.016

Ngan AHW, Tang B. 2009. Response of power-law-viscoelastic and time-dependent materials

to rate jumps. J. Mater. Res. 24:853–862.

Okur HI, Hladílková J, Rembert KB, Cho Y, Heyda J, Dzubiella J, and others. 2017. Beyond the Hofmeister Series: Ion-Specific Effects on Proteins and Their Biological Functions. J. Phys. Chem. B 121:1997–2014.

Olenskyj AG, Feng Y, Lee Y. 2017. Continuous microfluidic production of zein nanoparticles and correlation of particle size with physical parameters determined using CFD simulation. J. Food Eng. [Internet] 211:50–59. Available from: http://linkinghub.elsevier.com/retrieve/pii/S0260877417301668

Ottewill RH, Schofield a. B, Waters J a. 1996. Preparation of composite latex particles by engulfment. Colloid Polym. Sci. 274:763–771.

Paliwal R, Palakurthi S. 2014. Zein in controlled drug delivery and tissue engineering. J. Control. Release [Internet] 189:108–122. Available from: http://dx.doi.org/10.1016/j.jconrel.2014.06.036

Pan K, Zhong Q. 2016. Low energy, organic solvent-free co-assembly of zein and caseinate to prepare stable dispersions. Food Hydrocoll. [Internet] 52:600–606. Available from: http://www.sciencedirect.com/science/article/pii/S0268005X1530059X

Patel A, Hu Y, Tiwari JK, Velikov KP. 2010. Synthesis and characterisation of zein–curcumin colloidal particles. Soft Matter [Internet] 6:6192. Available from: http://xlink.rsc.org/?DOI=c0sm00800a

Qu Y, Huang R, Qi W, Su R, He Z. 2015. Interfacial Polymerization of Dopamine in a Pickering Emulsion: Synthesis of Cross-Linkable Colloidosomes and Enzyme Immobilization at Oil/Water Interfaces. ACS Appl. Mater. Interfaces [Internet]:150702095906003. Available from: http://pubs.acs.org/doi/abs/10.1021/acsami.5b03787

Rath A, Mathesan S, Ghosh P. 2015. Nanomechanical characterization and molecular mechanism study of nanoparticle reinforced and cross-linked chitosan biopolymer. J. Mech. Behav. Biomed. Mater. [Internet] 55:42–52. Available from: http://dx.doi.org/10.1016/j.jmbbm.2015.10.005

Roberts D, Keeling R, Tracka M, Van Der Walle CF, Uddin S, Warwicker J, and others. 2015. Specific ion and buffer effects on protein-protein interactions of a monoclonal antibody. Mol. Pharm. 12:179–193.

Sarrazin B, Tsapis N, Mousnier L, Taulier N, Urbach W, Guenoun P. 2016. AFM Investigation of Liquid-Filled Polymer Microcapsules Elasticity. Langmuir [Internet]:acs.langmuir.6b00431. Available from: http://pubs.acs.org/doi/abs/10.1021/acs.langmuir.6b00431

Shchukina EM, Shchukin DG. 2012. Layer-by-layer coated emulsion microparticles as storage and delivery tool. Curr. Opin. Colloid Interface Sci. [Internet] 17:281–289. Available from: http://linkinghub.elsevier.com/retrieve/pii/S1359029412000714

Sokolovskyy Y, Kroshnyy I, Yarkun V. Mathematical modeling of visco-elastic-plastic deformation in capillary-porous materials in the drying process. :52–56.

Su JF, Wang XY, Dong H. 2012. Micromechanical properties of melamine-formaldehyde microcapsules by nanoindentation: Effect of size and shell thickness. Mater. Lett. [Internet] 89:1–4. Available from: http://dx.doi.org/10.1016/j.matlet.2012.08.072

Subramaniam AB, Abkarian M, Stone H a. 2005. Controlled assembly of jammed colloidal shells on fluid droplets. Nat. Mater. 4:553–556.

Teh S-Y, Lin R, Hung L-H, Lee AP. 2008. Droplet microfluidics. Lab Chip [Internet] 8:198. Available from: http://xlink.rsc.org/?DOI=b715524g

Thompson KL, Williams M, Armes SP. 2014. Colloidosomes: Synthesis, properties and applications. J. Colloid Interface Sci. [Internet] 447:217–228. Available from: http://linkinghub.elsevier.com/retrieve/pii/S0021979714009187

Wang Q, Yin L, Padua GW. 2008. Effect of hydrophilic and lipophilic compounds on zein microstructures. Food Biophys. 3:174–181.

Wang Y, Lopes Filho F, Geil P, Padua GW. 2005. Effects of processing on the structure of zein/oleic acid films investigated by X-ray diffraction. Macromol. Biosci. 5:1200–1208.

Wang Y, Padua GW. 2010. Formation of zein microphases in ethanol-water. Langmuir 26:12897–12901.

Wang Y, Padua GW. 2012. Nanoscale characterization of zein self-assembly. Langmuir 28:2429–2435.

Wang Z, Ju X, He R, Yuan J, Wang L. 2015. The Effect of Rapeseed Protein Structural Modification on Microstructural Properties of Peptide Microcapsules. Food Bioprocess

Technol.:1305–1318.

Zellmer S, Lindenau M, Michel S, Garnweitner G, Schilde C. 2016. Influence of surface modification on structure formation and micromechanical properties of spray-dried silica aggregates. J. Colloid Interface Sci. [Internet] 464:183–190. Available from: http://linkinghub.elsevier.com/retrieve/pii/S0021979715303386

Zhang Y, Cui L, Che X, Zhang H, Shi N, Li C, and others. 2015. Zein-based films and their usage for controlled delivery: Origin, classes and current landscape. J. Control. Release [Internet] 206:203–219. Available from: http://dx.doi.org/10.1016/j.jconrel.2015.03.030

Zhong Q, Jin M. 2009. Zein nanoparticles produced by liquid–liquid dispersion. Food Hydrocoll. [Internet] 23:2380–2387. Available from: http://linkinghub.elsevier.com/retrieve/pii/S0268005X09001374

CHAPTER 6

Microencapsution of nisin in microfluidic chip for enhanced microbial activity

6.1 Abstract

Nisin-loaded zein microcapusles were prepared in microfluidic chips through internal phase separation method. The release profiles of nisin from microcapusules were tuned by changing the nisin loading and flow rate during microfluidic process. Rapid release of nisin was achieved with low dispersing phase flow rate (0.2 ml/hr) and high loading microcapsule, while slow release was achieved with high dispersing flow rate (0.3 ml/hr) and low loading microcapsule. Antimicrobial test results indicate that zein microcapsules with slow nisin release can effectively inhibit the growth of *L. monocytogenes* in cheese that is stored at 4°C. Compared to free nisin as controll, the microcapsule with slow release of nisin was able to reduce the *L. monocytogenes* concentration from 4.11 log CFU/g to non-detectable range, while the *L. monocytogenes* in nisin control sample climbed to 4.22 log CFU/g. However, rapid release of nisin is more feasible to inhibit the growth of *L. monocytogenes* in BHI broth. The AFM-IR spectrum suggests that the distribution of nisin in zein homogeneous, which indicates that co-assembling between zein and nisin occurred during the internal phase separation process.

Keywords

Microfluidics, nisin, Listeria *monocytogenes*, AFM-IR, controlled release, cheese

6.2 Introduction

Each year, foodborne pathogens contamination affects 48 million people in the United States and impose over $15.5 billion of economic burden to the industry and government (Hoffmann and others 2015). These foodborne illnesses further give rise to antibiotic resistance and present critical challenges to control the disease and infection (Mulholland and others 2016). Therefore, it is gaining interest to develop novel strategies to ensure food quality and safety during processing and consumption, such as the usage of antimicrobial packaging films (Vonasek and others 2014; Kashiri and others 2016; Mei and others 2017). Currently, the antimicrobial compounds present in packing films usually contain silver nanoparticles and other non-food grade materials (López-Carballo and others 2013; Mei and others 2017), which provided promising results and possessed safety concerns of the materials themselves at the same time. Therefore, many efforts were made in the past decade towards the application of natural food preservatives, and one famous example would be nisin (Liu and Hansen 1990; Xiao and others 2011) which is a peptide based antimicrobial chemical composed of 34 amino acids (Lins and others 1999). Nisin has shown potent effect on inhibiting the growth of *Listeria monocytogenes* (LM)(Abee and others 1994; Imran and others 2013). LM is a pathogen typically found in dairy products that can cause listeriosis, which is responsible for an annual economic loss of $2.6 billion in the United States (HOFFMANN and others 2012).

The application of nisin in food industry is limited due to its instability and insolubility in food matrices, where nisin can readily be degraded by other food ingredients such as sodium metabisulfite, titanium dioxide, Ca^{2+} and Mg^{2+} (Abee and others 1994), as well as neutral pH(Rollema and others 1995). Encapsulation of nisin using GRAS materials were investigated in previous study(Bernela and others 2014) to improve and extend their efficacy in food matrices. Zein, as a GRAS protein from corn, food and pharmaceutical industries due of its excellent physiochemical property, safety and cost-efficacy features (Shukla and Cheryan 2001). Previously nisin was encapsulated in zein using spray drying method. It lead to a porous microcapsule structure and resulted in poorer antilisterial properties than free nisin, then glycerol was used as a plasticizer to modify the morphology (Xiao and others 2011). The involvement of thermal treatment during conventional processing, such as spray drying, could also bring in detrimental effects on the stability and antimicrobial activity of nisin (Holcapkova and others 2017). On the other hands, those studies have demonstrated that zein, a water-insoluble protein, has a great potential as a releasing medium for antimicrobial agents (Zhang and others 2014; Kashiri and others 2016; Mei and others 2017). However, there is still lack of

study to reveal the molecular structure when nisin interacts with the wall materials.

Microfluidic technique has been developed in the 1990s, while it is still a new technique in food science and food industry, which is capable of manipulating fluids in small scale (10^{-9} to 10^{-18} liters) (Whitesides 2006). Recently, it is gaining more attention as a manufacturing tool to produce microparticles with sophisticated structures (Zhang and others 2007; Workman and others 2008; Shum and others 2010; Zhou and others 2014). Microfluidic processing features many advantages including simplicity, precise control over product quality, and the potential of assembling various physical structures (Muijlwijk and others 2016). Different from conventional encapulation methods like shear and high-pressure homogenization, there is no heat generation during microfluidic processing(Ali and others 2009). As such, nisin will be able to retain its chemical stability and antimicrobial activity during processing. Our previous work showed that zein can self-assemble to form hollow microcapsules in microfluidic chips, driven by diffusion induced internal phase separation (Feng and Lee 2017). The objective of this study is to encapsulate nisin in zein microcapsule in a microfluidic device through the internal phase separation approach, and control the release rate of nisin for the purposes of extending its antimicrobial efficacy.

6.3 Materials and methods

6.3.1 Materials

Zein (Z3625, Sigma-Aldrich, St. Louis, MO) dissolved in 70% (v/v) ethanol (200 Proof, Decon Laboratories, King of Prussia, PA) was used as the dispersing phase. Tributyrin (W222305, Sigma-Aldrich, St. Louis, MO) containing 2% (w/v) soy lecithin (MP Biomedicals Inc, Solon, OH) was used as the continuous phase. Nisin (Nisaplin, Danisco, New Century, KS) was extracted with 98% methanol and 70% ethanol to prepare the stock solution. The extracted nisin fraction was centrifuged at 4200 rpm (add g value for this centrifugation) for 20 min. into the dispersing phase at 2 mg/ml, to assess the rate of release. Hexane (Macron Fine Chemicals, Center Valley, PA) was used to wash the microcapsules. No. 42 (pore size 2.5 μm) Whatman filter paper (Whatman Inc., Florham Park, NJ) was used to collect final products.

6.3.2 Microfluidic fabrication

The dispersing phase was prepared by mixing 6% (w/v) of zein into an ethanol-water binary system containing 70% (v/v) ethanol with extracted nisin. The mixture was centrifuged

at 2000 g for 20 min to remove insoluble. The continuous phase was prepared by mixing 2% (w/v) of soy lecithin with tributyrin by stirring at 250 rpm for overnight, followed by centrifugation at 2000 g for 10 min to remove impurities. Nisin loaded microcapsules were then produced in a 100 μm T-junction microfluidic chip (Dolomite, UK) through internal phase separation that described in our previous study (Feng and Lee 2017). The samples prepared in this study are listed in Table 6.1. Two flow rate combinations were chosen for this study and flow rates were controlled using a Harvard Model 11 Elite syringe pump (Harvard Apparatus Inc., Holliston, MA). Once collected, the capsules were immediately washed with hexane for three times on a filter paper with vacuum. The final microcapsules were obtained by transferring the filtered samples into a convective oven to remove excessive water at 30°C for 6 hours. Nisin load was quantified using HPLC.

6.3.3 Characterization of microcapsules

Scanning electron microscopy (SEM)

The surface morphology of microcapsules was imaged using a scanning electron microscope ((S-4700, Hitachi company, Japan) with an accelerating voltage of 5 kV located in Beckman Institute at the University of Illinois, Urbana-Champaign. Samples were adhered to a conductive carbon tape and sputter coated (model Dest-1 TSC, Denton Vacuum LLC., Moorestown, NJ, USA) with a gold layer before imaging.

Circular dichroism spectrum (CD)

The CD spectra were recorded with a JASCO J-715 spectropolarimeter (Jasco Inc., Easton, MD). Samples were placed in a quarts cell with a 1 cm path length. The measurement was conducted over the range of 200-250 nm at 25°C, with the scanning speed of 50 nm/min, and the resolution of 1 nm. The content of α-helix, β-sheet, and random coil was calculated using the BeStSel software (Micsonai et al., 2015), which could be accessed online at http://bestsel.elte.hu. The Savitsky-Golay smoothing algorithm was used, with a polynomial order of 3 and a smoothing window of 20 points, according to a previous study (Greenfield, 2006).

Fourier-transform infrared spectroscopy (FTIR)

FTIR spectra were acquired using an ATR-FTIR Nicolet Nexus 670 IR spectrometer (Thermo Nicolet Corp., Madison, MI) which was equipped with a Germanium attenuated total reflection (ATR) accessory. The IR transmittance was acquired from 4000 to 800 cm^{-1} with a resolution of 2 cm^{-1}. 40 repeated scans were undertaken for each sample. All signals were

collected against a background spectrum recorded from the mica substrate only.

Atomic force microscopy - Infrared (AFM-IR)

The distribution of nisin was investigated with a AFM-IR equipment (NeaSNOM, Neaspec GmbH, Germany) following a method described in a previous work (Huth and others 2012). The nano-FTIR is based on an oscillating gold-coated AFM tip and a near-field interferometric signal from of scattered light. A wavenumber range from 1150 to 1800 was chosen to reflect the secondary structure, according to a previous study (Amenabar and others 2013). Three locations on each AFM scanning image were randomly selected to obtain the spectrum.

Nisin loading and release kinetics

To study the release kinetics, approximately 7 mg of microcapsules was dispersed in deionized (DI) water with constant shaking rate at 100 rpm. Six measurements were taken at 3, 10, 30, 60, 180, 360 min, respectively, to evaluate the rate of release by measuring the nisin. An equivalent volume of DI water was supplemented upon the removal of the sample. High performance lipid chromatography (HPLC) with a C-18 column was used to quantify the amount of nisin. Acetonitrile was used as mobile phase for the HPLC and the nisin was detected using a UV detector at 215 nm of wavelength. The peak of nisin was identified at 23 min. A standard curve was plotted with nisin concentration at 20, 50, 100, 200, and 300 ppm, respectively.

6.3.4 Microbial test

Listeria growth curve

The listeria growth curve was performed using a method described in a previous study (Mishra and others 2018). Briefly, the pathogen *L. monocytogenes* (10^6 CFU/mL) was mixed with or without commercial nisin and encapsulated nisin (nisin content was normalized at 5 ppm), and then incubated in brain heart infusion broth (BHI) at 37°C for 12 hours. Every two hours, the population of survived *L. monocytogenes* was deteremined by plate count method. The control was prepared without the addition of nisin.

Antilisterial properties in cheese

Antimicrobial activity of commercial nisin and encapsulated nisin were evaluated by their addition to Queso Fresco (QF). An equivalent amount of 250 mg/g nisin was added into the milk before renneting. Afterwards, all QF samples were stored at 4 °C, for up to 7 days,

until sampled. Complementary to plate- count enumeration, samples from each time point were also subjected to enrichment using the FDA-Bacteriological Analytical Manual standard enrichment/recovery method. By the end of QF storage, three random *L. monocytogenes* isolates per cheese treatment per independent experiment were recovered from PALCAM Listeria-Selective agar (EMD-Millipore) plates and cultured individually for antimicrobial susceptibility testing.

6.4 Results and discussion

6.4.1 Nisin loading and release kinetics of nisin

The loading of nisin was quantified with HPLC. The loading of nisin was about 5 μg/mg in the low load sample and approximately 11 μg/mg in the high load microcapsules. The differences in the nisin loading indicates that 70% ethanol (pH=3) is more efficient than 98% methanol in extracting nisin, which was contradictory to a previous study in which pH was not precisely controlled (Taylor and others 2007). Nisin is a hydrophobic compound that has poor solubility in water but soluble in alcohols, and the low pH of alcohol environment could further increased the solubility of nisin in alcohols(Liu and Hansen 1990). The release kinetics of nisin from different microcapsules was plotted in the Figure 6.1. Overall the capsule with low load of nisin showed the slowest rate of release, while two high load samples showed similar release patterns. The release of nisin from microcapsule is driven by diffusion, which is based the local concentration gradient(Calado and others 2016). In those microcapsules with less nisin, the concentration gap between hydrated zein capsules and surrounding fluid is less, and hence resulted in a slower release rate. However, the sample with high loading releases faster while the capsule prepared with low dispersing phase flow rate releases slightly faster than the other sample. It agreed with our previous study, because smaller particles were generated at low dispersing phase flow which tend to release the core materials faster (Feng and Lee 2017).

6.4.2 Morphology of microcapsules

The SEM image of microcapsules are shown in the Figure 6.2. Different from the samples prepared with high flow rate, the capsules prepared with low flow rate has an open and cracked structure. The cracked during internal phase separation has been reported due to too fast or too slow diffusion rate(Dowding and others 2004). In this case, a fast diffusion rate is expected, due to the formation of small droplet at low flow rate. The drastic shrinking of capsule during rapid diffusion then leads to the formation of cracking before zein could self-

assemble to from steady structure. When the flow rate of dispersing phase increased, the microcapsules has less tendency to crack.

6.4.3 Molecular characterization of zein-nisin interaction

The molecular-level interaction between zein and nisin was studied using FTIR, CD, and nano-FTIR spectrum. The FTIR spectrum is shown in the Figure 6.3. The peaks were identified according to previous studies (Bernela and others 2014; Khan and others 2014), and most peaks remain the similar intensity, including the O-H stretch peak at 3299.63 cm^{-1}, the C-H stretch at 2963.21 cm^{-1}, the C=O stretch at 1744.25 cm^{-1}, the O-H stretch at 1252.58 cm^{-1}, and the C-O stretch at 1172.89 cm^{-1} and 1102.96 cm^{-1}. On the other hand, an increased intensity of amide peaks (amide I at 1658.27 cm^{-1} that indicating C=O vibration, amide II at 1544.28 cm^{-1} that indicating N-H vibration, and amide III at 1452.80cm^{-1} that indicating C-N bond) were observed in nisin-loaded samples. A previous study also reported the increased intensity of amide absorbance as the evidence of nisin loading (Khan and others 2014). In addition, the nisin-loaded sample did not show new peaks, indicating no covalent bond formation between nisin and zein.

Figure 6.4 shows the secondary structure of microcapsules that were characterized with CD spectrum. According to the CD spectrum, it could be found that the loading of nisin altered the secondary structures of protein. The distribution of α-helix, β-sheet and random coils were calculated with BestSel algorithms (Micsonai and others 2015). In blank zein capsules, very small amount of α-helix (1.9%) presents, with relatively high fraction of β-sheet (43.3%) and random coil (54.8%), as we reported in our previous work(Feng and Lee 2017). Self-assembly of zein converted the majority of α-helix into β-sheet(Wang and Padua 2012) Similar distribution of secondary structures were also found in low loading (~5μg/mg) nisin sample (0% α-helix, 39.7% β-sheet, and 60.3% random coil). However, microcapsules with high-loading of nisin (~12 μg/mg) contains much higher fraction of α-helix, 4.9% in the low flow rate sample and 12.2% in the high flow rate sample. The results suggests the self-assembly of zein is hindered by the increased concentration of nisin, which is probably due to the hydrogen bonding between nisin and the amino acids that reside in the α-helical structure of zein. On the other hand, it could also be possible that the α-helix structure originally exists in nisin. However, previous study only suggested the formation of β-sheet in nisin when the pH is greater than 5.5(Dykes and others 1998).

Unlike conventional microcapsules with core-shell structure, the interaction between

peptide and protein makes it difficult to predict the spatial distribution nisin in this study. A possible scenario is that nisin is involved in the arrangement of self-assembled zein molecules and forms a mingled and complexed structure, instead of the classical core-shell structure. As such, we utilized an AFM-IR technology to study the surface composition of nisin-loaded microcapsules. A schematic diagram is shown in the figure 6.5 to illustrate the mechanism of AFM-IR. Briefly, a gold-coated AFM tip is paired with an IR device to probe the near-field spectrum during scanning. As such, it can provide the fingerprint to reflect the composition at the material surface, which could be used in this work to study the distribution of nisin. Two samples, blank zein capsule and high nisin loaded and high flow rate capsule were compared. For each capsule, three spots were randomly selected after the AFM scanning on the capsule surface (2μm * 1μm). All three spots showed similar spectrums, indicating a homogeneous surface composition. Comparing the spectrum from nisin-loaded zein capsules and blank zein capsules, the nisin-loaded zein capsule has two characteristic peaks of amide I and amide II(Amenabar and others 2013), which is shown in the yellow color. As is mentioned in the previous sections, these amide peaks are an indication of the presence of nisin. Hence, it is reasonable to speculate that nisin and zein mingle and form a co-assembled homogeneous structure, instead of the classical core-shell structure in microcapsules.

6.4.4 The antimicrobial activity of encapsulated nisin

The growth curves of *L. monocytogenes* in broth with or without nisin are plotted in the Figure 6.6(a). Compared to the commercial nisin, the encapsulated nisin with different processing conditions behaved differently. The sample low load 0.3-10 showed worse antiliterial effects than free nisin in the broth while high load samples were able to inhibit the growth of LM. The main difference of low load sample is the slow release rate. In a broth, a slow release of nisin may favor the accumulation of nisin-resistant *L. monocytogenes.* In a previous study, it has been found that an instant high concentration of nisin combined with constant further release of nisin is necessary to provide efficient inhibition of *Listeria* growth(Mishra and others 2018). Similarly, the high load samples in this study, which were able to release the majority of nisin at the beginning of incubation, showed acceptable antilisterial properties in broth.

Listeria contamination occurs frequently in dairy products (Greenwood and others 1991) including cheese(Ibarra-Sánchez and others 2018). In spite of incubating at 37°C, dairy products are usually refrigerated at 4°C where the growth of *Listeria* is much slower. The results of survived *Listeria* with/without nisin or encapsulated nisin in fresh cheese were shown

in the Figure 6.6(b). Opposite from the results from the *Listeria* growth curve, the slow released sample (low load 0.3-10) showed the most efficient inhibitory of listeria. This result indicates that a constant amount of nisin with low concentration is more feasible to inhibit slow growth of listeria at low temperature in fresh cheese.

Contradictory results from listeria survival tests were found in the broth and cheese, which were also performed at different temperature (37°C and 4°C). For different food matrices and storage conditions, completely different strategy should be used to prevent the growth of food pathogens. For designing a delivery system to release antimicrobial agents in foods, all the perspectives of foods matrices including pH, fat content, temperature and viscosity need to be taken into account.

6.5 Conclusions

In this study, an anti-microbial peptide nisin was encapsulated in zein using internal phase separation method. Different release patterns were achieved by adjusting the flow rates and nisin loading. The distribution of nisin in zein microcapsules was characterized with AFM-IR, and a homogeneous co-assemble pattern between nisin and zein was suggested. Microbial tests infers that microbial activity of encapsulated nisin is highly dependent on the food matrices and environmental conditions. Instant release of antimicrobial agent is helpful for inhibiting rapid grow of listeria in broth while sustained release is preferred in cheese. Future work could reveal more insights in terms of choosing the appropriate antimicrobial release media in different food matrices and environment.

6.6 Tables and figures

Table 6.1. A list of samples prepared in this study

Sample name	**Loading (μg/mg)**	**Dispersing flow rate (ml/hr)**	**Continuous flow rate (ml/hr)**
Commercial nisin	Commercial sample with 2.5% (w/w) of nisin	N.A.	N.A.
Low load 0.3-10	5	0.3	10
High load 0.3-10	11	0.3	10
High load 0.2-10	11	0.2	10

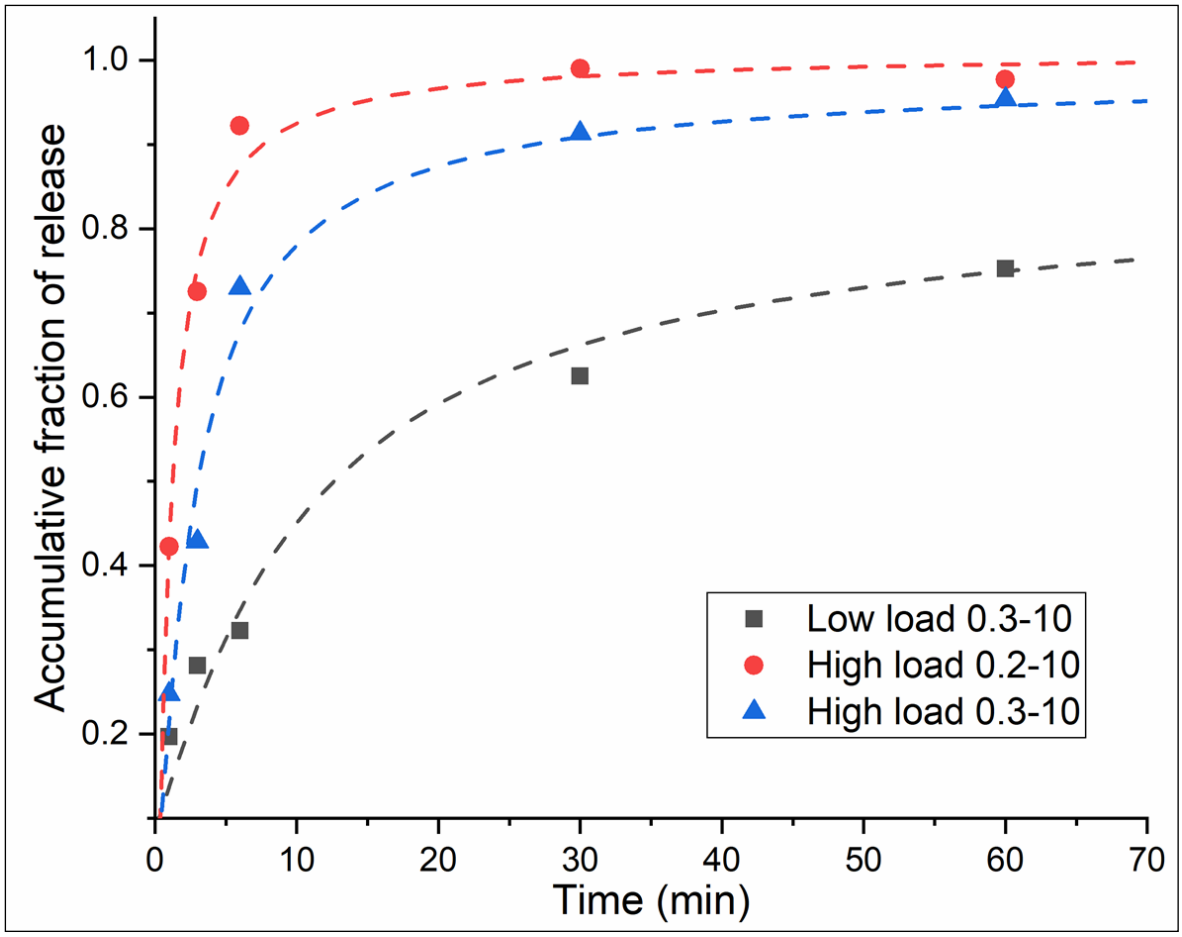

Figure 6.1. The release profiles of nisin from different capsules. sample low load 0.3-10 is the zein capsule with 5 μg/mg of nisin, prepared with 0.3 ml/hr of dispersing flow rate and 10ml/hr of continuous flow rate; sample high load 0.3-10 is the zein capsule containing 11 μg/mg of nisin, prepared with 0.3 ml/hr of dispersing flow rate and 10 ml/hr of flow rate; sample high load 0.2-10 is the zein capsule containing 11 μg/mg of nisin, prepared with 0.2ml/hr of dispersing flow rate and 10ml/hr of continuous flow rate.

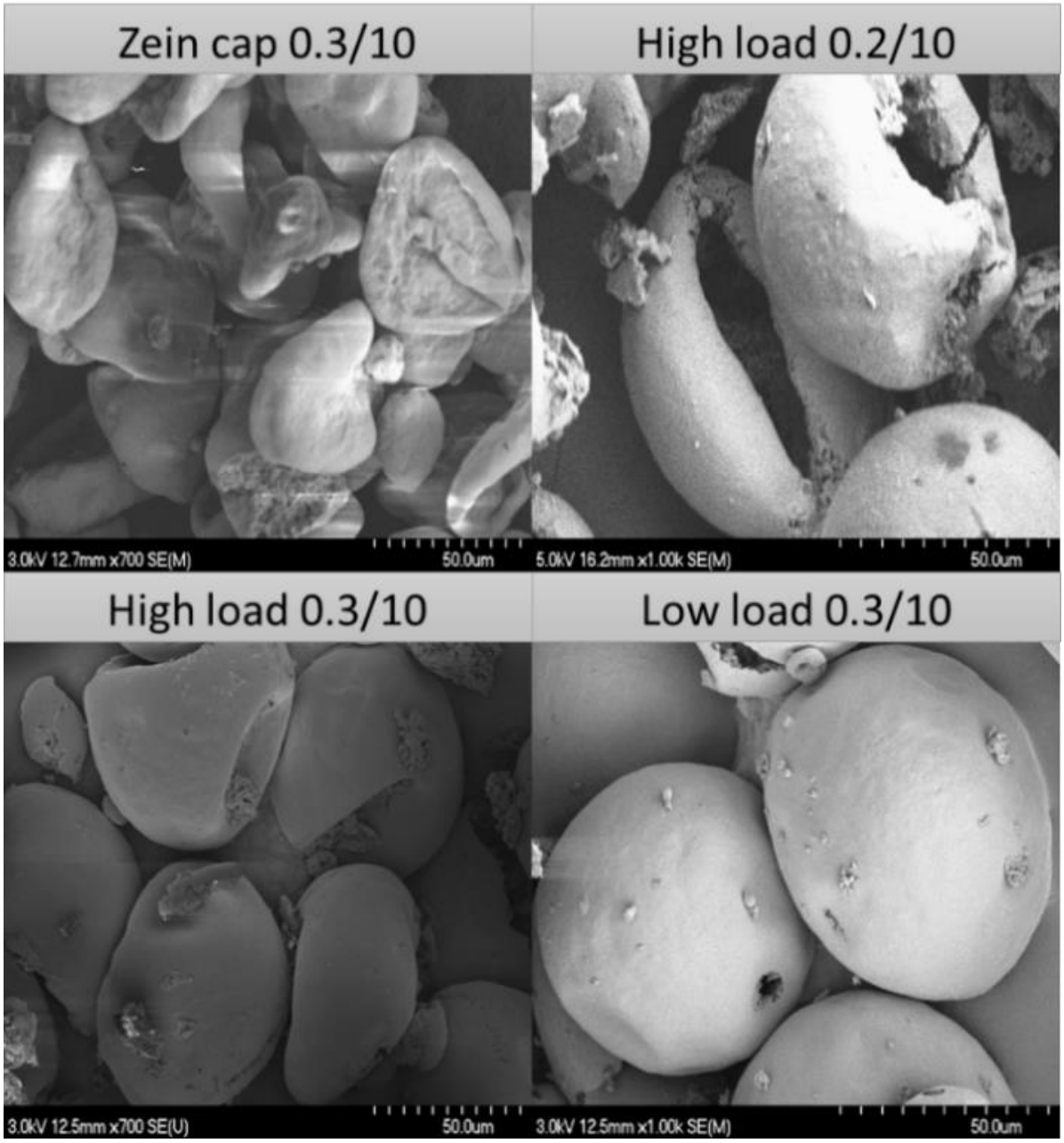

Figure 6.2. The scanning electron microscopy images of microcapsules formed at different conditions. Zein capsule is the blank that does not contain nisin; sample low load 0.3-10 is the zein capsule with 5 μg/mg of nisin, prepared with 0.3 ml/hr of dispersing flow rate and 10ml/hr of continuous flow rate; sample high load 0.3-10 is the zein capsule containing 11 μg/mg of nisin, prepared with 0.3 ml/hr of dispersing flow rate and 10 ml/hr of flow rate; sample high load 0.2-10 is the zein capsule containing 11 μg/mg of nisin, prepared with 0.2ml/hr of dispersing flow rate and 10ml/hr of continuous flow rate.

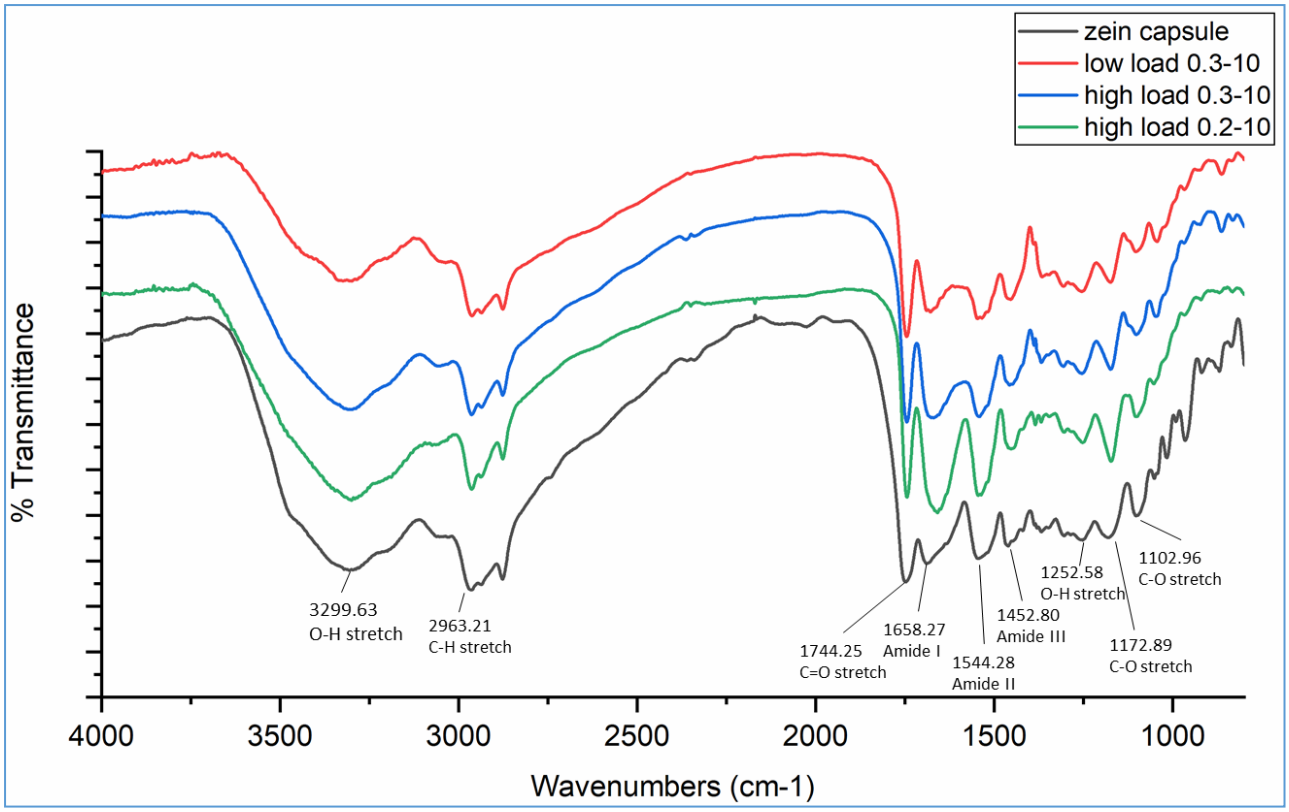

Figure 6.3. FTIR spectrum of microcapsules, zein capsule is the blank that does not contain nisin; sample low load 0.3-10 is the zein capsule with 5 µg/mg of nisin, prepared with 0.3 ml/hr of dispersing flow rate and 10ml/hr of continuous flow rate; sample high load 0.3-10 is the zein capsule containing 11 µg/mg of nisin, prepared with 0.3 ml/hr of dispersing flow rate and 10 ml/hr of flow rate; sample high load 0.2-10 is the zein capsule containing 11 µg/mg of nisin, prepared with 0.2ml/hr of dispersing flow rate and 10ml/hr of continuous flow rate.

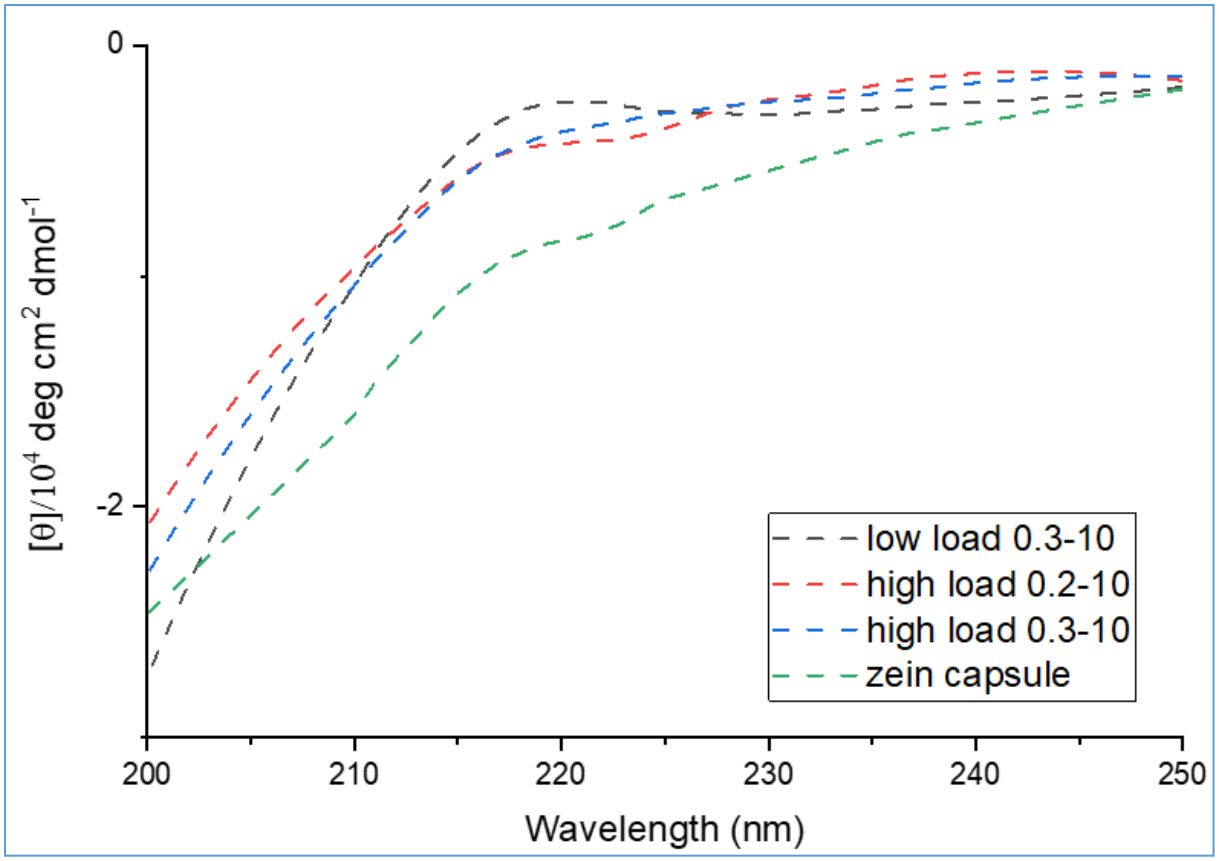

Figure 6.4. Circular dichroism spectrum of zein capsule and nisin-loaded zein capsules. zein capsule is the blank that does not contain nisin; sample low load 0.3-10 is the zein capsule with 5 μg/mg of nisin, prepared with 0.3 ml/hr of dispersing flow rate and 10ml/hr of continuous flow rate; sample high load 0.3-10 is the zein capsule containing 11 μg/mg of nisin, prepared with 0.3 ml/hr of dispersing flow rate and 10 ml/hr of flow rate; sample high load 0.2-10 is the zein capsule containing 11 μg/mg of nisin, prepared with 0.2ml/hr of dispersing flow rate and 10ml/hr of continuous flow rate.

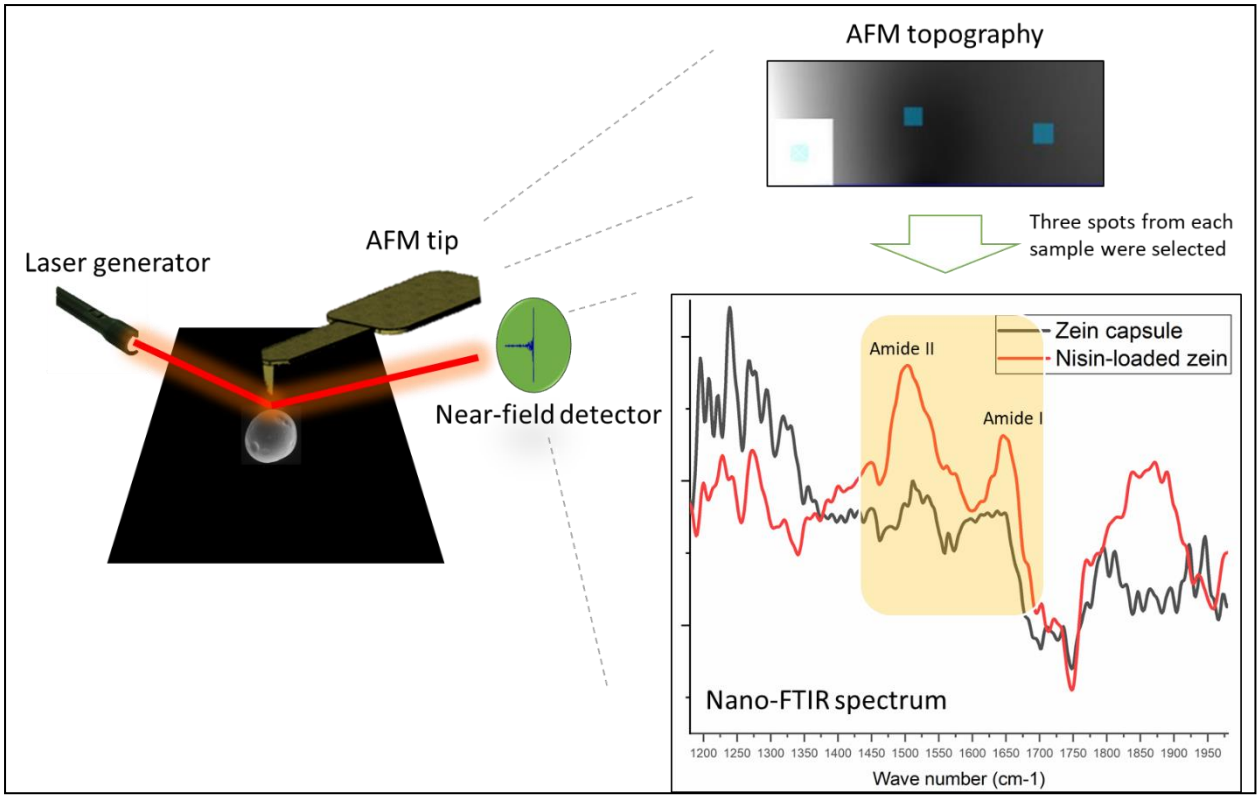

Figure 6.5. A schematic diagram of nano-FTIR measurement.

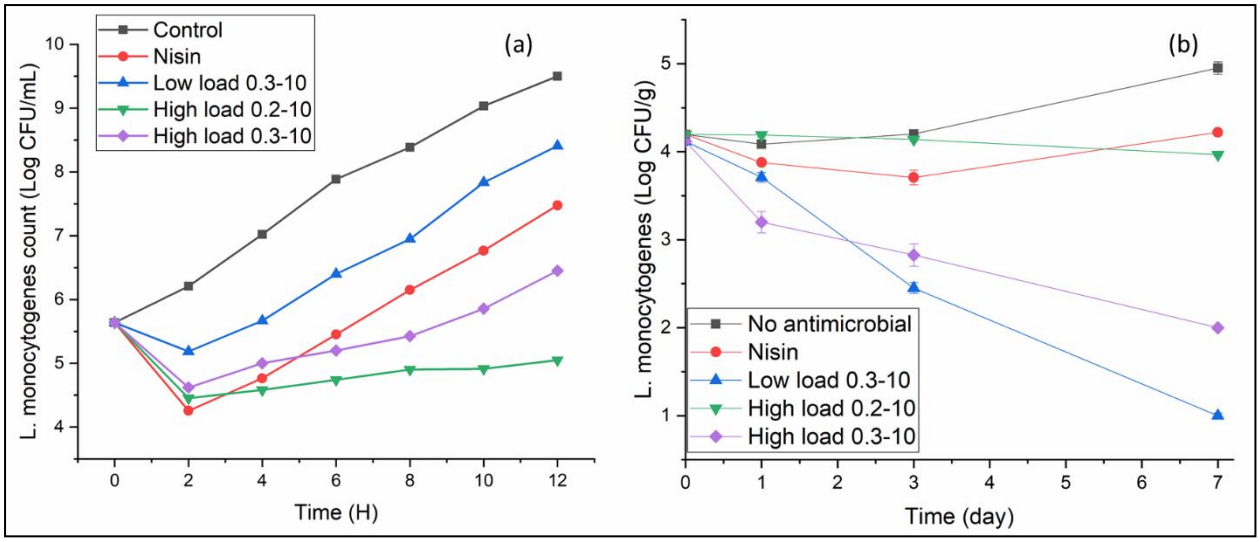

Figure 6.6. The L. *monocytogenes* survival test in (a) broth at 37°C (5 ppm nisin for all treatments) and (b) cheese at 4°C (250 µg/g nisin for all treatments). Sample low load 0.3-10 is the zein capsule with 5 µg/mg of nisin, prepared with 0.3 ml/hr of dispersing flow rate and 10ml/hr of continuous flow rate; sample high load 0.3-10 is the zein capsule containing 11 µg/mg of nisin, prepared with 0.3 ml/hr of dispersing flow rate and 10 ml/hr of flow rate; sample high load 0.2-10 is the zein capsule containing 11 µg/mg of nisin, prepared with 0.2ml/hr of dispersing flow rate and 10ml/hr of continuous flow rate. Sample nisin is the commercial nisin with the concentration of 2.5% (w/w).

6.7 References

Abee T, Rombouts FM, Hugenholtz J, Guihard G, Letellier L. 1994. Mode of Action of Nisin Z against Listeria monocytogenes Scott A Grown at High and Low Temperatures. Appl. Environ. Microbiol. [Internet] 60:1962–8. Available from: http://www.pubmedcentral.nih.gov/articlerender.fcgi?artid=201587&tool=pmcentrez&rendertype=abstract

Ali HSM, York P, Blagden N. 2009. Preparation of hydrocortisone nanosuspension through a bottom-up nanoprecipitation technique using microfluidic reactors. Int. J. Pharm. [Internet] 375:107–113. Available from: http://linkinghub.elsevier.com/retrieve/pii/S0378517309001732

Amenabar I, Poly S, Nuansing W, Hubrich EH, Govyadinov AA, Huth F, and others. 2013. Structural analysis and mapping of individual protein complexes by infrared nanospectroscopy. Nat. Commun. [Internet] 4:1–9. Available from: http://dx.doi.org/10.1038/ncomms3890

Bernela M, Kaur P, Chopra M, Thakur R. 2014. Synthesis, characterization of nisin loaded alginate-chitosan-pluronic composite nanoparticles and evaluation against microbes. LWT - Food Sci. Technol. [Internet] 59:1093–1099. Available from: http://dx.doi.org/10.1016/j.lwt.2014.05.061

Calado B, dos Santos A, Semiao V. 2016. Characterization of the mixing regimes of Newtonian fluid flows in asymmetrical T-shaped micromixers. Exp. Therm. Fluid Sci. [Internet] 72:218–227. Available from: http://www.sciencedirect.com/science/article/pii/S0894177715003337

Dowding PJ, Atkin R, Vincent B, Bouillot P. 2004. Oil core-polymer shell microcapsules prepared by internal phase separation from emulsion droplets. I. Characterization and release rates for microcapsules with polystyrene shells. Langmuir 20:11374–11379.

Dykes GA, Hancock REW, Hastings JW. 1998. Structural variations in nisin associated with different membrane mimicking and pH environments. Biochem. Biophys. Res. Commun. 247:723–727.

Feng Y, Lee Y. 2017. Microfluidic fabrication of hollow protein microcapsules for rate-controlled release. RSC Adv. [Internet] 7:49455–49462. Available from: http://xlink.rsc.org/?DOI=C7RA08645H

Greenwood MH, Roberts D, Burden P. 1991. The occurrence of Listeria species in milk and dairy products: a national survey in England and Wales. Int. J. Food Microbiol. 12:197–206.

HOFFMANN S, BATZ MB, MORRIS JG. 2012. Annual Cost of Illness and Quality-Adjusted Life Year Losses in the United States Due to 14 Foodborne Pathogens. J. Food Prot. [Internet] 75:1292–1302. Available from: http://jfoodprotection.org/doi/abs/10.4315/0362-028X.JFP-11-417

Hoffmann S, Maculloch B, Batz M. 2015. Economic Burden of Major Foodborne Illnesses Acquired in the United States. Econ. Res. Serv.

Holcapkova P, Kolarova Raskova Z, Hrabalikova M, Salakova A, Drbohlav J, Sedlarik V. 2017. Isolation and Thermal Stabilization of Bacteriocin Nisin Derived from Whey for Antimicrobial Modifications of Polymers. Int. J. Polym. Sci. [Internet] 2017:1–7. Available from: https://www.hindawi.com/journals/ijps/2017/3072582/

Huth F, Govyadinov A, Amarie S, Nuansing W, Keilmann F, Hillenbrand R. 2012. Nano-FTIR absorption spectroscopy of molecular fingerprints at 20 nm spatial resolution. Nano Lett. 12:3973–3978.

Ibarra-Sánchez LA, Van Tassell ML, Miller MJ. 2018. Antimicrobial behavior of phage endolysin PlyP100 and its synergy with nisin to control Listeria monocytogenes in Queso Fresco. Food Microbiol. 72:128–134.

Imran M, Revol-Junelles AM, de Bruin M, Paris C, Breukink E, Desobry S. 2013. Fluorescent labeling of nisin Z and assessment of anti-listerial action. J. Microbiol. Methods [Internet] 95:107–113. Available from: http://dx.doi.org/10.1016/j.mimet.2013.07.009

Kashiri M, Cerisuelo JP, Domínguez I, López-Carballo G, Hernández-Muñoz P, Gavara R. 2016. Novel antimicrobial zein film for controlled release of lauroyl arginate (LAE). Food Hydrocoll. 61:547–554.

Khan A, Salmieri S, Fraschini C, Bouchard J, Riedl B, Lacroix M. 2014. Genipin cross-linked nanocomposite films for the immobilization of antimicrobial agent. ACS Appl. Mater. Interfaces 6:15232–15242.

Lins L, Ducarme P, Breukink E, Brasseur R. 1999. Computational study of nisin interaction with model membrane. Biochim. Biophys. Acta 1420:111–120.

Liu W, Hansen JN. 1990. Some chemical and physical properties of nisin, a small-protein

antibiotic produced by Lactococcus lactis. Appl. Environ. Microbiol. [Internet] 56:2551–8. Available from: https://www.ncbi.nlm.nih.gov/pmc/articles/PMC184764/

López-Carballo G, Higueras L, Gavara R, Hernández-Muñoz P. 2013. Silver ions release from antibacterial chitosan films containing in situ generated silver nanoparticles. J. Agric. Food Chem. 61:260–267.

Mei L, Teng Z, Zhu G, Liu Y, Zhang F, Zhang J, and others. 2017. Silver Nanocluster-Embedded Zein Films as Antimicrobial Coating Materials for Food Packaging. ACS Appl. Mater. Interfaces [Internet]:acsami.7b08152. Available from: http://pubs.acs.org/doi/abs/10.1021/acsami.7b08152

Micsonai A, Wien F, Kernya L, Lee Y-H, Goto Y, Réfrégiers M, and others. 2015. Accurate secondary structure prediction and fold recognition for circular dichroism spectroscopy. Proc. Natl. Acad. Sci. [Internet] 112:E3095–E3103. Available from: http://www.pnas.org/lookup/doi/10.1073/pnas.1500851112

Mishra SK, Malik RK, Panwar H, Barui AK. 2018. Microencapsulation of reuterin to enhance long-term efficacy against food-borne pathogen Listeria monocytogenes. 3 Biotech [Internet] 8. Available from: https://doi.org/10.1007/s13205-017-1035-8

Muijlwijk K, Berton-carabin C, Schroën K. 2016. Cross-flow microfluidic emulsification from a food perspective. Trend food Sci. Technol. 49:51–63.

Mulholland S, Turpin ER, Bonev BB, Hirst JD. 2016. Docking and molecular dynamics simulations of the ternary complex nisin2:lipid II. Sci. Rep. [Internet] 6:1–11. Available from: http://dx.doi.org/10.1038/srep21185

Rollema HS, Kuipers OP, Both P, De Vos WM, Siezen RJ. 1995. Improvement of solubility and stability of the antimicrobial peptide nisin by protein engineering. Appl. Environ. Microbiol. 61:2873–2878.

Shukla R, Cheryan M. 2001. Zein: The industrial protein from corn. Ind. Crops Prod. 13:171–192.

Shum HC, Abate AR, Lee D, Studart AR, Wang B, Chen CH, and others. 2010. Droplet microfluidics for fabrication of non-spherical particles. Macromol. Rapid Commun. 31:108–118.

Taylor TM, Davidson PM, Zhong Q. 2007. Extraction of nisin from a 2.5% commercial nisin product using methanol and ethanol solutions. J. Food Prot. 70:1272–1276.

Vonasek E, Le P, Nitin N. 2014. Encapsulation of bacteriophages in whey protein films for extended storage and release. Food Hydrocoll. [Internet] 37:7–13. Available from: http://dx.doi.org/10.1016/j.foodhyd.2013.09.017

Wang Y, Padua GW. 2012. Nanoscale characterization of zein self-assembly. Langmuir 28:2429–2435.

Whitesides GM. 2006. The origins and the future of microfluidics. Nature [Internet] 442:368–73. Available from: http://www.ncbi.nlm.nih.gov/pubmed/16871203

Workman VL, Dunnett SB, Kille P, Palmer DD. 2008. On-chip alginate microencapsulation of functional cells. Macromol. Rapid Commun. 29:165–170.

Xiao D, Davidson PM, Zhong Q. 2011. Spray-dried zein capsules with coencapsulated nisin and thymol as antimicrobial delivery system for enhanced antilisterial properties. J. Agric. Food Chem. 59:7393–7404.

Zhang H, Tumarkin E, Sullan RMA, Walker GC, Kumacheva E. 2007. Exploring microfluidic routes to microgels of biological polymers. Macromol. Rapid Commun. 28:527–538.

Zhang Y, Niu Y, Luo Y, Ge M, Yang T, Yu L, and others. 2014. Fabrication, characterization and antimicrobial activities of thymolloaded zein nanoparticles stabilized by sodium caseinate-chitosan hydrochloride double layers. Food Chem. [Internet] 142:269–275. Available from: http://dx.doi.org/10.1016/j.foodchem.2013.07.058

Zhou J, Hyun DC, Liu H, Wu H, Xia Y. 2014. Protein capsules with cross-linked, semipermeable, and enzyme-degradable surface barriers for controlled release. Macromol. Rapid Commun. 35:1436–1442.

CHAPTER 7

Conclusions and future directions

Assembling food-grade delivery systems based on microfluidic platforms are gaining more and more interest. In this study, we found that surface modified zein colloidal particles can form stable emulsions by high-shear homogenization, while an immediate phase separation was observed when using a microfluidic approach. It is attributed to the limited mobility of the colloidal particles to adsorb onto the oil-water interface during microfluidic processes. As an alternative, we then demonstrated a facile approach to fabricate zein-based microcapsules in microfluidics through an internal phase separation that is driven by the self-assembly of zein at the oil-water interface. A series of properties including particle size, release rate, morphology, mechanical properties and internal structures were precisely controlled by adjusting the flow rates and formulation. A practical application of this technique was tested using a pH-sensitive antimicrobial peptide, nisin. By controlling the rate of release, nisin that encapsulated in microfluidics showed promising results in extending the efficacy of nisin in a fresh cheese at neutral pH.

A microfluidic process is suitable for handling delicate materials due to its mild processing conditions and highly controllable features. Recently, several types of food-grade materials have been successfully applied in microfluidic processes and most of them are carbohydrate-based polyelectrolytes and synthetic polymers. Nevertheless, very few studies have been reported using proteins and lipids as building blocks of the structure, which could be a promising future direction. Although many ideas have been proposed, scalability and reliability are still the main issues for the mass production using microfluidics, and future studies could focus more on prevention of clogging in the microfluidic channels during production, especially when the biomaterials are used.

Another challenge associated with the processing of food-grade materials in microfluidics is related to the heterogeneity of many food-grade materials. In conventional top-down processes, the existence of impurity may be a significant issue. However, the heterogeneity of food-grade materials could be detrimental in microfluidic processes, especially when the raw material is handled on a very small scale. For instance, a high local concentration of impurities could result in clogging in the microfluidic channels. Furthermore,

the impurities could accumulate in the microchannels, which would alter the flow parameters and hydraulic pressure in the channels. Those issues may be resolved by a periodical auto-cleaning system, but it will increase the cost in the meantime. Future work is still needed to increase the yield of microfluidic production and avoid clogging during the process with a cost-effective approach.

APPENDIX A-1 Permission and publication reprint for the contents of CHAPTER 2

American Physical Society Reuse and Permissions License

16-Apr-2018

This license agreement between the American Physical Society ("APS") and Yiming Feng ("You") consists of your license details and the terms and conditions provided by the American Physical Society and SciPris.

Licensed Content Information

License Number:	**RNP/18/APR/003488**
License date:	16-Apr-2018
DOI:	10.1103/PhysRevLett.99.094502
Title:	Dripping to Jetting Transitions in Coflowing Liquid Streams
Author:	Andrew S. Utada et al.
Publication:	Physical Review Letters
Publisher:	American Physical Society
Cost:	USD $ 0.00

Request Details

Does your reuse require significant modifications: No

Specify intended distribution locations:	United States
Reuse Category:	Reuse in a thesis/dissertation
Requestor Type:	Student
Items for Reuse:	Figures/Tables
Number of Figure/Tables:	1
Figure/Tables Details:	Figure 1
Format for Reuse:	Print and Electronic
Total number of print copies:	Up to 1000

Information about New Publication:

University/Publisher:	University of Illinois
Title of dissertation/thesis:	Microfluidic assembly of zein microcapsules
Author(s):	Yiming Feng
Expected completion date:	May. 2018

License Requestor Information

Name:	Yiming Feng
Affiliation:	Individual
Email Id:	yfeng15@illinois.edu
Country:	United States

APPENDIX A-1 (continue)

Order Completed

Thank you for your order.

This Agreement between University of Illinios -- Yiming Feng ("You") and Elsevier ("Elsevier") consists of your license details and the terms and conditions provided by Elsevier and Copyright Clearance Center.

Your confirmation email will contain your order number for future reference.

printable details

License Number	4331110551823
License date	Apr 16, 2018
Licensed Content Publisher	Elsevier
Licensed Content Publication	Chemical Engineering Journal
Licensed Content Title	Numerical and experimental investigations of liquid mixing in T-type micromixers
Licensed Content Author	A. Soleymani,E. Kolehmainen,I. Turunen
Licensed Content Date	Jan 15, 2008
Licensed Content Volume	135
Licensed Content Issue	n/a
Licensed Content Pages	10
Type of Use	reuse in a thesis/dissertation
Portion	figures/tables/illustrations
Number of figures/tables/illustrations	1
Format	both print and electronic
Are you the author of this Elsevier article?	No
Will you be translating?	No
Original figure numbers	Figure 5
Title of your thesis/dissertation	Microfluidic assembly of zein microcapsules
Expected completion date	May 2018
Estimated size (number of pages)	171
Attachment	
Requestor Location	University of Illinios 1304 W Pennsylvania Ave URBANA, IL 61801 United States Attn: University of Illinios
Publisher Tax ID	98-0397604
Total	0.00 USD

APPENDIX A-1 (continue)

License Number	4331110658099
License date	Apr 16, 2018
Licensed Content Publisher	John Wiley and Sons
Licensed Content Publication	Journal of Chemical Technology & Biotechnology
Licensed Content Title	Microfluidic synthesis of monodisperse pectin hydrogel microspheres based on in situ gelation and settling collection
Licensed Content Author	Chaeyeon Kim, Ki-Su Park, Jongmin Kim, et al
Licensed Content Date	Apr 28, 2016
Licensed Content Volume	92
Licensed Content Issue	1
Licensed Content Pages	9
Type of use	Dissertation/Thesis
Requestor type	University/Academic
Format	Print and electronic
Portion	Figure/table
Number of figures/tables	1
Original Wiley figure/table number(s)	Figure 1
Will you be translating?	No
Title of your thesis / dissertation	Microfluidic assembly of zein microcapsules
Expected completion date	May 2018
Expected size (number of pages)	171
Attachment	
Requestor Location	University of Illinios 1304 W Pennsylvania Ave URBANA, IL 61801 United States Attn: University of Illinios
Publisher Tax ID	EU826007151
Total	0.00 USD

APPENDIX A-1 (continue)

License Number	4331110731638
License date	Apr 16, 2018
Licensed Content Publisher	Elsevier
Licensed Content Publication	Chemical Engineering Journal
Licensed Content Title	Factory-on-chip: Modularised microfluidic reactors for continuous mass production of functional materials
Licensed Content Author	Tengteng Han,Li Zhang,Hong Xu,Jin Xuan
Licensed Content Date	Oct 15, 2017
Licensed Content Volume	326
Licensed Content Issue	n/a
Licensed Content Pages	9
Type of Use	reuse in a thesis/dissertation
Portion	figures/tables/illustrations
Number of figures/tables/illustrations	1
Format	both print and electronic
Are you the author of this Elsevier article?	No
Will you be translating?	No
Original figure numbers	Figure 1
Title of your thesis/dissertation	Microfluidic assembly of zein microcapsules
Expected completion date	May 2018
Estimated size (number of pages)	171
Attachment	
Requestor Location	University of Illinios 1304 W Pennsylvania Ave URBANA, IL 61801 United States Attn: University of Illinios
Publisher Tax ID	98-0397604
Total	0.00 USD

APPENDIX A-1 (continue)

License Number	4331110796936
License date	Apr 16, 2018
Licensed Content Publisher	Elsevier
Licensed Content Publication	Journal of Membrane Science
Licensed Content Title	Premix emulsification: A review
Licensed Content Author	Akmal Nazir,Karin Schroën,Remko Boom
Licensed Content Date	Oct 15, 2010
Licensed Content Volume	362
Licensed Content Issue	1-2
Licensed Content Pages	11
Type of Use	reuse in a thesis/dissertation
Portion	figures/tables/illustrations
Number of figures/tables/illustrations	1
Format	both print and electronic
Are you the author of this Elsevier article?	No
Will you be translating?	No
Original figure numbers	Figure 1
Title of your thesis/dissertation	Microfluidic assembly of zein microcapsules
Expected completion date	May 2018
Estimated size (number of pages)	171
Attachment	
Requestor Location	University of Illinios 1304 W Pennsylvania Ave URBANA, IL 61801 United States Attn: University of Illinios
Publisher Tax ID	98-0397604
Total	0.00 USD

APPENDIX B-1 MATLAB code for the image analysis of the degree of wrinkle

```
clear all;
close all;
clc;
[pathstr,name,ext] = fileparts('sample control 20XT4.tif')


original_filename=strcat(name,ext)
img3d=imread(original_filename)

img2d=im2bw(img3d,maps,0.01) %switch to binary image
imgnoise=imfill(img2d,'holes')  %fill holes
img2 = filter2(fspecial('average',3),imgnoise)/1;  %remove noise
SE = strel('rectangle',[20,20]);   %connect surface
img3 = imerode(img2,SE)   %smooth surface
img = imopen(img3, strel('disk',10));
%figure
%imshow(img);

imglb=bwlabel(img,4)
STAT_perimeter=regionprops(imglb,'perimeter') %calculate perimeter
STAT_area=regionprops(imglb,'area')       %calculate area


P=struct2cell(STAT_perimeter)
A=struct2cell(STAT_area)

xlswrite('sample control.xlsx',P,'sheet1','B5')
xlswrite('sample control.xlsx',A,'sheet2','B5')
[m n]=size(img);

imgn=zeros(m,n);
ed=[-1 -1;0 -1;1 -1;1 0;1 1;0 1;-1 1;-1 0];
for i=2:m-1
   for j=2:n-1
      if img(i,j)==1

         for k=1:8
            ii=i+ed(k,1);
            jj=j+ed(k,2);
            if img(ii,jj)==0
               imgn(ii,jj)=1;
            end
         end

      end
   end
end
```

APPENDIX B-1 (continue)

```
figure;
%imshow(imgn,[]);

se = strel('square',3);
imgn=imdilate(img,se)-img;
%figure;
%imshow(imgn)

I=img
[x,y]=size(I);

BW = bwperim(I,8);

P1=0;
P2=0;
Ny=0;
for i=1:x
   for j=1:y
      if (BW(i,j)>0)
         P2=j;
         if ((P2-P1)==1)
            Ny=Ny+1;
         end
         P1=P2;
      end
   end
end

P1=0;
P2=0;
Nx=0;
for j=1:y
   for i=1:x
      if (BW(i,j)>0)
         P2=i;
         if ((P2-P1)==1)
            Nx=Nx+1;
         end
         P1=P2;
      end
   end
end


SN=sum(sum(BW));
Nd=SN-Nx-Ny;

H=max(sum(I));
```

APPENDIX B-1 (continue)

```
W=max(sum(I'));
L=sqrt(2)*Nd+Nx+Ny;
A=bwarea(I);
C=2*3.1416*sqrt(A*0.3183)

outputimg=cat(2,img2d,img,imgn)
imshow(outputimg)

bundary_name=strcat(name,['_bundary.tif'])
area_name=strcat(name,['_area.tif'])
output_name=strcat(name,['_output.tif'])

imwrite (img,area_name)
imwrite (imgn,bundary_name)
imwrite (outputimg,output_name)
```

APPENDIX B-2 Matlab code for creep curve fitting

```
clear all;
close all;
clc;

[pathstr,name,ext] = fileparts('MS2T3_0006 LC.txt')
filename=strcat(name,ext)
[a1 a2 a3 a4 a5]=textread(filename,'%f %f %f %f %f',11999,'headerlines',2573)

distance = a1(1:2:end,:)
time = a3(1:2:end,:)

initial_depth=distance(1,1)
initial_time=time(1,1)

adjusted_depth=[distance(1:6000,:)-initial_depth;]
adjusted_time=[time(1:6000,:)-initial_time;]
relative_depth=initial_depth.\adjusted_depth

hplot=plot(adjusted_time,relative_depth)
ylabel('RelativeDepth')
xlabel('AdjustedTime')
saveas(hplot, name, 'jpg')

ft=fittype('m*log(1+x/n)')
fit(adjusted_time,relative_depth,ft,'StartPoint',[0.1,0.1])
```